Politecnico di Torino

Corso di Laurea in Ingegneria per l'Ambiente e il Territorio

TESI DI LAUREA
FEASIBILITY STUDY OF GROUND-SOURCE HEAT PUMPS IN NORTHERN QUÉBEC

Candidate: Luca Riggi

Tutor: ing. Alessandro Casasso
ing. Simone Della Valentina
prof. Rajandrea Sethi

ANNO ACCADEMICO 2017-2018

1 Sommario

Abstract (Ita)

Nella regione nord del Québec (Nunavik) esistono comunità remote totalmente scollegate con la rete stradale ed elettrica del resto del Paese, nelle quali il riscaldamento degli ambienti, l'acqua sanitaria e l'energia elettrica vengono prodotti interamente con caldaie e generatori a gasolio. Kuujjuaq è la comunità più popolosa (~2500 abitanti) del territorio degli Inuit del Québec e presenta un fabbisogno termico di circa 33 MWh/unità abitativa, con clima subartico e con una temperatura media annua di 0°, con presenza discontinua di permafrost. In tale contesto si è cercata la soluzione tecnologica migliore per ridurre le emissioni di CO_2 ed operare un efficientamento energetico nella comunità di Kuujjuaq sfruttando l'energia geotermica del terreno a basse profondità con la tecnologia delle pompe di calore accoppiate a sonde geotermiche verticali. La tesi presenta un'analisi di fattibilità economica e tecnologica mettendo a confronto lo scenario attuale, in cui si utilizzano caldaie a diesel, e quello in cui avviene una totale o parziale sostituzione delle caldaie a diesel con pompe di calore a compressione di vapore, alimentate da corrente elettrica, o assorbimento, alimentate da gasolio. Per ogni scenario è stato calcolato il tempo di ritorno (payback time) dell'investimento e il risparmio di CO_2 che ne deriva. Per studiare il funzionamento dell'impianto sono state effettuate simulazioni numeriche di trasporto di calore nel terreno con il codice agli elementi finiti FEFLOW®, attraverso il quale è stata verificata l'efficienza di scambio, la risposta termica del fluido termovettore circolante all'interno della sonda e del sottosuolo per un periodo di 20 anni. Le simulazioni hanno tenuto conto, attraverso il plugin FTM, del cambiamento di fase da liquido a solido dell'acqua di falda, che comporta una notevole variazione delle proprietà termiche e lo scambio isotermico di calore latente di solidificazione/fusione. La soluzione migliore in termini economici e tecnologici è stata ottenuta con pompe di calore ad assorbimento nel caso di una copertura del fabbisogno termico al 70% (integrando il resto con la caldaia), installando una sonda di lunghezza pari a 200m e diametro di perforazione 3 pollici. In questo contesto, è stato raggiunto un Gas Utilization Efficiency (GUE) pari a 1.25. Tutte le simulazioni effettuate, però, hanno evidenziato tempi di ritorno superiori alla vita utile d'impianto, rendendo quindi necessario adottare degli incentivi per promuovere la realizzazione di questi impianti.

Abstract

In the northern region of Quebec (Nunavik) there are remote communities totally disconnected from the road and electricity networks of the rest of the country, where space heating, domestic hot water and electricity are produced entirely with boilers and diesel generators. Kuujjuaq is the most populated community (~2500 inhabitants) in this region and has a heating demand of about 33 MWh/home unit, with a subarctic climate and an average annual temperature of 0°C, with discontinuous presence of permafrost. In this context, we have tried to find the best technological solution to reduce CO2 emissions and operate an energy efficiency in the community of Kuujjuaq by exploiting the geothermal energy of the ground at shallow depths with the technology of heat pumps coupled with vertical ground heat exchangers. The thesis presents an analysis of economic and technological feasibility comparing the current scenario in which diesel boilers are used and that in which a total or partial replacement of diesel boilers with steam compression heat pumps, powered by electricity, or absorption heat pumps, powered by diesel. For each scenario, the payback time of the investment and the resulting CO2 savings have been calculated. To study the operation of the plant, numerical simulations of heat transport in the ground were carried out with the finite element code FEFLOW®, through which the exchange efficiency and the thermal response of the heat carrier fluid circulating inside the probe and the subsoil were verified for a period of 20 years. The simulations took into account, through the FTM plugin, the phase change from liquid to solid of the groundwater, which involves a significant variation of the thermal properties and the isothermal exchange of the latent heat of solidification / fusion. The best solution in economic and technological terms was obtained with absorption heat pumps in the case of a 70% coverage of the heat requirement (integrating the rest with the boiler), coupled to a borehole with a length of 200m and a drilling diameter of 3 inches. In this context, a Gas Utilization Efficiency (GUE) of 1.25 was achieved. All the simulations carried out, however, showed payback periods higher than the plant lifetime, making it necessary to provide subsidies to promote the construction of these plants

Introduction

In northern Quebec, in the region called Nunavik, north of the 55th parallel, there are 14 Inuit communities totally disconnected from the national road network and hydropower grid.

These communities are electrically powered by autonomous networks using diesel generators, while the production of heat for heating buildings and domestic hot water is mainly based on the combustion of hydrocarbons. The sub-Arctic and harsh climate makes it difficult to supply diesel once a year by sea.

Despite widespread electrification and massive hydroelectric production in the rest of Quebec, it is unrealistic to connect all isolated communities to the grid as it would involve the development of a multi-million-dollar electricity transmission project for a community of a few hundred or thousands of inhabitants.

This is how it is necessary to think about decentralized solutions, with low environmental impact.

This work is based on a research and collaboration project between the Polytechnic and the University of Turin and the INRS (Institute National de la Recerque Scientifique - Quebéc city - Canada) for the energy efficiency and decarbonisation and reduction of CO_2 emissions of these communities with renewable energy.

In this view, the use of low-enthalpy geothermal energy can be a measure that can help to achieve these goals.

It is in fact a form of renewable energy that can be exploited through the technology of the Borehole Heat Exchange (BHE) coupled with a heat pump, which is able to extract heat from the ground even at low temperatures and transport it to the surface for domestic use, without producing polluting emissions on site. However, these systems are also characterized by high installation costs and, hence, the economic return must be fully assessed given the high installation costs and the absence of incentives.

The main objective of this thesis is to conduct a feasibility study of a closed loop vertical probe geothermal plant coupled with a ground-coupled heat pump (GCHP) in the community of Kuujjuaq which, with its 2775 inhabitants, represents the most populated community in Nunavik, to analyse the performance and thermal

response of the ground through the numerical code FEFLOW ® (Finite Element subsurface Flow system).

The analysis is developed by comparing the current scenario, in which diesel boilers are used, with a total and a partial replacement with vapour compression heat pumps, powered by electricity, and absorption heat pumps, powered by diesel.

The information useful for the analysis were collected in a collaboration between Politecnico di Torino and INRS (Québec) in June 2018, during the mission co-financed by the Ministry of Foreign Affairs and International Cooperation and the Government of Québec.

This work is divided into three macro sections: the first part presents the data collected in Canada and gives a description of the context, geographical, socio-economic, climate of the study area with a focus on the energy context and environmental policies to reduce CO_2 emissions. Chapter 2 introduces the technology of the heat pump coupled to the BHE and a description of the various types of heat pumps that can be installed in this context, and the operating characteristics of a closed-loop system. Chapter 3 deals with a theoretical point of view with the transport of heat in porous media, and the effects of freezing on the properties of water within it.

The second macro section corresponding to chapter 4 presents the method by which the feasibility analysis was developed. In a first phase this is characterized by the calculation of the investment cost, annual savings and Pay Back Time of the GCHP system.

The second phase is aimed exclusively at the construction of the model through the implementation of a suitable setup, through the numerical code FEFLOW®, to analyse the temperature behaviour of the probe coupled to an absorption heat pump, the efficiency of exchange with the ground, the performance of the pump and the thermal lumen of the ground.

In the last section are reported the results obtained from the economic feasibility analysis in which are highlighted the differences in the cost items of each type of plant and savings that can result also in terms of CO_2, and the results of simulations carried out with FEFLOW ®.

1 KUUJJUAQ

Kuujjuaq (58.10 ° N, -68.42 ° E) is the largest of 14 communities in northern Québec, in the Nunavik region. Kuujjuaaq is located 48 km upstream of the Bay of Ungava on the western bank of the river Koksoak (Fig. 1), which gives it a strategic geographical position from a commercial point of view [1]. Nunavik is an Arctic region north of Québec (Canada), it covers a land area of 443,684. km² delimited by the 55th parallel, it is surrounded to the east by the Ungaa Bay to the north by the Hudson Strait and to the west by the Hudson Bay (Fig. 1).

Fig. 1 Canada, Nunavik, Kuujjuaq

1.1 Socio-economic context

Kuujjuaq with about 2375 inhabitants represents the most populous community of Nunavik, around the 20% of the entire region [2], and the community with highest energy demand and emissions. In Nunavik the population is almost 90% Inuit with 14 communities distributed on a peninsula confined by Hudson Bay (W), Hudson Strait (N) and Ungava Bay (E).

Under the 2006 agreement between Canada, Makivik Corporation and Nunavut, the Inuit became the owner of 80% of the islands in the Nunavik marine region [3].

The social, political, administrative, economic and legal organization is controlled and implemented by several regional and local authorities. The most important are the KRG (Kativik Regional Government), the Makivik Corporation, Landholding corporation and other land corporations based in Kuujjuaq.

The KRG was created in 1978, to provide public services to residents of Nunavik and it is the privileged interlocutor of the Quebec government and is the main contributor to regional development projects. It also provides technical assistance to the 14 villages in the north.

The implementation of the overall financing method envisaged by the Kativik Regional Government, signed in 2004, allows the KRG to allocate the amounts autonomously according to its priorities and within the framework of the mandates it has to carry out.

Its responsibilities include local and regional government, local and regional economic development, airport operations and maintenance of marine infrastructure, Internet access, regional police, fire protection, Inuit hunting support, fishing and capture activities, environment, development and management. parks, employment, training and income support, development of municipal infrastructure.

Makivik Corporation, for its part, has a mandate to protect Inuit rights and to manage the interest and financial compensation resulting from the agreements. It manages large enterprises and contributes to the socio-economic development of the region, the improvement of Inuit housing conditions and the protection of the Inuit language and culture [3].

These communities, which are far from Québec, the capital of the region of the same name, about 1,000 ÷ 1,900 km, are not connected to the rest of the region by a road or rail network, nor are there road links between the different communities.

The connection with the ocean combined with the presence of an airport with two runways makes Kuujjuaq a commercial hub of primary importance for the entire region. Two airlines deliver air transportation services in Nunavik: Air Inuit and First Air [4][5]. They offer scheduled and charter flights, but this service is expensive. For example, a return flight between Quebec City and Kuujjuaq costs about 200 Canadian $ (1 CAN $ = 0.67 €). NEAS and Desgagnés Transartik are the only two shipping companies that serve the region. All the communities possess marine infrastructure that permit the unloading of supplies [6].

The population in this region is much younger than in the rest of Quebec with about 40% under the age of 15 and has a higher growth rate and household size than in the rest of Quebec with housing containing on average 5 people. On the other hand, life expectancy in Nunavik (63.3 years) is much lower than in the rest of Québec (79.4 years) [7].

The economic pillar of Nunavik is the public administration, together with the various public services, retail sales and transport. The primary and secondary sectors are mainly dominated by mining and the construction industry. Although employment is higher than in the rest of Quebec, the average income received by 60% of Nunavik households is below 30,000 per year, with poverty two times higher.

At the same time, the cost of consumer goods prices is higher in Nunavik mainly because of the costs of transport and storage, which results in a significantly reduced purchasing power, to this should be added tax rates (income tax, consumption tax, etc..) are equal to those present throughout Quebec. On the other hand, there are credit programmes and measures that do not compensate for this deficit.

Low levels of schooling, poor work experience or mobility due to family obligations and housing make it particularly difficult for the inhabitants of this region to increase their income.

Indeed, with a few exceptions, home ownership is not an option and there is no freedom to choose it as it is allocated by public authorities or employers, depending on availability. These are low rental housing with high management costs, but they are not reflected in the monthly rents, which in 2007 reached a maximum of 148$ to

$505 depending on the type of housing and the conditions of the household, compared to monthly management costs estimated by the State at 2615$.

In 2008, Nunavik's housing stock consisted of 1950 low-rent dwellings and several hundred homes for staff from government departments and agencies and regions (Table 1). Despite the absence of a private real estate market, there were also 80 private dwellings, most of which were purchased through special property programmes set up, by the Société d'habitation du Québec (SHQ) in the mid-1990s.

Nunavivik, in 2013 counted about 2 734 residential housing.

The typical dwellings rest on piles which are in turn resting on the foundations, in such a way as to isolate the internal environment from the outside temperature and from the freezing effects which it would encounter (Fig. 3 and Fig. 4).

Table 1 - Population and housing trends in Nunavik (2008-2013)(source:[2],[3])

Site	2008		2011		2013		
	Population	N° Houses	Population	N° Houses	Population	N° Houses	% Houses
Akulivik	551	117	620	125	662	163	6.0%
Aupaluk	196	46	198	46	202	60	2.2%
Inukjuak	1689	306	1619	368	1661	429	15.7%
Ivujivik	358	63	372	75	381	75	2.7%
Kangiqsualujjuaq	786	155	882	171	914	187	6.8%
Kangiqsujuaq	623	129	703	145	736	145	5.3%
Kangirsuk	507	120	554	138	587	138	5.0%
Kuujjuaq	**2236**	**373**	**2403**	**373**	**2520**	**451**	**16.5%**
Kuujjuarapik	593	133	665	150	675	166	6.1%
Puvirnituq	1523	263	1703	325	1773	387	14.2%
Quaqtaq	324	64	379	70	397	85	3.1%
Salluit	1361	229	1360	256	1377	284	10.4%
Tasiujaq	263	73	305	73	314	89	2.5%
Umiujaq	446	79	448	80	465	95	3.5%
TOTAL	**11.456**	**1950**	**12.211**	**2395**	**12.664**	**2734**	**100%**

Fig. 2 house type years 2000 (source: Le longement au Nunavik, 2014)

Fig. 3 house type in Kuujjuaq (Source: Nicolò Giordano 2018)

One of the elements that most influence the economy of the northern regions is certainly the supply of fuel. Due to the harsh climate, the cost of heating is a very important cost item for public administrations and rare homeowners. It is also an important component of the cost of domestic transport and food collection (snowmobile and boat).

The purchase is made once a year, before the tankers leave for other regions to supply farms and the price paid at that time determines the price to pay for fuel for the whole year, from 1th September. To this, must be added the costs of transporting, storing and distributing fuel in sometimes very small communities.

These constraints produce a disparity with the rest of Quebec throughout the year, where the price varies every time refuelling takes place, while in Nunavik it is generally higher.

However, Nunavik communities benefit from gasoline subsidy programs. The amount of the grant is determined based on the $/litre price of gasoline, past and projected sales figures for the following year, and of course the funds available.

1.2 Energy context

In addition to being disconnected from the rest of the region by roads, Kuujjuaq and the other 13 communities are not connected to the regional electricity grid (Fig. 5). Electricity, space heating and domestic hot water are produced locally by means of diesel-fired generators and furnaces.

It is the same public utility Hydro Québec that deals with the production of electricity through diesel generators (Fig. 6), that is then distributed with independent networks community by community to users with higher costs than the Distribute System powered by hydroelectric power (0.30$/kWh).

The production cost for the operator of this energy varies between 0.30 ÷ 1$/kWh depending on the latitude, with an average of 0.75$/kWh. The expenditure one in 2010 was covered per kWh in the best case only 17% with a cost for resident consumers of 5.71 cents per kWh. [8].

Since 2007, the regional and administrative authorities (KRG and Makivik) have agreed on a subsidy of 0.16$/l and in 2008 of 0.48$/l. In 2009, KRG undertook to finance 45% of the entire amount, to keep the price of gasoline at 1.40$/l, even though this price was still about 40% higher than the price of gasoline in other Québec [9].

Energy costs for the residential and medium-power sectors are presented in Table 2.

Fig. 4 - Power generation systems and grid lines in Quebec (b) (Hydro-Québec Sustainability report 2012-modified)

Fig. 5 Kuujjuaq's power plant. (PHOTO BY JANE GEORGE)

Table 2 Hydro-Québec's electricity rates (source: Hydro-Québec, 2016).

Tariff	On grid	Off grid
Residential rate and agricultural	5.71¢ per kWh to a maximum of 30 kWh per month	5.71¢ per kWh to a maximum of 30 kWh per month
	8.68¢ per kWh for the remaining energy consumed	37.62¢ per kWh for the remaining energy consumed
The average tariff for power of at least 50kW	4.93¢ per kWh for the first 210 MWh monthly	4.93¢ per kWh for the first 390 MWh monthly
	3.66¢ per kWh for the remaining energy consumed	15.22¢ per kWh for the remaining energy consumed plus $30.78 per kW for the power demand

In 2015, Arctic diesel was sold to 1,929 $/L (50.22/GJ) to Nunavik and generally the cost increases with the isolation of communities [10].

Almost all buildings and homes are heated with oil-burning furnaces. Each community has furnace oil reservoirs and delivery trucks (Fig. 6).

FCNQ Petro and Halutik are responsible for the distribution of fuel products in the region [6].

Hydro-Québec's autonomous diesel generators have a total capacity of 45 MW (referring only to the 14 Inuit communities) for 2006 with an average efficiency of 33.2%, and about 26-27 MW for Nunavik alone, producing about 65,300 MWh/a (2007) with an average capacity factor of 28.8% (Table 3). [11].

In 2006 a total of 37.2 million litres were consumed, for a diesel bill of 52 million dollars and 93,000 tonnes of CO_2 equivalent emissions with a total emission, in 2015, from all Hydro-Québec power stations, of 232,424 tonnes of CO_2 equivalent [12].

Itshould also be added that historical data and forecasts on energy demand in the Nunavik area indicate that it is progressively increasing because of population growth rates higher than in other regions in the North (Table 4).

Table 3 summary of energy demand and capacity, CO_2 emission of off-grid in Nunavik (Status of remote/Off-grid Communities in Canada 2011) (Hydro Québec, 2006) - efficiency (Deslauries, 2008)

Site	Annual Energy Demand (MWh/y)	Capacity of diesel power plant (kW)	Efficiency (kWh/l)	Efficiency (%)	Estimated CO_2 emission x10^3 teq
Akulivik	2300	900	3.37	31.3	2.1
Aupaluk	1200	780	3.43	31.8	1.1
Inukjuak	7400	2990	3.78	35.1	6.4
Ivujivik	1400	1015	3.4	31.5	1.3
Kangiqsualujjuaq	3800	1975	3.55	32.9	2.9
Kangiqsujuaq	3200	1520	3.61	33.5	2.7
Kangirsuk	2800	1360	3.53	32.8	2.4
Kuujjuaq	15100	4555	3.78	35.1	12.2
Kuujjuarapik	9800	3405	3.68	34.1	8.8
Puvirnituq	7400	2870	3.75	34.8	6.4
Quaqtaq	1900	1085	3.42	31.7	1.7
Salluit	5500	2960	3.78	35.1	4.3
Tasiujaq	1600	850	3.36	31.2	1.3
Umiujaq	1900	1050	3.47	32.2	1.7

Table 4 Estimated energy and power demand in Nunavik (2016-2026)

	NUNAVIK								Increase 2016-2026	
	2016	**2017**	**2018**	**2019**	**2020**	**2022**	**2024**	**2026**	**Δ**	**%**
GWh	93.7	95.8	98.2	100.7	103.5	107.9	112.8	116.8	23.0	2.2%
MW	17.5	17.9	18.4	18.9	19.3	20.2	21.0	21.4	3.9	2.3%

Fig. 6 Steel tank of a common house in Kuujjuaq (2018)

1.3 CO_2 emissions and environmental issues in the Artic

CO_2 emissions represent the main side effect of all those combustion phenomena used for human activities for electricity production. According to an IPPC emissions report of 2016, the activities that produce the most greenhouse gases are certainly those dedicated to the production of energy with 58% of total global emissions starting from the oxidation of fossil fuel carbon[13].

Although the debate on the climate effect of man and the direct link between human activity and climate change is still the subject of debate today [14], it can be said that since the last century carbon dioxide has undergone a significant increase of 44% when compared to the level of 1800 or the pre-industrial period with 280ppm compared to 2016 where the average concentration was found to be 403 ppm with a growth of 2 ppm/y in the last decade. By 2018, the concentration had already exceeded 410 ppm.

On the other hand, the climate system continues to warm up, with an increase of almost twice the global average rate of average Arctic temperatures over the last 100 years, resulting in widespread melting of snow and ice and rising sea levels [15].

The effects of climate change are more influential in the polar regions than elsewhere in the world, it is essential to consider its impact on the Inuit of Nunavik and their homes. Among the many effects observed are permafrost melting, landslides and an interrupted seasonal cycle, which can have negative and worrying impacts on building stability.

Other effects of climate change include an interruption of the seasonal cycle and an interruption of traditional Inuit activities (hunting, fishing, trapping, etc.).

1.4 Hydro Québec - Environmental Policy

While Hydro Québec's users bear very high costs, the annual emission of thousands of tons of CO_2 contributes to air pollution and warming of the Arctic climate with the degradation of permafrost and effects on fauna and in general the ecosystem and society [16].

In the plan for the management of autonomous networks published in 2016, the distributor Hydro-Québec has developed an action plan in which it actively promotes the conversion of existing networks into less expensive and more efficient energy networks, through the publication of calls for the submission by 2020 of projects technically feasible, sustainable from the economic and environmental point of view. The call for proposals process considers the opportunities and characteristics associated with each network, as well as the needs of each community, in order to choose the most appropriate technologies.

The main objective of the distributor is to reduce the cost of supplying fossil fuel from thermal power plants and the CO_2 emissions associated with it (Table 3),

and at the same time to stimulate the private market so as to be able to propose solutions that are more economical than the current method of production.

At the same time, the distributor has implemented a policy against the use of electricity produced by plants for domestic heating and energy efficiency by using as a leverage disincentive tariffs applied to customers north of the 53th parallel for the efficient use of energy, thus encouraging customers to use customers stand-alone systems to use a source other than electricity produced by a plant for space heating.

At the end of 2015, was registered a decrease in power requirements of 4 MW (4.3%), to which corresponded interventions in autonomous systems with 16.2 GWh (4% of sales), results that reflect the good performance of the distributor's energy saving programs in stand-alone systems [17].

1.5 Climate and geological setting

The environment Nunavik is characterized by the presence of boreal forest, tundra and permafrost with a marked latitudinal gradient that determines average annual temperatures that differ in extreme latitudes of almost 10 degrees (4.6 ° C in Kuujjuarapik and -6.8 ° C in Inukjuak for the reference period 1961-1990 according to climatological records by Environment Canada)[18].

There are two types of climate in this region: a subarctic climate and an arctic climate. Winters are long and very cold, while in summer, the region enjoys prolonged sunshine. The winds are strong with the speed that is greatly increased by the absence of trees (with winds that can reach 160km/h) [3]. [3], Temperatures can reach -37°C, during winter, in some places with the freezing of the surrounding seas while in summer temperatures easily exceed 20°C even if the average surface temperature remains close to the freezing point [12].

Annual temperatures are up to 15 ° C cooler than in northern European marine areas on similar latitudes.

In Kuujjuaq the climate is sub-Arctic with an average temperature of 0 °C and is characterized by significant rainfall during the year with a difference in precipitation between the driest month and the rainiest of 40 mm while it is 34.2 °C is the variation in average temperatures during the year. The coldest month is January, where the temperature is -23.3 °C, while July is the hottest month of the year, with an average temperature of 10.9 °C. [19].

Such a climate explains why the heating period of the buildings lasts longer than elsewhere in Quebec and why, in Kuujjuaq, the ground is permanently frozen.

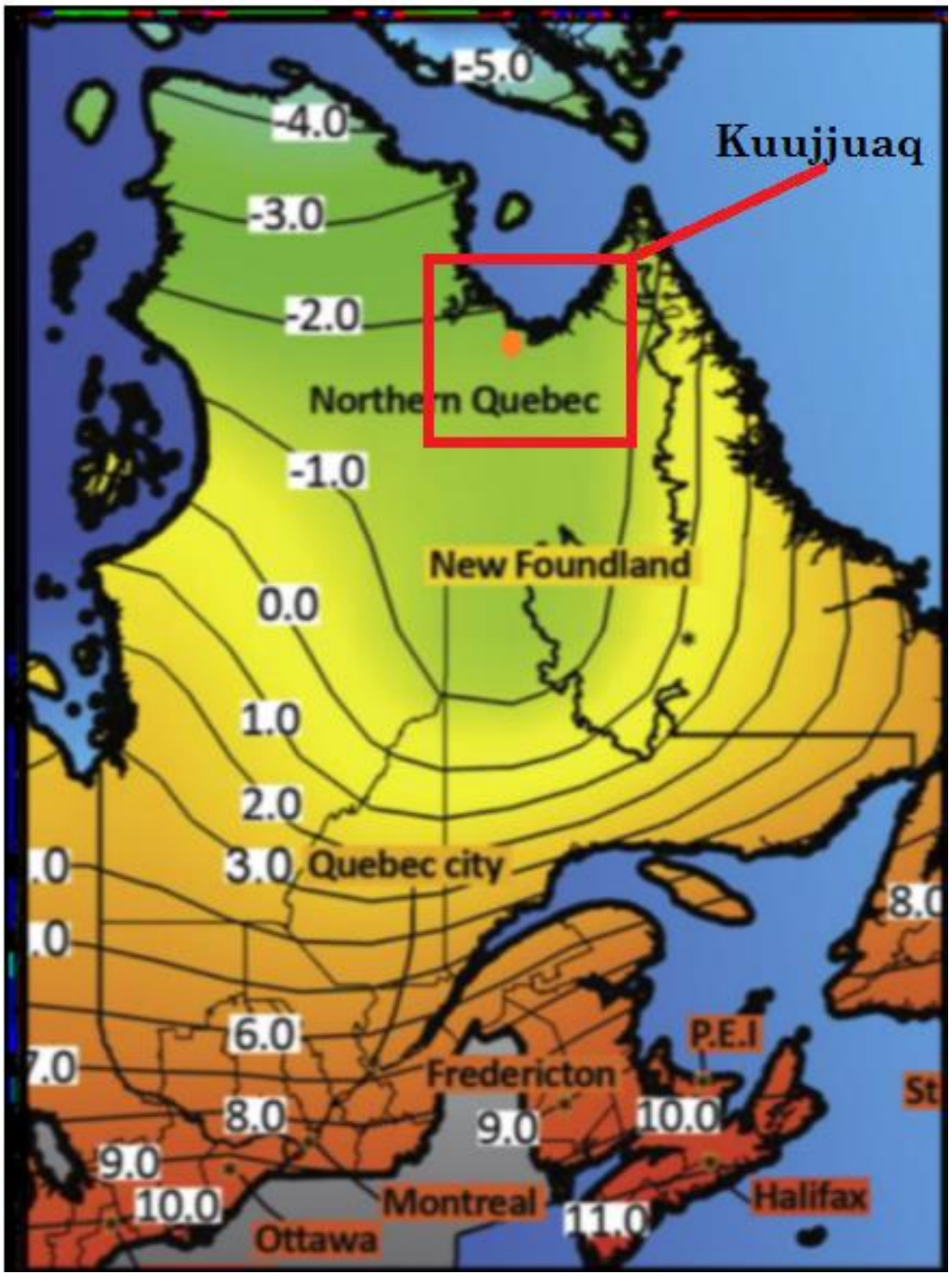

Fig. 7 Ground temperatures in Québec (Source: Ouzzane et al 2015-modified).

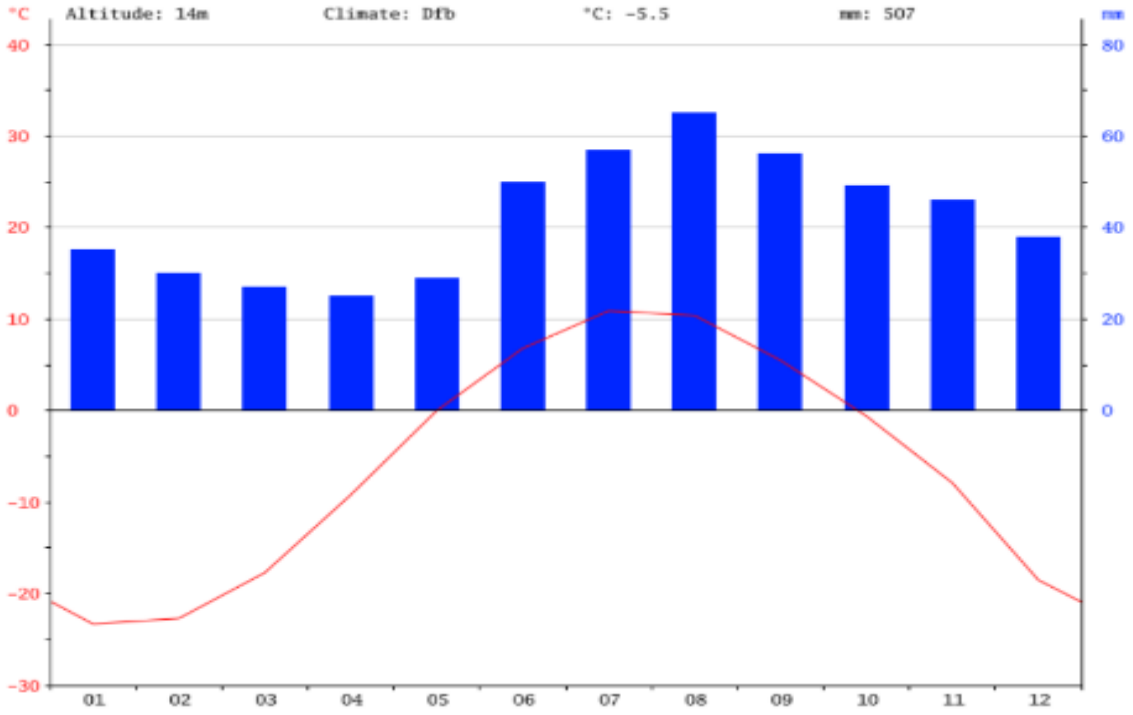

Fig.8 Average temperature trend and average monthly rainfall during the year in Kuujjjuaq (Source: climate-data.org-not modified)

Such a rigid climate determines the formation and maintenance of permafrost,that it is mainly present in fine, low-permability, unconsolidated deposits (silts and clays). [20]

"Permafrost is a soil whose temperature remains below 0°C for at least two consecutive years" [21]. The active layer is the surface layer of the soil above the permafrost which is subject to annual freeze-thaw cycles (C.A.R.R.G., 1988). Permafrost, being essentially a periglacial climatic phenomenon, is very sensitive to the latitudinal gradient and therefore climatic. This is reflected in the thickness and distribution in the region.

In the south there is a sporadic and discontinuous presence while in the north the thickness varies from decimetres to hundreds of meters passing through a coverage of the territory from 2% to 100% except under the great lakes and rivers of the extreme north.

Unlike permafrost, the thickness of the active layer is smaller, from a few decimetres to a few meters, while it is always influenced by the surface and thermal conditions of the soil.

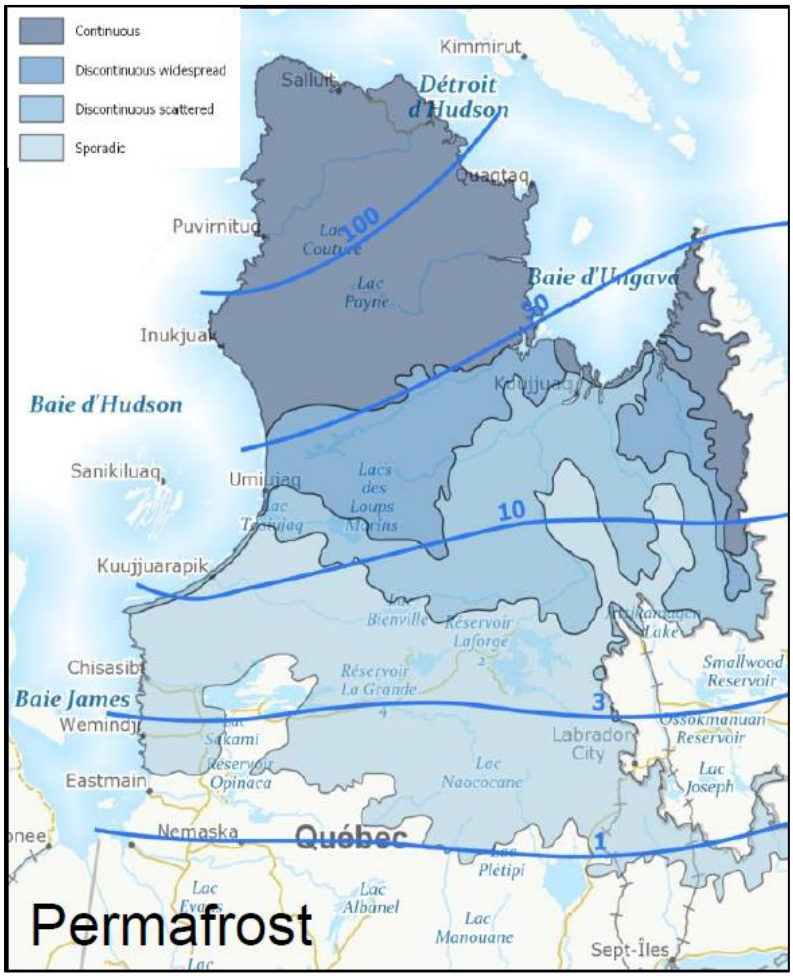

Fig. 9 Map of permafrost (source: OHMI-Giordano et al.2017-not modified)

In Kuujjuaq there is a discontinuous presence of permafrost at a depth of 25m with a thickness of a few meters.

The main lithological units present in and around Kuujjuaq are diorites and gabbros, gneisses and paragneisses. (*Fig. 10*) [22].

Quaternary sediments mainly consist of coastal and pre-littoral sediments alternating with intertidal deposits linked to different transgression and regression cycles of the Iberville Sea (*Fig. 11*). From a geomorphological point of view, in the territory of Kuujjuaq there are two small parallel valleys, both sloping south towards the river Kosoak, whose estuary flows into the bay of Ungava at about 50 km in the direction of NNE. The glacial deposits often cover outcrops of bottom rock and it is common to find them at the base of marine sediments. Coarse-grained alluvial materials can only be found along the small streams of the above-mentioned valleys.

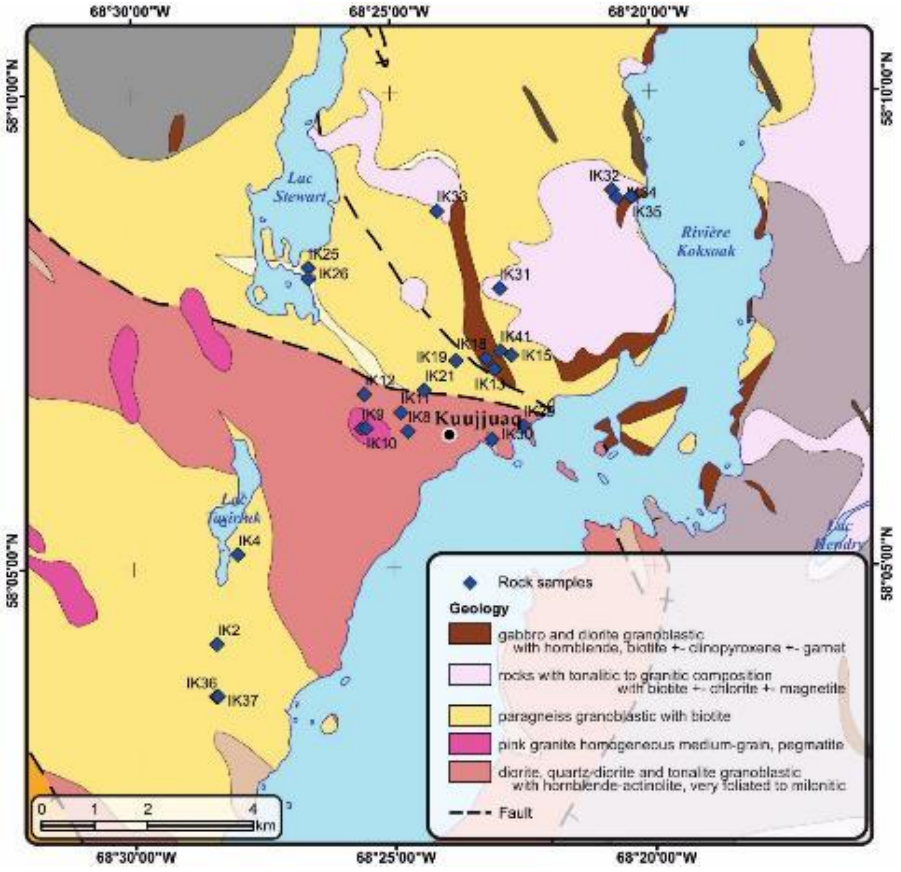

Fig. 10 Geological map (Source:Miranda et al., 2018-not modified)).

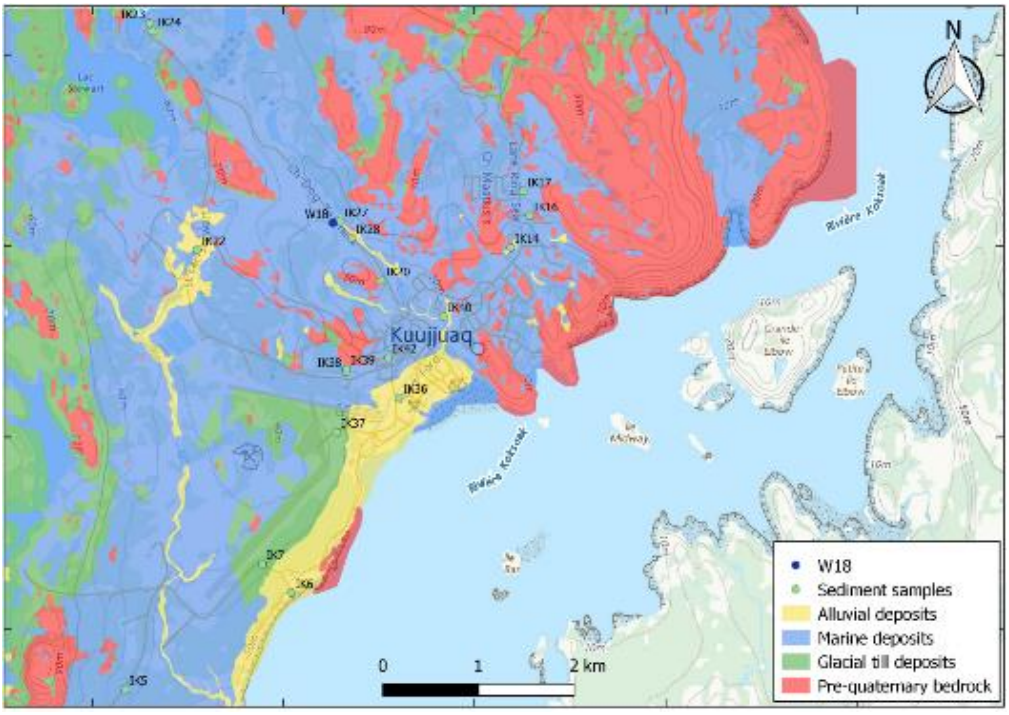

Fig. 11 Map of quaternary deposits (source: Giordano et al. 2017-not modified)).

The shallow underground temperature in the study area is slightly higher than 0°C and the vertical geothermal gradient is very low (~ 20 °C/km), (Fig. 12). This is a limiting factor for the efficiency of geothermal applications.

The temperature profile has minimum values at the glaciall till layer at a depth of about 20m, from which it increases as the depth increases(Fig. 12).

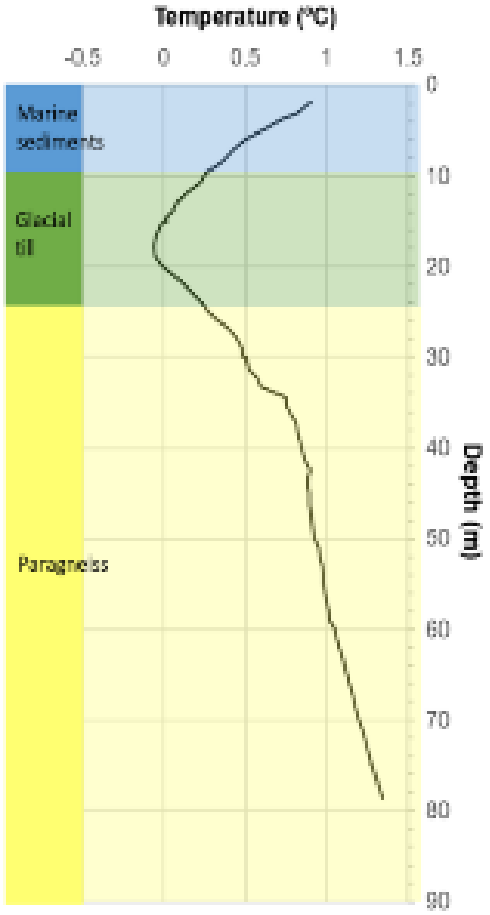

Fig. 12 Temperature vertical profile in W18 (source: Della Valentina et al. 2018-not modified)

2 LOW ENTHALPY GEOTHERMAL SYSTEM

The building conditioning (heating and cooling) with geothermal energy has spread considerably since the 80's following the introduction and spread of heat pumps [23].

The various heat pump systems make it possible to extract and economically use the heat present inside the ground at low temperatures, as well as in aquifers and surface water masses [24].

Low enthalpy systems are suitable for any type of site, unlike high enthalpy systems that require sites with thermal anomalies present only in a few sites and often too far from the users. The main peculiarity is to exploit a thermal resource that during the seasons maintains a constant temperature even in those regions with extreme seasonal temperatures, from hot heat in summer to cold below zero in winter.

Their operating principle is based on the transfer of heat from a colder source (well) to a warmer one (heating system). In the heat exchange, for the second law of thermodynamics, mechanical work is required at the expense of a heat pump.

The winter heat source can also be used as a summer heat sink, with the same system it is possible to both heat and cool a building releasing the heat in the subsoil in the summer and use it as a reserve in the winter period.

Low-enthalpy geothermal energy is considered a renewable source, in fact, although the system is powered by electricity and/or fossil fuels, with a correct sizing the heat can be hypothetically exploited for an infinite time.

A low-enthalpy geothermal plant consists of three basic elements (Fig. 10):

- Heat pump
- Ground heat exchangers
- Heat distribution system to the user

Sizing this type of plant means considering the maximum thermal power of heating and cooling, but above all the trend of the thermal load over time. The energy performance of the system strictly depends on the thermal stresses suffered by the ground during the exchange phase.

2.1 Heat Pump

The heat pump is a thermal machine, operating according to a cyclic process, which allows heat to be transferred in the opposite direction to that in which it would tend to flow naturally, from a low temperature body T_0 to a high temperature body T_c, with $T_0<T_c$. It is the refrigerant fluid present inside the heat pump that absorbs the quantity of heat q_0 at temperature T_0 and makes it available q at a temperature T_c at the terminals, through the transformation phases according to a thermodynamic cycle of evaporation and condensation. This is in fact characterized by a relatively low evaporation temperature and a high latent heat of vaporization that allows it to absorb and release a large amount of heat [19].

Most heat pumps are so-called 'reversible' because, depending on the desired effect, they can heat or cool an environment. In fact, both conceptually and in terms of operation, there is no difference between a refrigeration machine and a heat pump.

These are generally made up of an evaporator, a condenser and a compressor (Fig. 13).

During operation, the fluid undergoes four transformations [25]:

- *Compression:* the refrigerant in the gaseous state at low temperature and pressure, coming from the evaporator is brought to high pressure by the effect of a compressor becoming "hot".
- *Condensation:* the heat purchased is released through a condenser that cools and liquefies the "hot" steam.
- *Expansion:* passing through the lamination valve, the "hot" liquid refrigerant loses pressure and cools down.
- *Evaporation:* the refrigerant absorbs heat from the outside and passes from the "cold" liquid phase to the "cold" vapour.

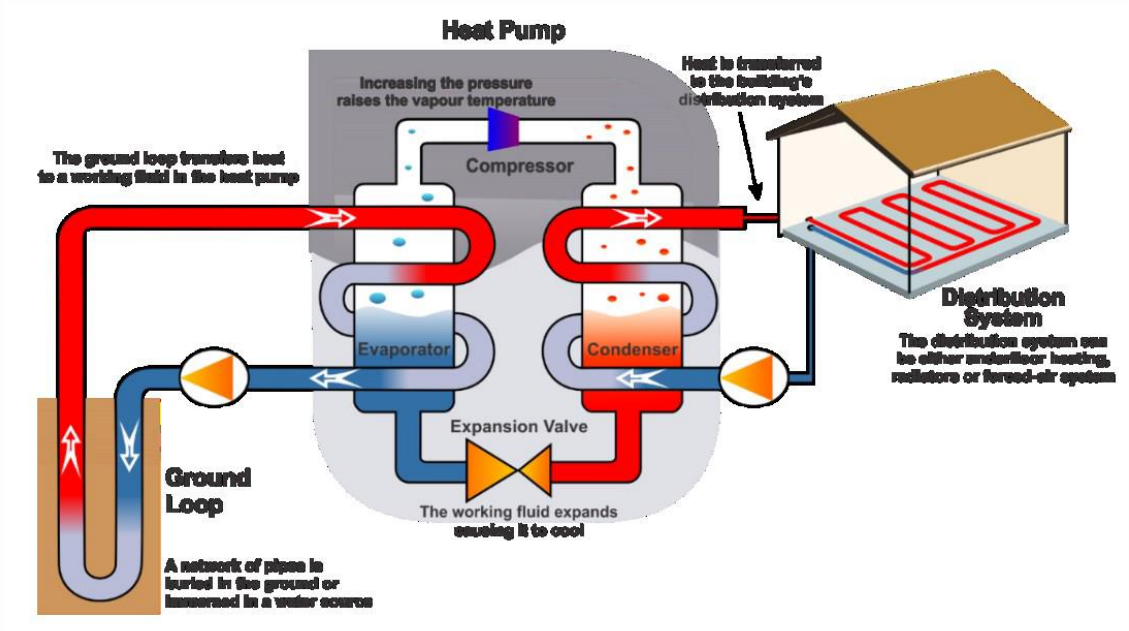

***Fig. 13* Thermodynamic cycle: heating.**

Below is explained in detail the thermodynamic cycle of the heat pump together with the *COP* performance coefficient.

2.1.1 Thermodynamic Cycle

These machines follow the thermodynamic cycle of reverse compression Carnot, which in turn is based on the theoretical reversible cycle of Carnot, which is represented in the Fig. 14 on the entropic diagram (*T-s*) and on the enthalpy pressure diagram (*P-h*), has the following transformations [26]:

1) *1-2 isentropic compression:* the gas is heated from T_E to T_C without heat transfer;

2) *2-3 isothermal compression*: the gas is compressed keeping the temperature constant. During this phase, the gas gives off a quantity of heat equal to q_C to the cold source;

3) *3-4 isentropic expansion:* the steam expands without heat transfer, reducing the temperature of the same from T_C to T_E;

4) *4-1 isothermal expansion:* the gas draws a quantity of heat equal to q_E from the hot source, causing an increase in the volume of the gas and a decrease in pressure. During this phase the temperature remains constant.

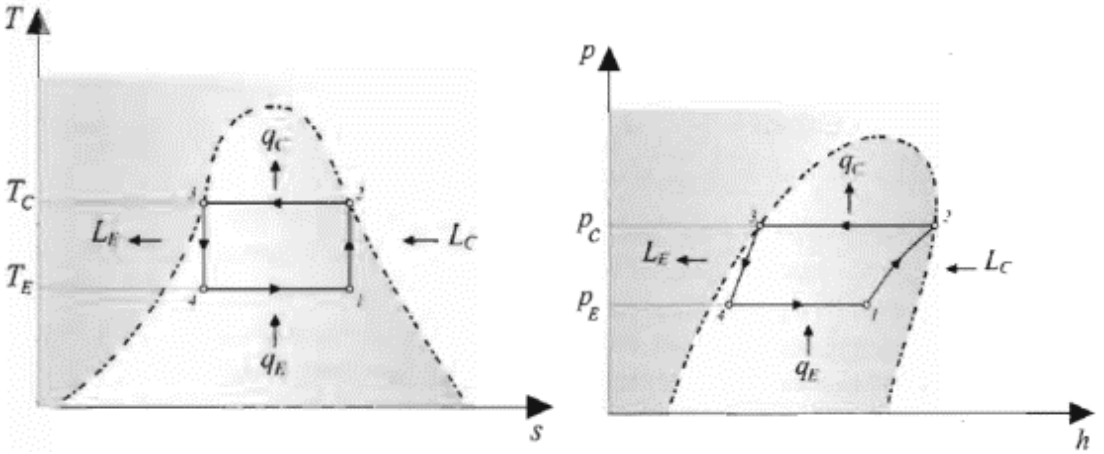

***Fig. 14* Reversible Carnot cycle: entropic diagram (T-s) and pressure digram (P-h); (Source: Delmastro 2009 - not modified)**

The Carnot cycle is said to be theoretical since to achieve it requires the use of perfect gas without friction and an ideal thermal machine, such as to evolve between two sources with the highest possible thermodynamic efficiency with thermodynamic transformations totally reversible. These conditions are not achievable, despite this it is used as a reference cycle with which to compare real applications such as the heat pump.

The real cycle of which the diagram is shown in the figure, the rolling and compression phases are irreversible and therefore not isentropic, and the following transformations are present:

1) *1-1' compression:* The steam coming from the evaporator is overheated to avoid the presence of a liquid phase in the compressor, thus cooling the lubricating oil of the compressor and avoiding overheating of the compressor.

2) *1'-2 compression:* the pressure and temperature increase occur at the expense of the mechanical work carried out by the compressor.

3) *2-3 isothermal condensation:* the steam at high temperature and pressure enters the condenser where it first cools down and then condenses, releasing heat.

4) *3-4 expansion:* the refrigerant passes through the lamination valve and is transformed into partially saturated cold steam.

5) *4-1 isothermal expansion:* partially saturated cold steam absorbs a quantity of latent heat q_E from the cold source and partially evaporates.

.

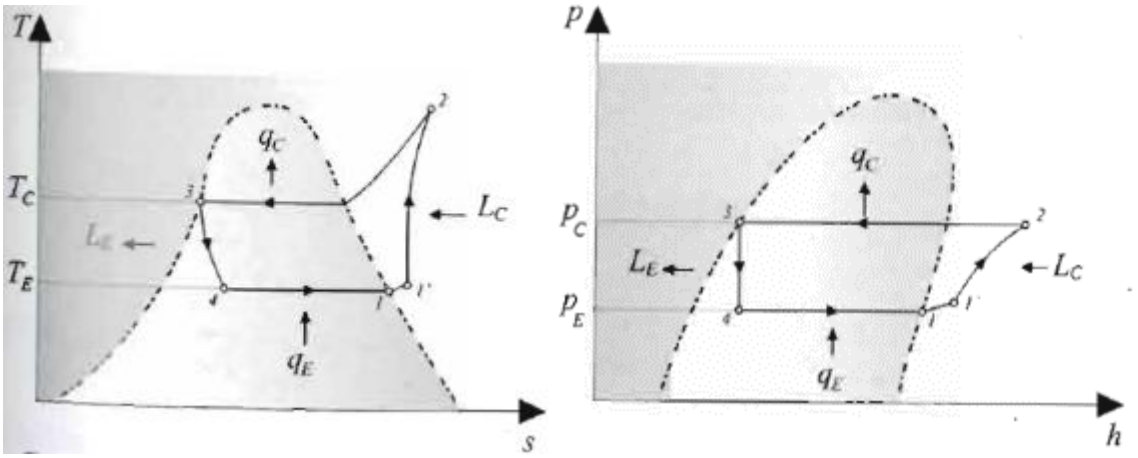

Fig. 15 **Reversible Carnot cycle: entropic diagram (T-s) and pressure digram (P-h); (Source: Delmastro 2009 - not modified)**

The efficiency of the system is measured by a parameter called *COP* (*Coefficient Of Performance*) which expresses the ratio between the amount of heat introduced or removed in a system and the work used to perform it (energy consumption of the heat pump) [27].

The *COP* in the reverse cycle can be expressed as follows:

$$COP = \frac{q_C}{L} = \frac{T_C}{T_C - T_E} \qquad \textbf{(2.1)}$$

During the cooling phase this is called *EER* (Energy Efficiency Ratio):

$$ERR = \frac{q_E}{L_C - L_E} = \frac{T_C}{T_C - T_E} \qquad \textbf{(2.2)}$$

where: q_C is the heat released during condensation, q_E is the heat extracted during evaporation, Lc is the energy consumption of the pump and L_E is the work gained through the expansion valves while T_C and T_E represent the condensation and evaporation temperatures.

The steam compression cycle will obviously have a performance coefficient or *COP* lower than the ideal cycle or that of Carnot. To calculate it we can use the classic Carnot formula and then multiply the result by a coefficient called "Carnot Yield" which varies according to the type of fluid used and the temperatures of the evaporator, as shown in the Fig. 13:

$$COP_H = COP_{Carnot} * \eta c \qquad \textbf{(2.3)}$$

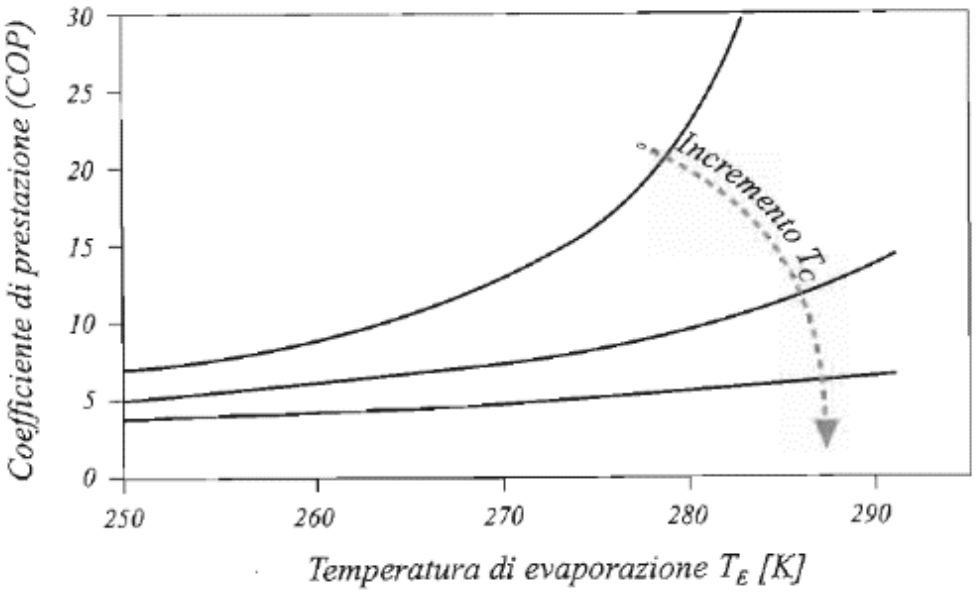

Fig. 16* Trend of the *COP* with variation of T_E and T_C *(source: Delmastro 2009 – not modified)

Observing the Fig. 13 it can be noticed how the *COP* increases keeping a condensation temperature as low as possible and having an evaporation temperature as high as possible. These are the ones to consider when designing a system to optimize its performance. Therefore, the greater the difference in temperature through which the heat pump operates, the smaller the quantity of heat pumped and the greater the power required by the pump. In other words, the greater the temperature differential between the source and the terminal, the lower the efficiency of the heat pump. In other words, the smaller the temperature difference between source and terminal, the higher the efficiency of the heat pump.

For this reason, the geographical and climatic context in which these systems are installed is important in the preliminary choice of the best source and type of heat pump.

The sources can be multiple and, in some cases, limiting for a good efficiency of the system. The geothermal source, unlike air or surface water, in harsh climatic contexts, where you can reach temperatures of varying degrees below 0 °C, is the

best answer for a good efficiency of the heat pump since the temperature in the subsoil is not affected by seasonal temperature variations. Just think that an air source heat pump becomes inefficient at temperatures less than -5 °C [28].

2.2 Types of heat Pumps

The types of heat pumps are many and can be classified according to different parameters but if you tighten the field to those used in geothermal, the most common heat pumps coupled to geothermal BHE on the market are:

- Electric compression
- Absorption

The compression mode in fact constitutes a further categorization of heat pumps [29].

2.2.1 Electrical compression

This type of heat pump uses electrical energy to drive the compressor (Fig. 15) and has a coefficient of performance (*COP*) with values around 3.

This means that for 1 kWh of electricity consumed, it will supply 3 kWh of heat to the vehicle to be heated.

To calculate more accurately the efficiency of an electric heat pump in terms of electricity consumption, the energy consumed in power plants to produce electricity should be considered. Estimating an average efficiency of the power plants of 36%, the COP of the electric heat pumps will be: $COP = 3 \times 0.36 = 1.1$ [28].

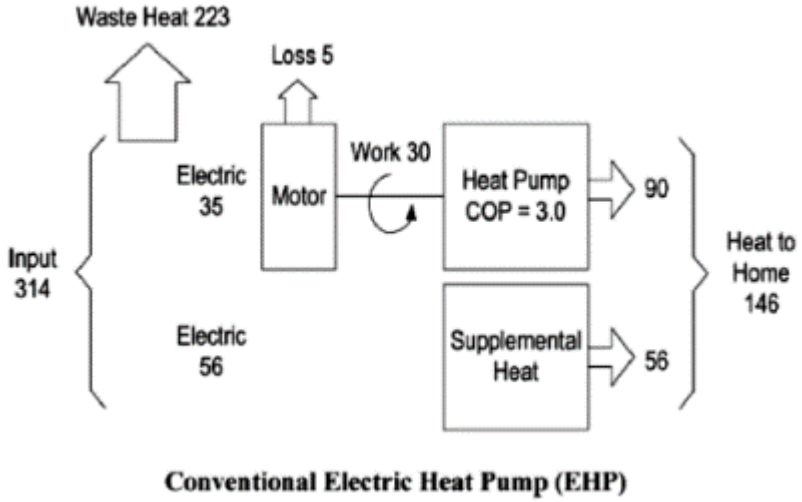

Fig. 17* Energy balance of *EHP (source :Lian et al., 2005-not modifies)

2.2.2 Absorption

Absorption heat pumps do not use mechanical compressors but a "thermal compressor" based on a chemical absorption reaction. The electrical system is replaced by a heat source generated by the combustion of natural gas, propane, water heated by the sun. Commercial heat pumps with diesel fuel as a source have not been identified during this research.

In residential heat pumps, the electric compressor as shown in the Fig. 15 is replaced by a sub-circuit consisting of an absorber and des-sorber inside which circulates a water-ammonia solution. Instead of being compressed as in normal electric heat pumps, the refrigerant is absorbed by the water and, with a relatively low power pump, it is brought to higher pressure and the ammonia is evaporated through the external heat source, restarting the cycle.

While the efficiency of an electric heat pump is measured by the *COP*, the efficiency of a gas heat pump is measured by the efficiency of gas utilization (*GUE*), which is the ratio between the energy supplied (heat released to the medium to be heated) and the energy consumed by the burner.

The *G.U.E.* varies according to the type of heat pump and the operating conditions and has, in general, values around 1.5.

This means that for 1 kWh of gas consumed it will supply 1.5 kWh of heat to the medium to be heated[30].

This heat pump coupled with BHE is called GCAHP has been introduced to provide a solution to remote and cold regions. They have a very low *GUE* compared to the types of heat pumps, extracting little heat from the ground during the Winter.

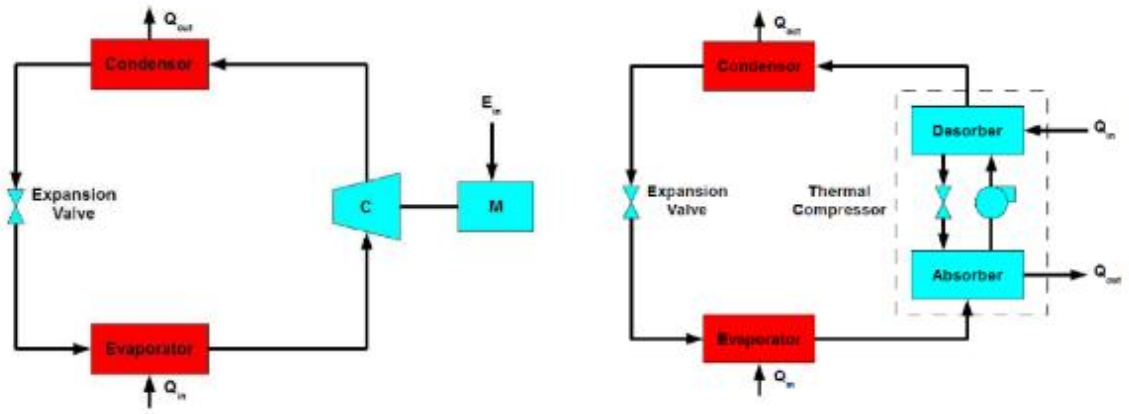

Fig. 18 Schematic diagrams of an electric heat pump (left) and an absorption heat pump (right) (Garrabrant, 2015 -not modified, Belzile 2017)

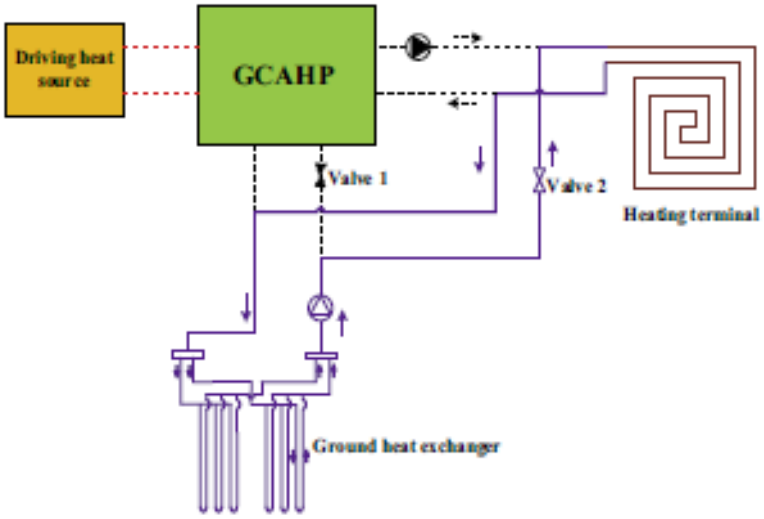

Fig. 19 GCAHP scheme.

2.2.3 Diesel Heat Pump

An alternative would be to feed the compressor of the heat pump with a diesel engine with a recovery of the heat losses of the engine thus increasing the efficiency.

Considering that an HP assumes a *COP* between 2÷4 and that the diesel engine has an efficiency of 30% one could expect an efficiency between 60÷120%.

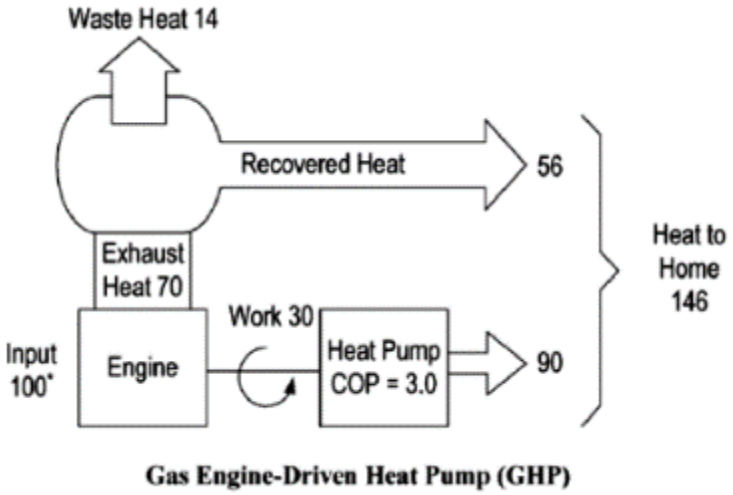

Fig. 20–Energy balance of DEHP (source : Lian et al., 2005-not modified).

2.2.4 Hybrid systems

In some cases, due to the limited space available for the probe field or due to the very low temperature of the ground in which they are installed, and therefore the low temperature of the operating fluid, it is not always possible to cover the entire energy and power requirements for the building's air conditioning.

In these situations, it is normally advisable to work with the geothermal heat pump to cover the base load of the building's heating or cooling needs and to use an auxiliary system to cover the peaks in heating or cooling capacity.

This is called hybrid systems. Normally, if the thermal peak to be covered is relative to the winter it would be advisable to cover the summer cooling energy demand with the geothermal heat pump, leaving it to work to cover the base load in winter and use an additional system to produce thermal energy. The additional system may consist of a boiler fuelled by fossil fuel or biomass, or even an electric heater (in the latter case, it is necessary to check the sporadic use of the electric heater during the season so as not to penalize the overall efficiency of the system)[27].

2.3 Heat distribution system to the user

In heat pump systems coupled with BHE, the containment of energy consumption by means of good containment construction techniques and the choice

of suitable system terminals is very important to maximise the performance of the entire system.

In fact, lowering the power required to supply heat to the environment, lowers the specific power and therefore it is possible to supply heat at lower temperatures, containing the thermal jump and obtaining a major *COP*.

Geothermal energy becomes convenient when using heating systems that operate at low temperature (30 ÷ 40 °C), compared to traditional ones that require temperatures of the order of 70 °c instead.

The most common system terminals in the residential field are:

- radiators
- radiant panels
- fan coils.

The former, are the most common in traditional systems and therefore in old buildings. They are not recommended for geothermal plants because of the high temperatures reached by the fluid (even 90°C). These are shell and tube heat exchangers made of metallic material in which the heat transmission is mainly due to conduction and to a lesser extent to convention.

The alternatives are therefore the diffuse systems (radiant panels in the figure) in which the transmission takes place by irradiation and the concentrated systems (fan Coil) in which a transmission takes place for convective motion.

The fan coil units are the best heat exchangers in a power/size ratio. The high efficiency makes it possible to use smaller Batteries. The advantages are to be realized in the reduced cost per unit of energy yield and extreme ease of regulation.

However, they can create noise and dust movement problems due to ventilation.

The radiant panels, thanks to the low temperature required by the heat transfer fluid, constitute the best coupling option with the heating pumps. They are composed of polyethylene serpentines where the heat transfer fluid flows and can be placed behind the surfaces of the environment to be heated (floor, ceiling, side walls).

For these reasons it is advisable to think of the exploitation of geothermal energy only in the case of new constructions or complete restructuring, where it is possible to foresee the installation of a suitable distribution plant.

In the case of partial and total replacement of a boiler system combined with traditional radiators already installed in favour of a geothermal system, it is possible to intervene by means of certain measures without incurring excessive costs.

For example, it is possible to use the same radiators, after having verified their correct sizing with the addition of some elements or replace them with radiators designed to have efficiencies comparable to traditional radiators with the same size but lower operating temperatures.

In the case of mixed systems, it is possible to exploit the geothermal heat for the domestic water and provide the thermal input for the mid-seasons and exploit the boiler in the coldest days or months.

Fig. 21 Radiators, fan coils and radiant panels (source: PhDThesis Casasso 2012-modified)

2.4 Typology of system

Geothermal heat pumps have the advantage of relying on a source that has a very low variation in temperature during the day and seasons compared to air heat pumps.

The systems can be open or closed, but in this work, we will refer only to the latter type, leaving a brief description of the technical aspects and problems of the so-called open systems so that we can understand the specific choice made.

Specifically for ground heat exchanger ASHRAE, proposes a classification based on the type of source on which the heat exchange is operated [29].

- GCHP (Ground-Coupled Heat Pump): closed-loop heat exchangers, closed circuit, or also indicated as BHE (Borehole Heat Exchanger) or geothermal probes, where the heat exchange takes place between a

circuit of underground pipes and the ground through a heat transfer fluid that circulates within the circuit.

- GWHP (Ground Water Heat Pump): more commonly open-loop or open circuit, the heat exchange takes place between a pair of wells and the groundwater that is then discharged.

Both types can be presented in different configurations depending on the properties of the territory and the needs to be met.

2.4.1 Closed-Loop

This type of system consists of a closed system. Inside the probes there are U-shaped pipes connected to the bottom of the well (Fig. 24). Inside the pipes flows the heat transfer fluid that exchanges the heat drawn from the ground with the heat pump.

Closed-circuit heat pumps are the most common and can be applied anywhere. They do not need aquifers with extractable flow rates and exploit the heat in the subsoil that remains constant during the season even in regions with extremely harsh climates such as the one under study.

In addition, there are no major environmental problems since there is no direct use of groundwater. Proper grouting of the borehole is therefore requested by many administrative authorities, which makes approval procedures easier and faster. Propwhich makes approval procedures easier and faster.

The best geological conditions for the installation are in the presence of rock formations.

These in fact have good thermal properties (conductivity and thermal capacity), while loose deposits (clays, sands, gravel) have very poor thermal properties if dry, but good conductivity (1.5÷2) and excellent capacity (~3) if saturated. In addition, if in these porous media, there is a significant underground flow, the addition improves the performance of the exchanger because you have a continuous recharge of thermal energy[26].

There are different configurations:

- Vertical geothermal BHE
- Horizontal geothermal BHE
- Geothermal pieles

In the first configuration pipes are installed in boreholes with variable lengths (50÷300m) and the grouted with common sand-bentonite mixture or thermally enhanced grouts. Grout mixtures avoid the interconnection between different aquifer levels and improve the thermal contact between the plastic pipe and grout. The main peculiarity is the reduced installation space, which makes it extremely versatile, especially for urban environments. The systems built with this system, ranging from small houses with a single hole, to large buildings, which require real fields of geothermal probes.

On the other hand, perforations are very expensive and, together with the completion of the probe, they account for 40÷75% of the entire installation cost[26].

Horizontal geothermal probes are the easiest to install but require a larger area. They are installed at modest depths to exploit the heat generated by the radiation with lower system yields (coil configuration 10÷40 W/m2 , linear development 4÷16 W/m2) [31] compared to the previous types. For this reason, installations under roads or foundations should be avoided.

The largest expense in the installation of this type of system is related to the excavation of the trenches to host the heat exchangers.

On the contrary, the geothermal piles exploit the heat exchanged with the ground by fixing the pipes for the heat exchange to the reinforcement of the foundation pole. The operating principle is like vertical BHE, but they differ in the lower yield due to the type of soil used and the structural needs that prevent excessive thermal contractions of the foundation. Nevertheless, the considerable saving in terms of drilling makes it a valid option but with a lower yield (10÷30 W/m) compared to vertical probes (30÷60 kW) and can only be used for new buildings [29].

Fig. 22 **Borehole Heat Exchanger (BHE),(Source: GEAM, Casasso 2013 - not modified)**

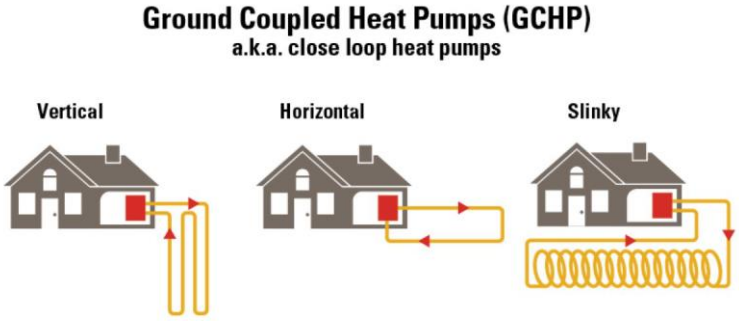

Fig. 23 **GCHP system configurations. (Source: www.mississippipower.com).**

The pipeline usually made of high-density polyethylene HDPE must have good values of thermal conductivity, corrosion resistance, good mechanical resistance and a durability equal to the useful life of the plant.

Different types of exchange circuits can be used (shown in the Fig. 24) and can be divided as follows:

- Single U pipes, consisting of a pair of straight tubes, connected by a 180° curved fitting at the bottom end of the hole.
- Double U pipes used to obtain a more effective heat exchange and have a redundant system that can allow the system to work even in the event of a pipe breakage.

- Coaxial pipes, i.e. concentric pipes of different diameters or in more complex configurations connected at the bottom of the perforation. In the case of heat exchange with the ground, the heat transfer fluid must necessarily carry out this phase in the crown. The main disadvantage is the short-circuiting effect it encounters due to the absence of distance between the cold and hot fluid.

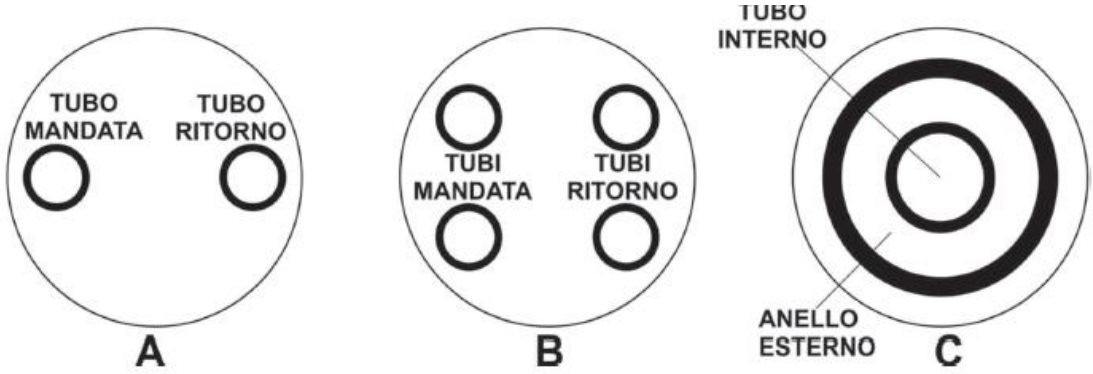

Fig. 24 **Pipes configuration in Borehole Heat Exchangers. (Source: GEAM, Casasso 2013 - not modified)**

The advantage of the U- and double U-tube is the low cost of the manufacturing material, and the possibility to place special spacers between the tubes along the entire extension of the hole, to ensure maximum reciprocal distance and mitigate as much as possible the effect of short circuiting and at the same time minimize the thermal resistance to the ground [26].

The well where the BHE is inserted is dug with a rotary drilling machine, shown in Fig. 22, which uses air or mud as drilling fluid, depending on the type of soil.

The hole must be filled with highly conductive material to minimise the overall resistance. Except in rare cases where water or quartz sand has been used, holes are commonly cemented with specific ready-mixed concrete with a high content of bentonite and additives to reduce porosity and hydraulic conductivity and improve thermal characteristics [32]. Furthermore, when working in climates, the filling must not show phenomena of expansion or shrinkage during the curing of the concrete due to the formation of ice, because the formation of cracks would be harmful to the transfer of heat between the BHE pipes and the ground.

The fluid flowing inside the pipes, through a recirculation pump, has the task of exchanging heat with the source and the heat pump.

It must have a high thermal conductivity, a low viscosity and a reduced toxicity and when working in soils where in winter cold temperatures are reached, it will be made up of a compound of water plus antifreeze to ensure a low point of solidification.

The most used fluids are solutions of propylene glycol, ethylene glycol and calcium chloride, the concentration of which depends on the freezing temperatures expected during the operation of the plant. In the use of these substances it is necessary to pay great attention both from the environmental point of view given in some cases their toxicity and the possibility of their spillage into the ground and into the aquifers, as they could pollute the aquifers, both from the technical point of view, relating to the concentration to be inserted. According to the design choices and the context in which it is worked, very often the heat carrier fluid works at temperatures below 0 °, with high concentrations of antifreeze that make the solution more viscous and dense going to burden the pressure losses (number of Reynolds is inversely proportional to the viscosity) and consequently on the recirculation pump that will have to have more power and higher energy costs (which usually accounts for about 1/10 of the consumption of the heat pump). The increase in concentration in parallel is reflected in the thermal properties of the fluid, in its thermal capacity and conductivity. The thermal resistivity of BHE in fact increases if the fluid is in laminar mode, compared to turbulent.

Propylene glycol compared to ethylene glycol is non-toxic, so much so that it is used in the food industry, but it is more viscous and expensive, which makes it less performing from a technical point of view.

Finally, the calcium chloride, despite its viscosity values, at the same solidification temperature, and much lower costs compared to glycols, is very corrosive and requires the design of special components, which overall makes it economically no longer valid.

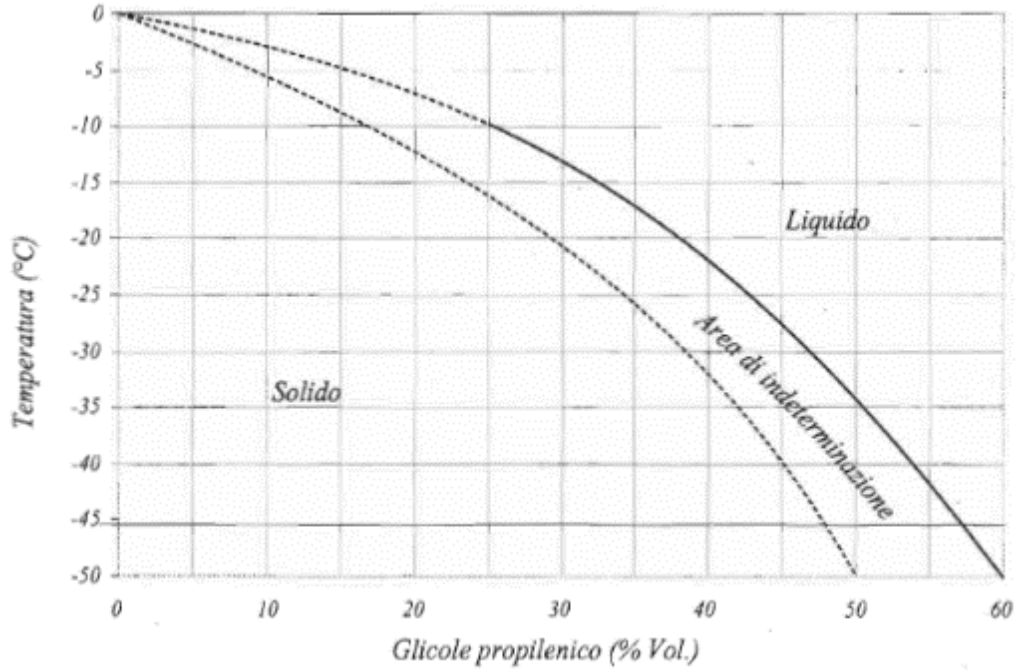

Fig. 25 **Phase diagram of propylene glycol water solutions at different volume concentrations (source: Delmastro 2009-not modified)**

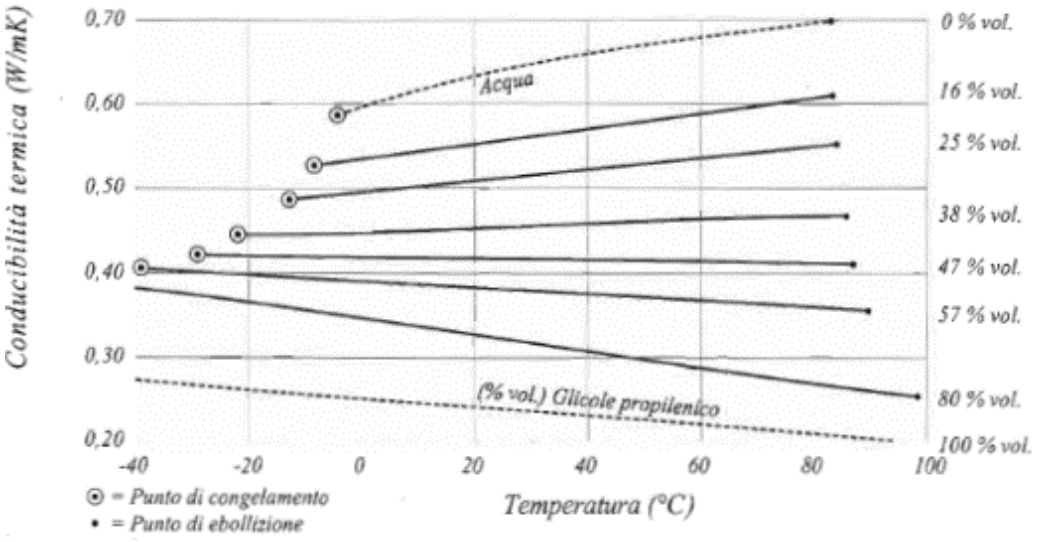

Fig. 26 **Thermal conductivity of propylene glycol water solution at different volume concentrations (source: Delmastro 2009- not modified)**

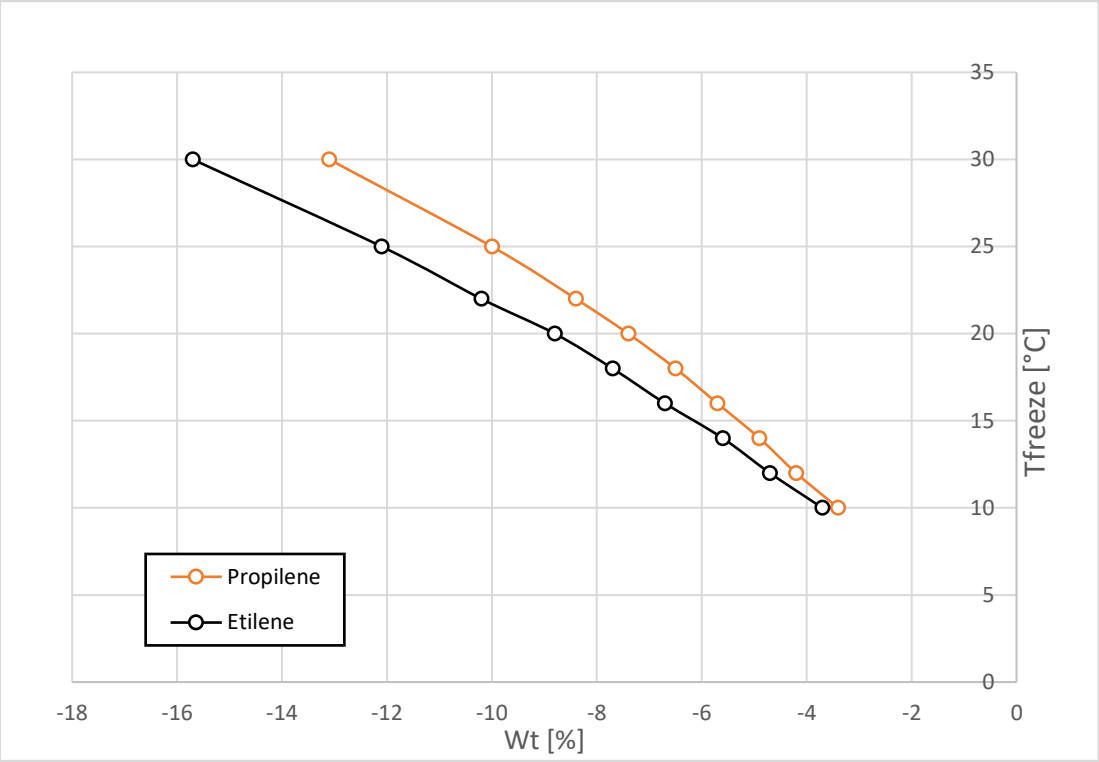

***Fig. 27*– Relation between the weight concentration of the antifreeze additives and their freezing point.**

2.4.2 Open-Loop

In this type of system, the heat pump operates a heat exchange with the water circulating freely underground or on the surface.

The water can be collected from the groundwater table or from lakes or rivers, which then, for economic and technical simplicity, is reintroduced into a body of surface water.

In this way, the return of cooled or heated water to the withdrawal well and the so-called thermal short circuit (Fig. 26), whose treatment refers to In this type of system the heat pump operates a heat exchange taking the heat possessed by the water that circulates freely underground or on the surface, depending on whether the intake takes place in the groundwater table in lakes or rivers, which then, for an economic and technical simplicity, is fed back into a body of surface water such as a river or irrigation channel, thus avoiding the return of cooled or heated water to the withdrawal well that could cause the so-called thermal short-circuit (Fig. 28) [34].

In open circuit systems, groundwater wells require maintenance and are limited to those sites with a discreet availability of aquifers and sufficient

permeability to allow the required flow rate to be achieved with a limited depression cone. The groundwater impoverishment is one of the main problems related to this type of plant.

In addition to this, a careful hydro-chemical analysis must be carried out during the design phase in order to avoid scaling caused by bacterial activity, which could require periodic removal treatments, and to verify, in the case of a re-injection well in the stratum, that the difference in inlet and outlet temperature is not too high in order to preserve the geochemical characteristics and microbial activity of the stratum [26].

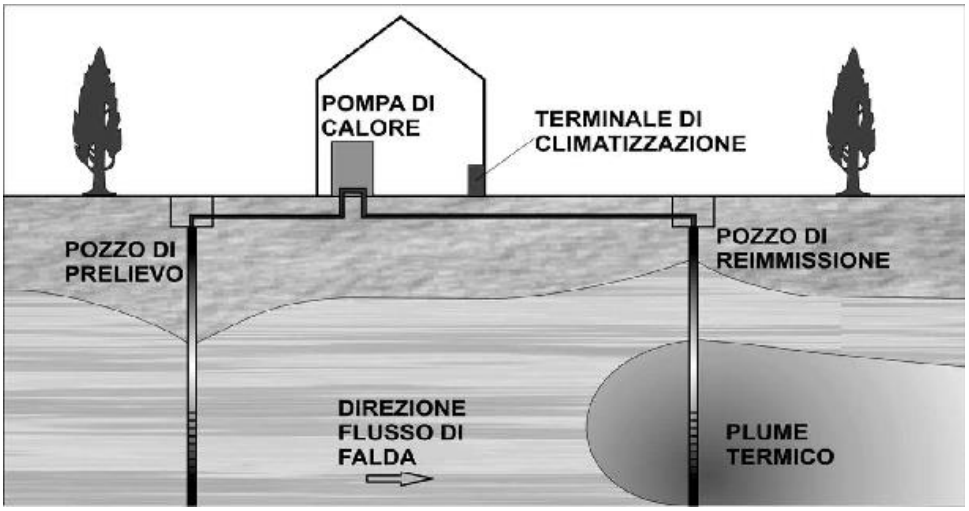

Fig. 28 Open loop system. Source [16].

2.4.3 Advantages and disadvantages Open and Closed Loop

The advantages of such a system mainly concern the economic aspect and depend, as always, on the context in which they are installed. They have a low installation cost and a limited size, and a high efficiency of the heat pump compared to a closed-loop if well designed, and in the absence of short circuit in addition to this they use a natural medium (aquifer) with a high thermal capacity.

A limiting economic factor is the depth in which the aquifer is located, in fact too high depth to water table makes the energy consumption for pumping up to the heat pump too high and higher than a closed system.

The presence of a productive aquifer implies the need for a deep hydrodynamic [30] and hydro-chemical characterization and an often difficult and long procedural procedure due to the risk of connecting different aquifers. This represents one of the

disadvantages combined with the already mentioned depletion of the aquifer and the spread of the thermal plume.

For this reason, open circuit systems are more recommended for high power, so that the costs of characterization and design have less weight on the total cost.

2.4.4 Design of ground coupled heat pump in Kuujjuaq

The typical diesel plant of a building in Kuujjuaq consists of a boiler and an external tank containing the diesel that is injected into the burner producing heat that is transmitted inside through the appropriate terminals ensuring thermal comfort throughout the year (Fig. 29).

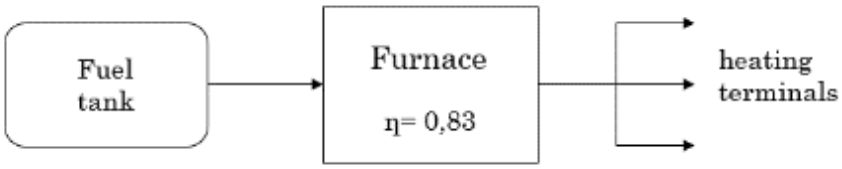

Fig. 29 Oil furnace scheme operating in Kuujjuaq.

The total replacement of the plant (Fig. 30-Fig. 31) presupposes the coverage of the heat requirement by the geothermal plant.

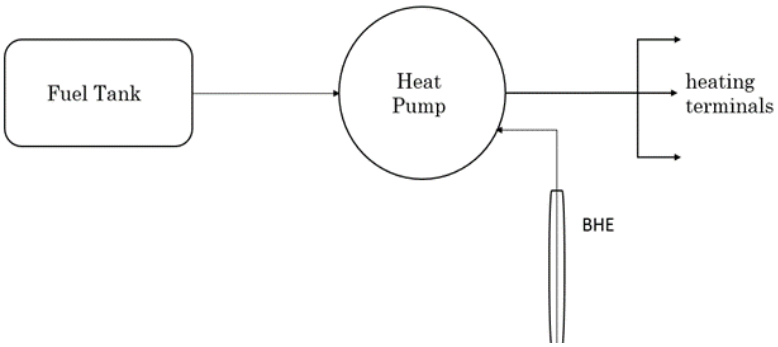

Fig. 30 GCAHP system scheme.

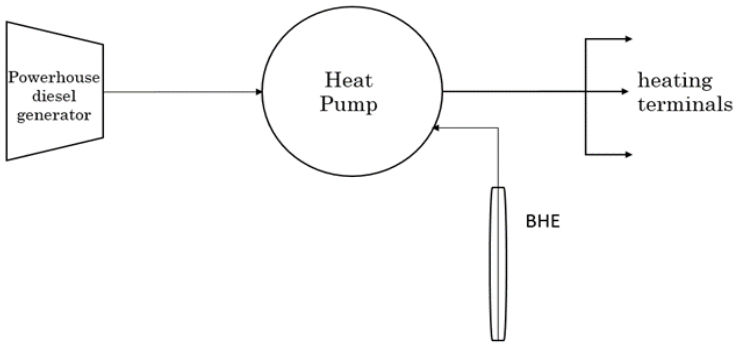

Fig. 31 GCEHP system scheme

The extremely harsh climate, a low thermal gradient (ΔT=+*20°C/Km*) and the presence of permafrost, are obstacles in meeting the entire heat demand, especially during the coldest months.

As suggested in the literature [29] at such high latitudes and so cold climates, integrating the geothermal plant with the existing one can be a good compromise, especially at an economic level (Fig. 32-Fig. 33). In fact, covering the entire need of the whole year can lead to an excessive exploitation of the heat present in the ground with consequent freezing of the plant and decrease of the *COP* and a freezing and swelling of the ground with potential harmful effects on the foundations of the houses surrounding the plant.

Moreover, integration would mean lowering the initial investment costs by avoiding the replacement of heating terminals and the decommissioning of old systems, and/or complex and costly renovation of homes, avoiding problems of temporary rental and alternative to be provided to residents.

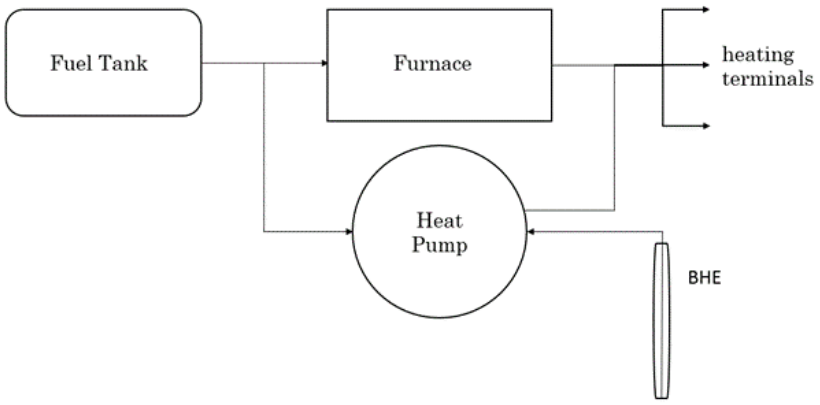

Fig. 32 Hybrid system scheme: GCAHP coupled with oil furnace.

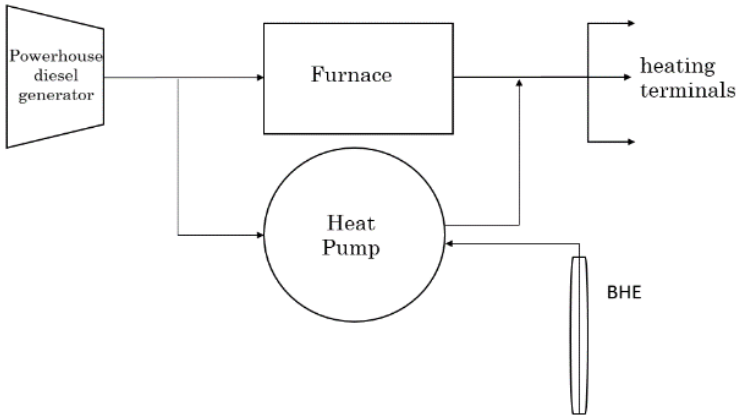

Fig. 33 Hybrid system scheme: GCEHP coupled with oil furnace

Of course, the precondition for these considerations would be the verification of the actual suitability and compatibility of the internal terminals in Kuujjuaq for the new type of installation. It should be noted that no information is available at this stage.

3 HEAT TRANSPORT MODELS

The heat exchange always takes place from the body at a higher temperature to the body at a lower temperature and is interrupted as soon as the balance is reached and can be done in three ways:

Conduction: it is the transfer of energy that occurs because of the interaction or rather collision of the molecules with the highest temperature to those with low temperature during their random motion [35].

It is never accompanied by movement of matter (apart from the movement of electrons in metals), so it is the method of heat transfer typical of solid bodies [29].

The process is described by Fourier's postulate:

$$Q_{xi} = -\lambda_{cond,xi} A \frac{\partial T}{\partial xi} \qquad (3.1)$$

Where the proportionality constant λ is a physical characteristic of the material called thermal conductivity $\lambda_{cond,xi}$ (W m^{-1} K^{-1}); Q_{x_i} (J s^{-1}) is the heat flow along the direction x_i; A (m^2) is the area affected by the flow; $\frac{\partial T}{\partial x_i}$ (K m^{-1}) is the temperature gradient.

Since the heat is transmitted as described above in the downward direction of temperatures and the thermal gradient becomes negative when the temperature decreases as the thickness increases *xi* is added the negative sign to make the thermal power positive in the direction of *xi*.

Convection or advection: is the mode of transfer of thermal energy that occurs whenever there is transmission of heat through macroscopic molecules of fluid. This means both the transmission between a solid surface and the liquid or adjacent gas moving at different temperatures and that between non-miscible fluids.

Heat transmitted by convection is directly proportional to the temperature difference as evidenced by Newton's law:

$$q = h\,(T_s - T_f) \qquad (3.2)$$

where T_s is the surface temperature, T_f the temperature of the fluid that laps it, q (W m^{-2}) the heat flow per unit area, h (W m^{-2} K^{-1}) is the convention coefficient. The latter is not a physical characteristic of materials but is determined experimentally whose value depends on several factors including the nature of the fluid, the flow rate, the coefficient of expansion of the fluid, the temperatures, the orientation and size of the exchange surfaces.

Dispersion: due to the heterogeneity that distinguishes any natural porous medium and linked to the presence of a flow of groundwater (non-uniform distribution of velocities within a flow channel, diversification of velocities from pore to pore, transversal speed components linked to the tortuosity of the routes). As in the case of the transport of the solute, also in this case the dispersion is given by the union between conduction and thermal kinematic dispersion. It is therefore more correct to use the term "hydrodynamic thermodispersion". The parallelism also applies to the equation that describes the phenomenon:

$$\boldsymbol{Qxi = -\lambda_{disp,xi}\, A \frac{\partial T}{\partial xi}} \qquad \textbf{(3.3)}$$

where $\lambda_{disp,xi}$ (W m^{-1} K^{-1}) is the thermal conductivity which is expressed as a function of dispersivity by the following relationship:

$$\boldsymbol{\lambda_{disp} = \rho_w\, c_w\, \alpha_{xi}\, v} \qquad \textbf{(3.4)}$$

with:

- ρw (kg m^{-3}) water density;
- cw (J kg^{-1} K^{-1}) specific heat of the water;
- α (m) thermal dispersity;
- v (m s^{-1}) effective velocity.

Irradiance: is the energy emitted by a substance in the form of electromagnetic waves because of changes in the electronic configurations of atoms or molecules. This phenomenon does not require the presence of an interposed medium and assumes a relative importance in our applications because it is predominant on large scales [36] [28].

3.1 The heat conservation equation

The phenomenon of heat transport presents itself as a combination of the processes described in the previous paragraph, which gives it a very complex behavior.

This phenomenon is described with the equation of energy conservation in the fluid and solid phase.

Below are the steps to obtain the transport equation that describes the behavior of heat in the aquifer from the above equation.

The energy conservation of a generic phase α is:

$$\frac{\partial}{\partial t}(\varepsilon_\alpha \rho_\alpha E^\alpha) + \frac{\partial}{\partial x}\left(\varepsilon_\alpha \rho_\alpha v_{i,\alpha} E^\alpha\right) + \frac{\partial}{\partial x}(j_{iT}^\alpha) = \varepsilon_\alpha \rho_\alpha Q_T^\alpha \qquad (3.5)$$

Where the energetic term dE^α, ignoring the effects of density variation and concentration, is proportional to the temperature difference:

$$dE^\alpha \approx c^\alpha \, dT^\alpha \qquad (3.6)$$

And the solid and liquid phases in balance:

$$T_\alpha = T_f = T_s = T \qquad (3.7)$$

The conservation equation can be rewritten as follows:

$$\frac{\partial}{\partial t}(\varepsilon_\alpha \rho_\alpha c_\alpha T^\alpha) + \frac{\partial}{\partial x}\left(\varepsilon_\alpha \rho_\alpha v_{i,\alpha} c_\alpha T^\alpha\right) + \frac{\partial}{\partial x}(j_{iT}^\alpha) = \varepsilon_\alpha \rho_\alpha Q_T^\alpha \qquad (3.8)$$

With:

- ε (-) effective porosity;
- QT (J m^{-3}) heat extracted/injected per unit volume;
- $jiT\alpha$ (W m^{-2}) the heat flux;

This last term represents the process of dispersion, and is described by Fourier's law:

$$j_{iT}^{\alpha} = - \lambda_{iT} \frac{\partial T_{\alpha}}{\partial x_j} \qquad (3.9)$$

with the coefficient of proportionality given by the sum of the term conductive and dispersive:

$$\lambda_{iT} = \left(\lambda_{iT}^{cond_{\alpha}} + \lambda_{iT}^{disp_{\alpha}} \right) \qquad (3.10)$$

For a saturated porous medium the term of conductivity becomes such:

$$\lambda_{ij} = \lambda_{ij}^{cond_s} + \lambda_{ij}^{disp_f} + \lambda_{ij}^{cond_f} \qquad (3.11)$$

with the term of dispersiveness of the solid phase absent since the speed is zero.

The individual terms are set out below:

$$\lambda_{ij}^{cond_s} = (1 - \varepsilon)\lambda^s \, \delta_{ij} \qquad (3.12)$$

$$\lambda_{ij}^{cond_f} = \varepsilon \lambda^f \, \delta_{ij} \qquad (3.13)$$

$$\lambda_{ij}^{disp_f} = \rho_f c_f \left[\alpha_T V_q \delta_{ij} + (\alpha_L - \alpha_T) \frac{q_i q_j}{V_q} \right] \qquad (3.14)$$

Con:

λ^s thermal conductivity of the solid phase (W m^{-1} K^{-1});

λ^f thermal conductivity of the fluid phase

δij Kronecker tensor,

αL and αT (m) longitudinal and transverse thermal dispersivity;

Vq (m s^{-1}) is the flow of Darcy;

$qi=\varepsilon \cdot vi$ (m s^{-1}) is the vector of the speed of Darcy [37].

Concluding the heat preservation equations for the solid and liquid phase are, respectively:

$$\frac{\partial}{\partial t}[(1-\varepsilon)\rho_s c_s T)] + \frac{\partial}{\partial x_j}\left(\lambda_{ij}^{cond_s}\frac{\partial T}{\partial x_j}\right) = (1-\varepsilon)\rho_s Q_T^s \qquad (3.15)$$

$$\frac{\partial}{\partial t}(\varepsilon\rho_f c_f T) + \frac{\partial}{\partial x_j}(\rho_f q_i^f c^f T) + \frac{\partial}{\partial x_j}\left[\left(\lambda_{ij}^{cond_f} + \lambda_{ij}^{disp_f}\right)\frac{\partial}{\partial x_j}\right] = \varepsilon\rho_f Q_T^f \qquad (3.16)$$

Putting together the three previous equations we obtain the equation of heat preservation in an aquifer:

$$\frac{\partial}{\partial t}\left[\left(\varepsilon\rho_f c_f + (1-\varepsilon)\rho_s c_s\right)T\right] + \frac{\partial}{\partial x_i}(\rho_a q_i^f c^f T) + \frac{\partial}{\partial x_i}\left[\left(\lambda_{ij}^{cond_s} + \lambda_{ij}^{cond_f} + \lambda_{ij}^{disp_f}\right)\frac{\partial T}{\partial x_j}\right] = Q_T \qquad (3.17)$$

The product between ρ and c represents the volumetric thermal capacity [36] [38] and in a porous medium is defined as the weighted average of the solid rock part and the fluid present in the pores:

$$\rho c = \varepsilon\rho_f c_f + (1-\varepsilon)\rho_s c_s \qquad (3.18)$$

Eq. 3.16 can be rewritten as follows:

$$\rho c\frac{\partial T}{\partial t} + \frac{\partial}{\partial x_i}(\rho_f q_i^f c^f T) + \frac{\partial}{\partial x_i}\left[\left(\lambda_{ij}^{cond_s} + \lambda_{ij}^{cond_f} + \lambda_{ij}^{disp_f}\right)\frac{\partial T}{\partial x_j}\right] = Q_T \qquad (3.19)$$

3.2 Soil Freezing

The lowering of the temperature inside the porous medium can lead to the phase change of the water present inside it, from the liquid phase to the solid phase (ice) and vice versa, substantially modifying its physical properties.

A porous medium is a solid material, such as soil, unconsolidated, fractured rocks, which has a porous volume within which it can contain a liquid or gaseous phase.

From a hydraulic point of view, the freezing of water causes a reduction of porous space available for the movement of groundwater, and therefore of the permeability and hydraulic conductivity.

The properties of water that change considerably are:

- *Volumetric heat capacity* ($Jm^{-3}K^{-1}$): represents the capacity of a medium to store heat or rather the amount of heat blocked in the medium of unit volume for each degree Kelvin of temperature;
- *Density* (kg m^{-3}): the ratio between the mass of a body and the volume it occupies;
- *Viscosity*: expresses the resistance opposed by a fluid to its flow and can be dynamic (Pa s) and kinematic (m2s-1);
- *Thermal conductivity* $\lambda cond$ (W m^{-1} K^{-1}): is a physical characteristic of the material and represents the capacity of a medium to transmit heat.

At the beginning of the phase change the movement of the water is greatly reduced due to the increase in viscosity which makes the convective contribution of the negligible underground flow negligible, especially in unconsolidated rocks rich in clays and in the grout of BHE where the permeability is very low. In these conditions, the transport of heat takes place mainly by conduction.

Typical density changes upon freezing are in the range of 5% to 10% but can be as high as 30% [39].

The dependence of these parameters on temperature variation is described through various semi-empirical relationships present in the literature.

Among the numerous relationships we report those used to modify the equation of heat transfer in porous media present inside the external plug-in used in the following phases of the following work.

The thermal conductivity is modified using the empirical approach of Alexiades and Solomon (1993):

$$\lambda_i = 2.240 + (5.975)(10^{-3})(-T)^{1.156} \qquad T < 0°C \qquad (3.20)$$

$$\lambda_w = (1.017)(10^{-1}) + (1.695)(10^{-3})(273.15 + T) \qquad T > 0°C \qquad (3.21)$$

where λ_i and λ_w are the thermal conductivities of ice and water ($Wm^{-1}K^{-1}$) and T is the temperature (°C).

The variation of the specific thermal capacity of water and ice as a function of temperature is calculated with the following relationships (modified after Alexiades and Solomon 1993):

$$c_i = 7.16(273.15 + T) + 138.0 \qquad T < 0°C \qquad (3.22)$$

$$c_w = 4186.8 \qquad T > 0°C \qquad (3.23)$$

where c_i and c_w indicate respectively the specific heat of the ice and water ($Jm^{-3}K^{-1}$).

Below are the graphs of the functions of conductivity and specific heat capacity just mentioned compared with other reports in the literature.

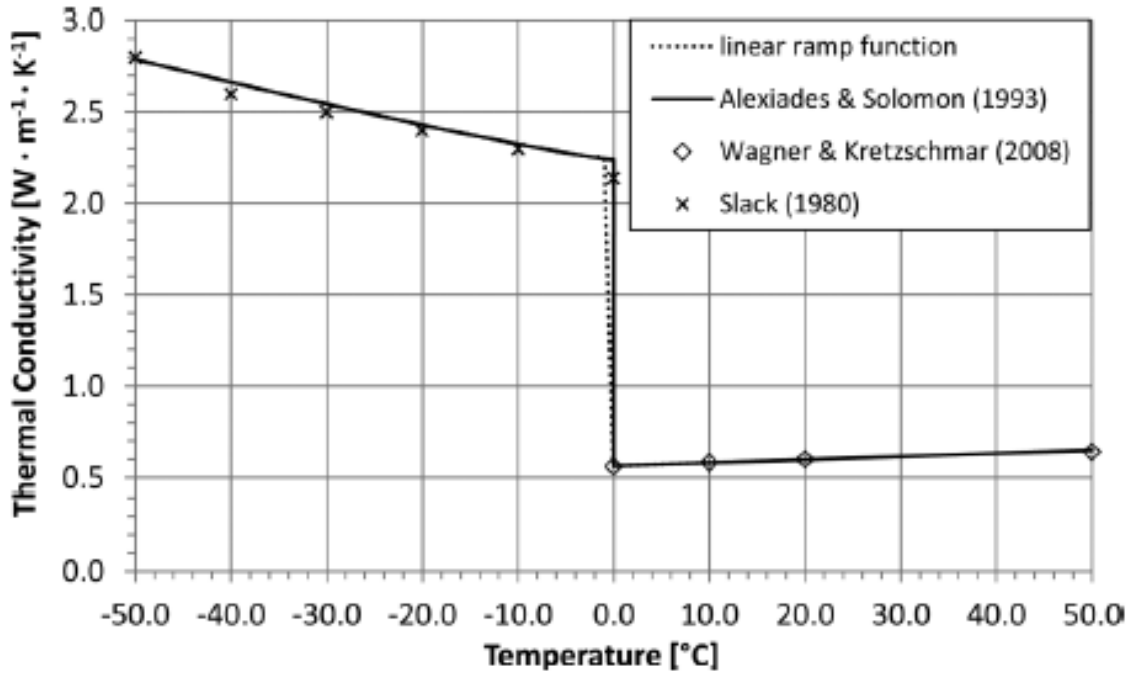

Fig. 34 Models for temperature- and phase-dependent heat conductivities of water and ice according to Alexiades and Solomon (1993), Wagner and Kretzschmar (2008), and Slack (1980); (source: Anbergen 2014, not modified).

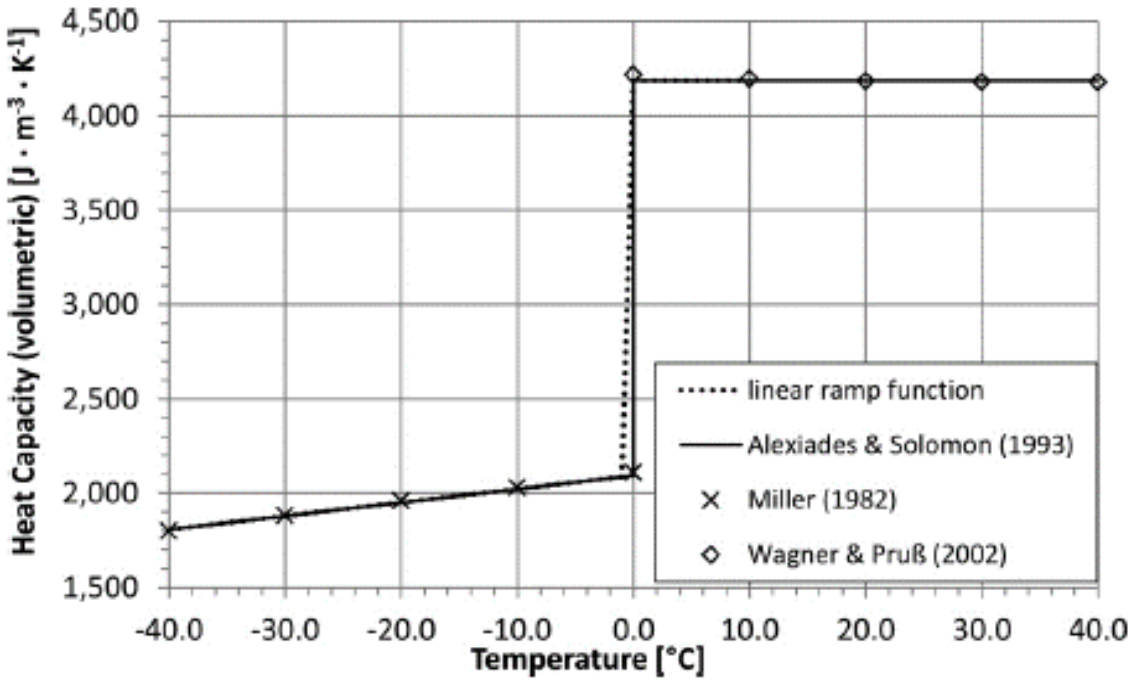

Fig. 35 Heat capacity of water and linear interpolation based on Alexiades and Solomon (1993), Wagner and Prus (2002), and Miller (1982); (source: Anbergen 2014, not modified).

As the temperature decreases, the conductivity increases while the thermal capacity decreases while as it increases it is the exact opposite with the only difference being the thermal capacity of the water, which assumes almost constant values for T>0°C.

The transformation process, depending on the temperature, is simplified in three phases: entirely fluid, transition state and entirely solid [40].

As can be seen in Fig. 34 and Fig. 35 for the transition area from solid to liquid and vice versa, there is a linear type of interpolation with freezing temperature set at 0°C.

Freezing occurs in a temperature range that depends on many factors such as the structure of the porous medium, pressure and chemical composition.

In this range, latent heat is released with a consequent increase in thermal capacity.

In order to take into account this heat and the variation that the heat capacity undergoes, a specific apparent heat capacity (c_{app}) is introduced:

$$c_{app} = \begin{cases} S_w \rho_w c_w & T \geq T_w \\ S_w \rho_w c_w + S_i \rho_i c_i - \rho_i (LF) \frac{\partial S_i}{\partial T} & T_w > T > T_i \\ S_i \rho_i c_i & T_i \geq T \end{cases} \quad (3.24)$$

where T_w (°C) and T_i (°C) are respectively the temperature at which the water is entirely liquid and solid, where LF (Jkg^{-1}) is the latent bonding energy, and e S_w and S_i respectively the saturation of the fluid and frozen water.

The new thermal capacity is replaced in equation (3.13):

$$\rho c = \varepsilon \rho_f c_{app} + (1-\varepsilon) \rho_s c_s \quad (3.25)$$

The phase variation, due to the new modified volumetric thermal capacity, and with the addition of thermal energy due to the latent heat is decelerated.

As far as saturation is concerned, a totally saturated porous medium is assumed in the absence of a gaseous phase:

$$S_w(T) + S_i(T) = 1 \quad (3.26)$$

With the variation of the two saturations in function of the temperature proportional to each other:

$$\frac{\partial S_w}{\partial T} = -\frac{\partial S_i}{\partial T} \quad (3.27)$$

With S_w, in the case of linear transition function between fluid and liquid will be expressed as follows:

$$S_w = \begin{cases} 1 & T \geq T_w \\ T + 1 & T_w > T > T_i \\ 0 & T_i \geq T \end{cases} \quad (3.28)$$

That in partial derivative with respect to the temperature will be:

$$\frac{\partial S_w}{\partial T} = \begin{cases} 0 & T \geq T_w \\ 1 & T_w > T > T_i \\ 0 & T_i \geq T \end{cases} \quad (3.29)$$

Alternatively, an exponential approach can be applied, depending on the function of Euler [41]:

$$S_w = \begin{cases} 1 & T \geq T_w \\ exp\left[-\left(\frac{T-T_w}{W}\right)\right] & T < T_w \end{cases} \qquad (3.30)$$

where W is a form factor that defines the slope of the function.

With the exponential approach in expressing the variation of saturation as it is possible to observe in Fig. 36 the freezing interval, which in the linear case was between 0°C and -1°C, is defined less clearly, with the advantage of continuous differentiability.

The slope of the relative saturation curve will change as a function of the freezing range considered, consequently the amount of latent heat released per kelvin will also change even if the total amount in the freezing range does not change. The smaller the field, the more concentrated is the release of latent heat and consequently the curvature of the graph within the transition field.

With the addition of this energy released in the range considered (0 ÷ -1°C) there will be an increase in thermal capacity with a strong impact with the result of a steeper transformation curve shown in Fig. 37.

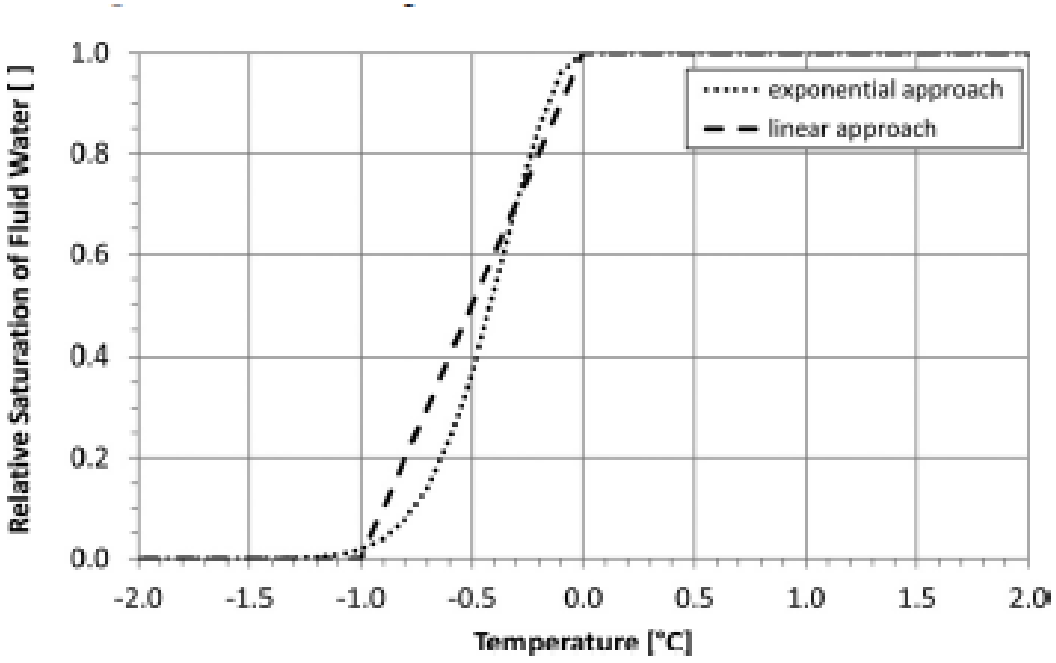

Fig. 36 Degree of saturation of fluid water in pore space. Linear freezing interval of 1 K; exponential form factor w = 0.5. (source: Anbergen 2014, not modified).

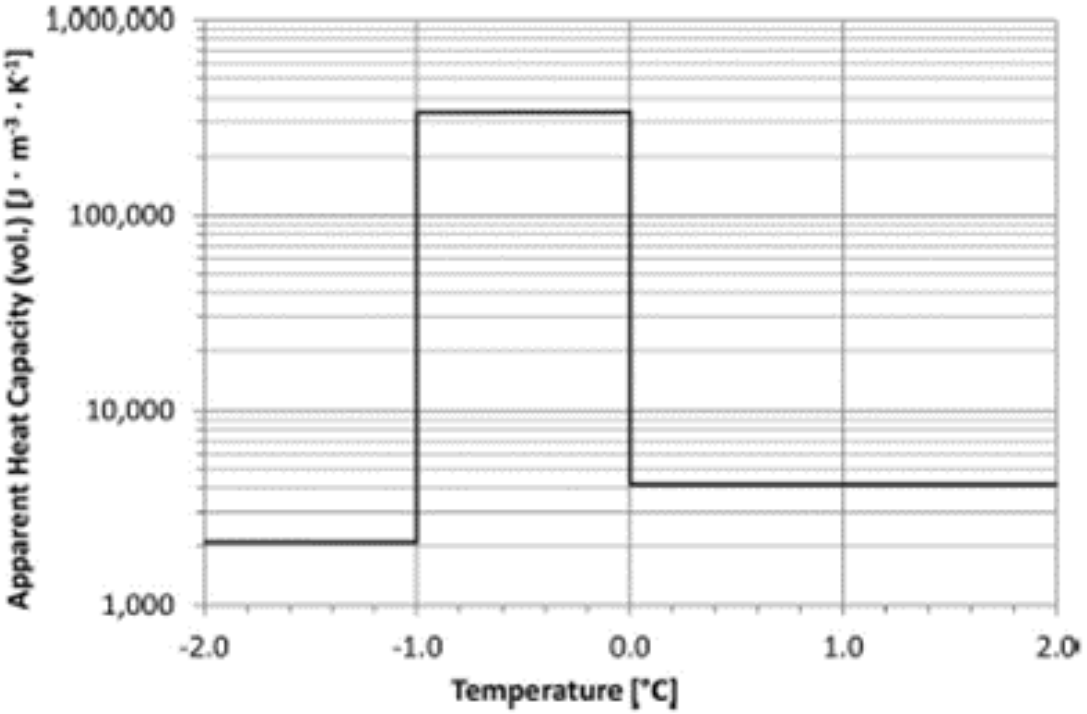

Fig. 37 Apparent heat capacity (linear approach; freezing interval 1 K) (source: Anbergen 2014, not modified).

3.3 Energy balance

This section analyses the thermal behaviour of the subsoil and the influence of the main energy supplies that exert on the geothermal probe inserted inside it. These can be summarized in the following (Fig. 34):

- Absorbed and net adsorbed solar radiation (W m^{-2})
- Geothermal flow

The geothermal heat flow that is dissipated from the earth to the outside is estimated to be on average equal to 0.03 (W m-2) value that has been calculated from the ratio of the amount of energy produced by processes within the Earth that, for the principle of energy conservation, is distributed on the outer surface and the total area. In Nunavik assumes a value around 40÷45 (mWm^{-2}).

Using the Fourier formula $Qxi = -\lambda_{cond,xi} A \frac{\partial T}{\partial x_i}$ (3.1*)*, considering a conductive transmission only (hypothesis valid for the Earth's crust) and knowing the value of the thermal conductivity of rocks (average 1 W m^{-1} K^{-1}) it is possible to calculate the geothermal gradient:

$$q = \frac{\lambda}{s}(T_1 - T_2) = \lambda \frac{(T_1 - T_2)}{\Delta z} \qquad (3.31)$$

The wall thickness of the earth is replaced by the difference in height Δz e T_1 e T_2 are two temperatures measured at different altitudes:

$$\nabla T = \frac{q}{\lambda} \qquad (3.32)$$

Calculating the overall energy balance by overlapping effects is very difficult due to the mutual influence of different factors.

Nevertheless, it is possible to obtain a temperature profile that will be nothing more than the result of all these factors.

In general, in the shallow portion of the earth's crust (<200-500m), the temperature is basically determined by the temperature of the atmosphere. At 10-30 m of depth, the difference in temperature between the atmospheric air on the surface and the subsoil increases with the increase in depth and is generally 1÷2 °C higher than the annual average of the air, a difference essentially due in the most

superficial part to the insulation due to the type of soil cover, evapotranspiration and in some cases from the snowpack.

As you go deeper you will feel the influence of the geothermal gradient, so it will tend to increase by about 3 degrees every 100 meters.

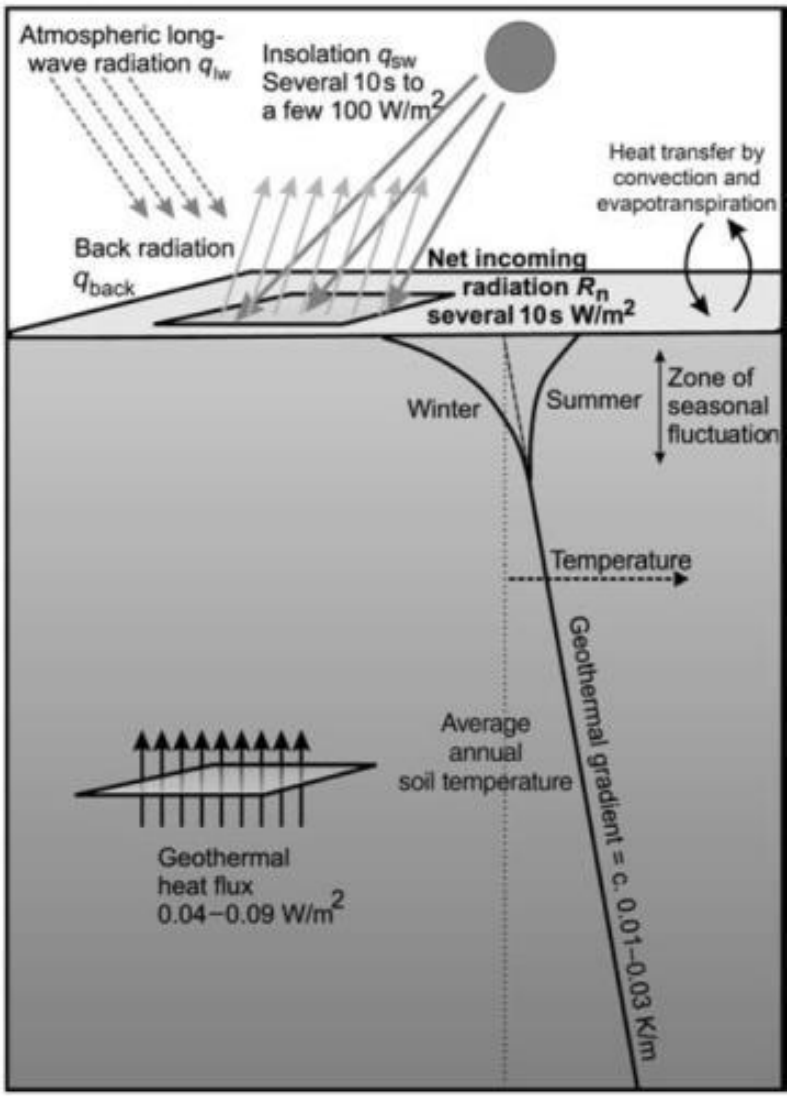

Fig. 38 Energy balance of the shallow ground (Banks 2012)

4 METHODS

Low-enthalpy geothermal plants, as already explained in Chapter 2, can be used almost everywhere, since they do not require high thermal anomalies and exploit the heat naturally present in the ground even at shallow depths.

However, it is always necessary to verify that a geothermal plant is feasible in technological and economic terms.

The study carried out takes into consideration these two aspects that are connected to each other.

The economic feasibility analysis starts from the evaluation in the study area of the geothermal potential, the capacity of a probe of defined length and diameter to exchange heat with the ground and satisfy a certain thermal load of a domestic/public building in the winter period, taking into account the geological and thermal characteristics of the subsoil with which it exchanges heat and the characteristics of the heat pump that operates this exchange.

The geothermal potential can be used as an economic and technical feasibility indicator for the installation of BHE in a given site as the number of probes, the total drilling depth to provide the required thermal load and consequently the payback time depend on it.

The economic feasibility analysis is then developed considering the types of heat pump (vapour compression or adsorption) to be coupled to the geothermal system GCHP and the total or partial replacement of the existing system.

For each of these scenarios, the savings of diesel and annual CO_2 emissions and the payback were calculated in function of the different *COP*s of the heat pump to which the system should be coupled.

Of these, the best one was chosen in economic terms and therefore defined the thermal load to which the probe is subjected and then passed to the verification of the efficiency of the thermal exchange of the probe.

For the technological analysis we used the numeric code FEFLOW® through which the exchange efficiency and the thermal response of the subsoil were verified.

The open software VersaGLD that allowed to calculate and set the physical characteristics of the heat carrier fluid circulating inside the BHE.

Below is a detailed description of the methods and software used.

4.1 G.POT method

To assess whether the area is suitable for the use and installation of geothermal probes, the method G.POT [42] developed within the Politecnico di Torino was used which numerically expresses the geothermal potential $\bar{Q}_{BHE}$ of a given region through an empirical relationship.

Geothermal potential can be defined as the average annual thermal load that can be exchanged sustainably with a Borehole Heat Exchanger of a length L and with certain soil conditions during the cooling or heating period.

Sustainable means the highest average thermal load value that can be extracted from the ground without excessive heating or cooling and freezing of the ground and the heat transfer fluid during the entire life cycle of the probe.

The geothermal potential can be calculated for both cooling and heating using the following empirical relationship:

$$\bar{Q}_{\mathrm{BHE}} = \frac{0.07\,(T_0 - T_{lim})\,\lambda\; L\; t_c'}{-0619\,t_c'\;\; log(u_s') + (0.532 t_c' - 0.962)\, log(u_c') - 0.455 t_c' - 1.619 + 4\pi\lambda\, R_b} \qquad (4.1)$$

The model depends on:

Ground parameters:

- λ Thermal conductivity [W/mK]
- ρc Thermal capacity [J/m^{3}K]
- T_0 Initial temperature [°C]

BHE parameters:

- r_b Borehole radius [m]
- r_p Pipe radius [m]
- n Number of pipes
- λ_{bf} Grout thermal conductivity [Wm^{-1}K^{-1}]
- R_b Borehole thermal resistance [mKW^{-1}]

Operational and design parameters of the plant:

- $q(t)$ Cyclic thermal load per unit length [Wm^{-1}]
- t_c Length of the heating/cooling season [s]
- t_s Operational lifetime of the plant [s]
- T_{lim} Minimum or maximum temperature heating or cooling mode [°C]

The following non-dimensional quantities:

- $t_c' = \frac{t_c}{t_y}$ ***(4.2)***
- $u_s' = \frac{r_b^2\, pc}{4\lambda t_s}$ ***(4.3)***
- $u_c' = \frac{r_b^2\, pc}{4\lambda t_c}$ ***(4.4)***

With

$$q(t) = \begin{cases} \boldsymbol{qmax\ sin\left(\frac{\pi t}{t_c}\right)} & \boldsymbol{for\ 0 \le t \le t_c} \\ \boldsymbol{0} & \boldsymbol{for\ t_c \le t \le t_y} \end{cases} \qquad \textbf{(4.5)}$$

The method is based on certain assumptions, such as:

- the ground thermal properties are homogeneously distributed
- thermal load of BHE annual cyclic with a semi-sinusoidal profile
- the BHE is modelled as a linear heat surce with infinite lenght, the heat flux is purely radial (Carslaw and Jaeger, 1959).
- The heat transfer between the BHE and fluid is governed by borehole resistence model of Claesson and Eskilson (1988).

The geothermal potential is an indicator of the technical feasibility of geothermal probes in certain areas,but can also can give preliminary indications about the economic feasibility, in fact a high geothermal potential allows to install shorter probes and thus reduce costs.

4.2 Calculating energy potential

In this paragraph the procedure for estimating the extractable geothermal potential with a standard depth probe (100-200-300 m) is explained, varying between three different drilling diameters (2.97, 3.77, 6 inches) applied only to the study area.

The calculation of this potential allows in fact to give a first estimate of the number of probes needed to meet the energy needs of a typical building for domestic use in the municipality of Kuujjuaq.

A total of 9 geothermal potential values have been calculated.

The input data are closely linked to the geological, stratigraphic and thermal characteristics of the site in question and to the specific choices regarding the *BHE* and the operation of the entire plant.

Ground parameters:

- λ *Thermal conductivity* [$Wm^{-1}K^{-1}$], ρc *Thermal capacity* [$Jm^{-3}K^{-1}$]: have been calculated as an equivalent value (λ_{eq}, ρc_{eq}) starting from of λ_{bulk} and ρc_{bulk}, provided by Giordano et Al 2017 [43], of the two geological formations by means of a weighted average with respect to the relative stratigraphic thicknesses.
- T_0 *Initial temperature* [°C]: the same values used in the mapping of the geothermal potential of Kuujjuaq with BHE length (100-200-300m) conducted by Della Valentina et al. 2018 [22] were used .

BHE parameters:

- R_b *Borehole thermal resistance* [mKW^{-1}]: were calculated using the VersaGLD software by editing the borehole radius r_b [m], the grout thermal conductivity λ_{bf}, the number, the configuration, the thickness and radius r_p of the pipes inside of the borehole.

Carrier fluid during temperature:

- T_{lim} *Minimum heating mode* [°C]: has been fixed at a value of -10°C, assuming to insert a quantity of antifreeze to allow the correct operation of the system even reaching this temperature.

Operational and design parameters of the plant:

- t_c *Lenght of the heating season* [s]: was set at 270 days or 9 months (September to May), ignoring the summer heat load.

The following are the input data:

Table 5 Input data for G.POT method

D 2.97 inch											
L	T_0	λ	ρc	r_b	R_b	T_{lim}	t_c	t_s	t'_c	u'_s	u'_c
m	°C	W/mK	MJ/m^{3}K	m	mK/W	°C	d	y	-	-	-
100	1	2.51	2.42	0.038	0.07	-10	270	50	0.740	2e^{-7}	1.3e^{-5}
200	1.75	2.67	2.42	0.038	0.07	-10	270	50	0.740	2e^{-7}	1.3e^{-5}
300	2.75	2.74	2.42	0.038	0.07	-10	270	50	0.740	2e^{-7}	1.3e^{-5}
D 3.77 inch											
L	T_0	λ	ρc	r_b	R_b	T_{lim}	t_c	t_s	t'_c	u'_s	u'_c
m	°C	W/mK	MJ/m^{3}K	m	mK/W	°C	d	y	-	-	-
100	1	2.51	2.42	0.048	0.1	-10	270	50	0.740	3.2e^{-7}	2.2e^{-5}
200	1.75	2.68	2.42	0.048	0.1	-10	270	50	0.740	3.2e^{-7}	2.2e^{-5}
300	2.75	2.74	2.42	0.048	0.1	-10	270	50	0.740	3.2e^{-7}	2.2e^{-5}
D 6 inch											
L	T_0	λ	ρc	r_b	R_b	T_{lim}	t_c	t_s	t'_c	u'_s	u'_c
m	°C	W/mK	MJ/m^{3}K	m	mK/W	°C	d	y	-	-	-
100	1	2.51	2.42	0.076	0.06	-10	270	50	0.740	8.3e^{-7}	5.6e^{-5}
200	1.75	2.68	2.42	0.076	0.06	-10	270	50	0.740	8.3e^{-7}	5.6e^{-5}
300	2.75	2.74	2.42	0.076	0.06	-10	270	50	0.740	8.3e^{-7}	5.6e^{-5}

Dividing the calculated thermal load of 33.58 MWh/y by the $\bar{Q}_{BHE}$ potential, the number of probes required to satisfy this thermal load was calculated as a first approximation:

$$n\,(L) = \frac{E}{\bar{Q}_{BHE}} \qquad \textbf{(4.6)}$$

4.3 Calculating effective n° of BHE coupled with a heat pump

As already explained in chapter 2, the heart of the system is the heat pump which, depending on the type, will have different *COP*s.

Starting from the *COP* value it is possible to calculate the maximum quantity of thermal power [kW] extracted from the ground through the following relation:

$$\boldsymbol{Gpeak = P\left(\frac{COP-1}{COP}\right)}\ [kW] \qquad \textbf{(4.7)}$$

Where G_{peak} is called "*Ground peak load"* and *P* "*Peak load"*.

Starting from the ground peak load and defining a plant operation currently as done in the G.POT method of 9 months or 2960h, the energy supplied during the year by the probe could be calculated:

$$\boldsymbol{E = \frac{Gpeak\ h}{1000}}\ [MWh/y] \qquad \textbf{(4.8)}$$

Once the energy *E* [MWh/y] supplied by the ground with a given *COP* has been calculated, the number of probes necessary to supply this energy can be calculated by fixing the 3 standard BHE lengths (100-200-300m). The drilling diameters are linked by the geothermal potential values previously calculated by this relationship:

$$\boldsymbol{n°eff(L,D) = \frac{E}{\overline{Q_{BHE}}}} \qquad \textbf{(4.9)}$$

L_{BHE}= 100-200-300m

$D_{drilling}$= 2.97-.3.77-6inch

the values obtained have been rounded up for precautionary reasons, in fact in the literature it is often advisable to design probes slightly longer than those actually needed [29].

4.3.1 Choice of heat pump

Given the energy context described in Chapter 2, with only two sources of power consisting of diesel and electricity, only two types of heat pumps coupled to geothermal probes were examined:

- absorption heat pumps;
- electrical compression heat pump.

Campaigns have been conducted by public utilities to discourage the use of electrical energy for heat production and, for this reason, the absorption heat pump with diesel fuel is preferable. The analyses performed in this thesis are aimed at verifying if this also applies to electrical heat pumps, compared to adsorption ones.

To date, however, as confirmed by the main manufacturers (Robur and Danstoker) who were contacted personally, there is no absorption heat pump on the market powered by diesel; the only existing types are powered by natural gas.

Therefore, we have worked according to the hypothesis of being able to use absorption heat pumps on the market but still feeding them with diesel, adapting them with any changes to the plant.

Finally, it has been assumed that, on average, the *GUE* value of gas-fuelled pumps is the same as that of diesel-fuelled pumps.

Given the uncertainty of a correct *GUE* value, in the calculation of the number of effective probes coupled with a heat pump, the variation of the number of standard length probes has been analysed, varying from a range of values which, for the absorption heat pump, is between 1.1÷2, given that on average it has a *GUE* of 1.5.

The electric heat pump coupled to *BHE* with an average *COP* value of around 4 [44] has been calculated the number of probes to vary a range of *COP* between 3.5÷4.6.

A low *COP/GUE* determines a low extraction of geothermal energy, and most of the heat supplied by the internal burner while a high *COP/GUE* determines a high extraction of heat from the ground and less thermal energy given by the burner of the refrigerant compression system.

Once the range of *COP* or *GUE* to be used has been defined, for the actual calculation of the number of probes (L_{BHE}, $D_{drilling}$), all that remains is to define the *Peak load* (*P*). For precautionary reasons, it was decided to use the peak load instead of the basic load, the definition of which derives from economic considerations and evaluations that are referred to in the next paragraph.

4.4 Economic feasibility assessment

This chapter assesses and calculates the annual operating costs, payback time and CO_2 emissions of a geothermal system coupled to a heat pump (absorption, electrical) compared with the existing system consisting of a diesel boiler.

In addition, for the new type of system, 2 different scenarios have been studied:

1. total replacement with a geothermal plant with vertical probes coupled to a heat pump (absorption and electrical);
2. partial replacement with coverage of the base load and domestic water and coverage of the peaks by the already existing diesel boilers.

For each of these two alternative scenarios to the existing system, the economic feasibility was assessed by calculating the number of probes needed to meet the energy needs, an estimate of the cost of the heat pump to be used, with its payback and the annual saving of tons of CO_2.

The annual heat requirement of a residence for domestic use in the municipality of Kuujjuaq, which is shown in Fig. 39, was calculated by the INRS [45] and has a value of 33.58 MWh/y, of which 1 MWh/y for domestic water.

During the winter months (Dec-Jan-Feb-Mar), as can be seen in Fig. 40, the figure exceeds 5MWh, where hourly load peaks (Fig. 41) of more than 25 kW are reached, with a maximum of 26.4 kW in March. In the summer months, the load does not exceed 2 MWh, while in the spring and autumn months, the values range from 2 to 4 MWh with a maximum hourly peak value in April of 15.7 kW.

In the study conducted to calculate the return time and the energy consumption to provide the annual thermal load, a 12-month system operation was considered.

Based on this requirement, the number of probes coupled to an absorption and electric heat pump was calculated.

The annual heating demand was ordered in descending order and, depending on the two case studies (total and partial replacement), the peak values P (kW) were defined (*Fig. 42*).

In the scenario of total replacement of the existing system with total coverage of demand, the maximum value of hourly demand P=26.4 kW was set as the peak load, while in the scenario of partial replacement 6 different undercurrents were studied in which a partial coverage of demand occurs up to peak loads equal to P =

10-11-12-13-15-17 kW, corresponding respectively to 32-37-41-46-57-70% (Table 6) of the total annual thermal load (Fig. 40).

As mentioned in chapter 2, thermal peaks in hybrid systems of this type are covered by the diesel boiler and depending on the percentage will be dominant called "dominant furnace" or not.

Table 6 Peak load related to the share of thermal load coverage with GCHP.

	Total	**Partial**					
***P* (kW)**	26.4	17	15	13	12	11	10
% of thermal load coverage	100%	70%	57%	46%	41%	37%	32%

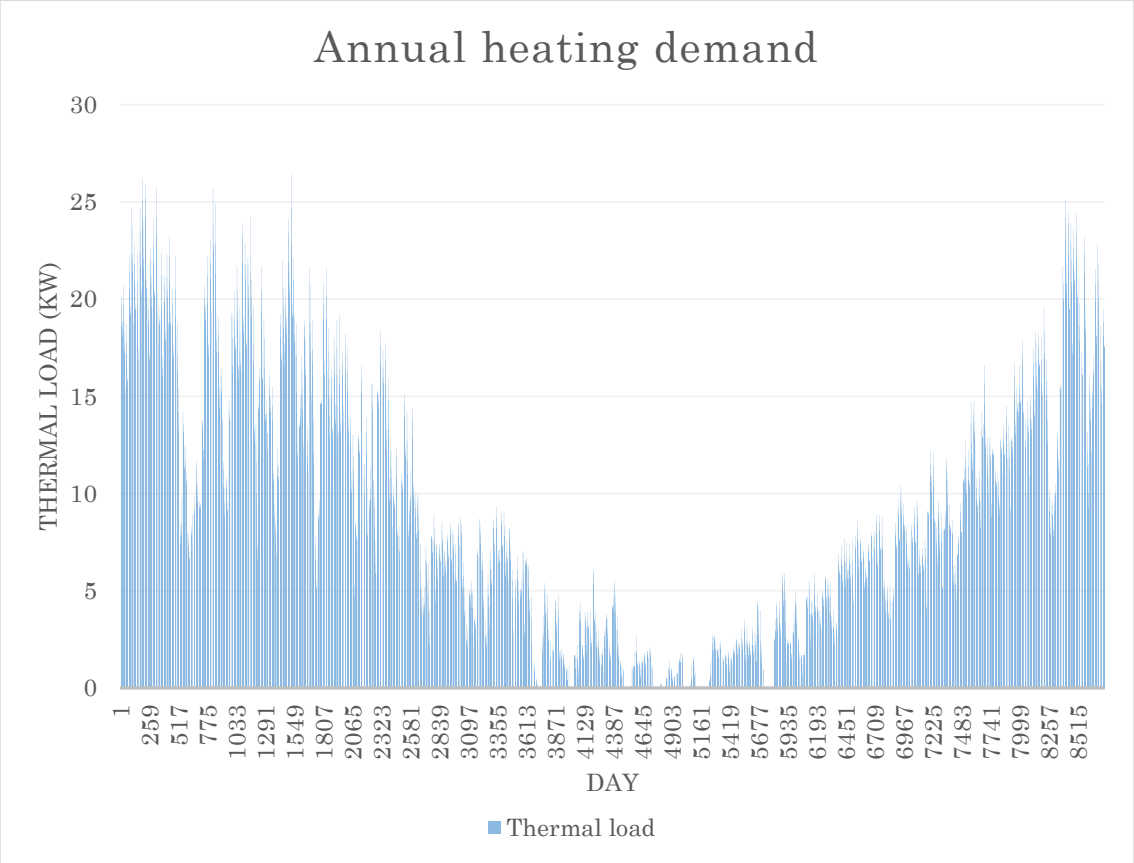

Fig. 39 Annual heating demand trend [kW] for a standard domestic housing in Kuujjuaq.

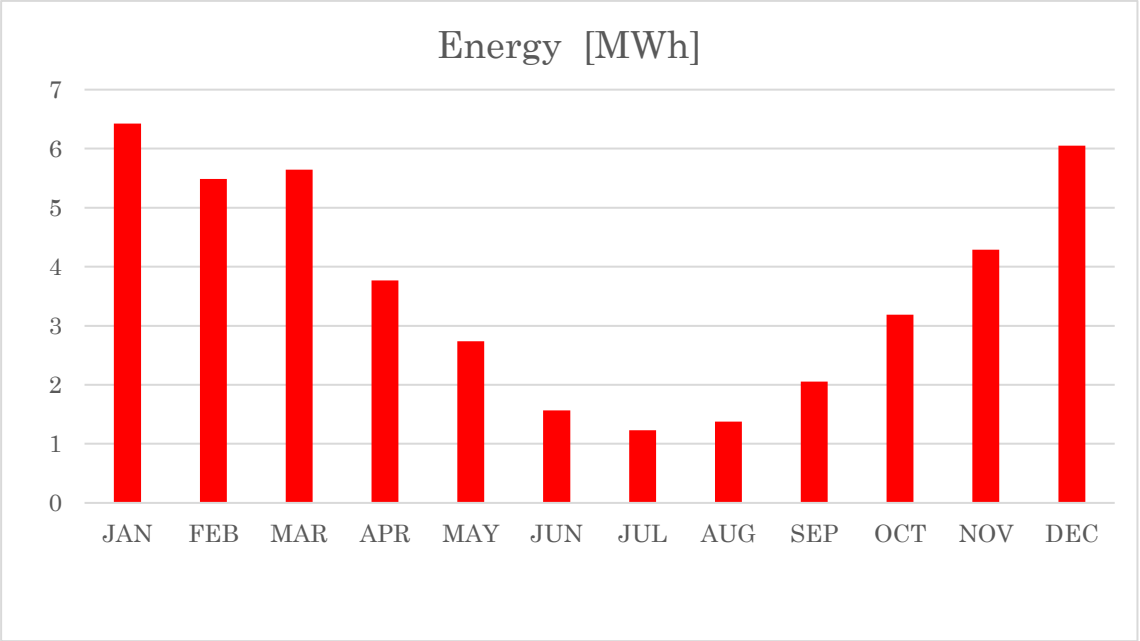

Fig. 40 Thermal demand [MWh] monthly for a standard domestic housing in Kuujjuaq.

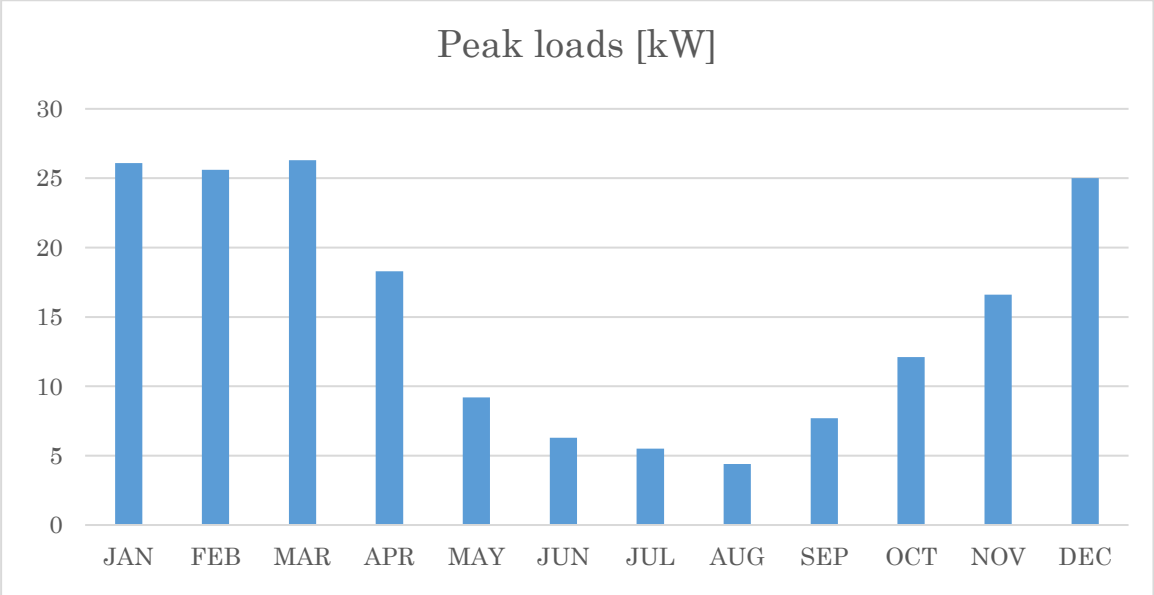

Fig. 41 Maximum thermal peak loads [kW] monthly for a standard domestic housing in Kuujjuaq.

The ascending order heating loads is show:

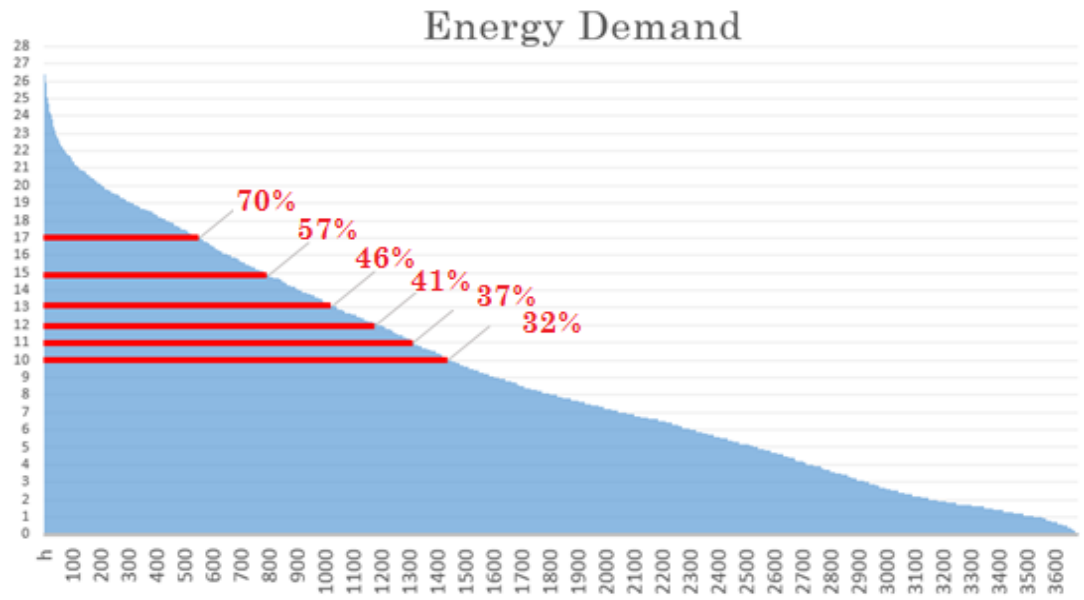

Fig. 42 Annual thermal load in discending order and coverage percentage of the different sub-scenarios of partial replacement of diesel furnace with GCHP.

4.5 Calculation of Pay Back Time

Payback time is defined as the period necessary to recover the investment cost. It is an important factor in the primary phase of a project, useful for deciding whether or not to undertake [46].

The payback time (*PBT)* for each scenario and for the *COP* ranges was calculated by dividing the *Initial investment cost* divided by the *Annual savings cost* compared to the existing system to be replaced:

$$\boldsymbol{PBT} = \frac{\boldsymbol{Initial\ investment}}{\boldsymbol{Annual\ saving}}\ [y] \qquad \boldsymbol{(4.10)}$$

The *Initial investment* cost has been calculated for all scenarios in which partial and total replacement is expected (*COP/GUE, $Dd_{rilling}$-L_{BHE}*), adding the *Drilling cost of BHE* and installation to the cost of purchasing the heat pump.

$$\boldsymbol{Initial\ investmet = Drilling\ cost\ of\ BHE + heat\ pump\ cost}\ \ [\$CAD] \qquad \boldsymbol{(4.11)}$$

To estimate the cost of drilling, INRS contacted two drilling companies near Kuujjuaq operating in the mining and industry: CanaDrill and Forages ROUILLIER. They have provided drilling estimates that have been increased by 50% to take into account the grout, pipes and installation. Each company has drilling rigs with different diameters.

Table 7 Drilling Companies cost per meter

	Forages ROULLIER		**Canadrill**
D	D2.97	D3.77	D6
$CAD/m	200	225	340

Fixed the cost per meter of drilling was multiplied by the number of probes needed for the standard length of reference thus obtaining the total price:

$$Drilling\ cost\ of\ BHE = n°\ BHE\ x\ L_{BHE}\ (100\text{-}200\text{-}300)\ x\ cost/m\ \ [\$CAD] \quad \textbf{(4.12)}$$

As far as the price of the Heat Pump is concerned, two world leaders in this field have been personally contacted: Robur and Danstoker.

These companies confirmed the absence on the market of a diesel-fired absorption heat pump but provided a rough estimate of about 15,000 $CAD including shipping for a type of gas-fired absorption heat pump GCAHP with a nominal capacity of 35 kW.

Assuming therefore to adapt such type of machine to the new supply, such price has been considered however valid and indicative of the order of magnitude of the cost of such machine and used for the calculation of the initial investment cost for all the scenarios.

For the electric heat pump GCEHP the price list of the manufacturer Rossato has been consulted, where it was found the price of about 25000 $CAD[47] with different nominal capacities for each scenario (Table 9).

Once initial investment costs had been obtained, it was decided to analyse some alternatives and technical solutions that would allow further reduction of costs

through the choice of the heat pump, linking the analysis made to the real availability on the market of the heat pumps and their technical characteristics.

Some choices have been made to reduce the initial investment cost of some of the multiple scenarios presented above, choosing for both the GCAHP and GCEHP systems the heat pumps that actually exist on the market.

For the GCAHP system it was decided to combine the system with a Ground Source Gas Fired Absorption Heat Pump by the manufacturer Robur[48], with a standard heat capacity of 35 kW and an average *GUE* of 1.25.

A higher heating capacity than the thermal powers under examination where in the extreme scenario of total replacement ninth we reach 27 kW. Given the absence of models with a lower nominal capacity and the limited choice, it was decided to use the same heat pump for several users, exploiting the potential it offers as much as possible, on the one hand, and to divide the costs for several users, on the other. On the basis of this hypothesis, the scenarios for covering the needs were chosen in such a way that they did not exceed or were not excessively inferior to the capacity of 35kW. It was therefore decided to divide the pump for 3 users in the case of an 11kW cover, reaching a thermal power of 33kW, and in the case of 17 kW to use the pump for 2 users with a total thermal power of 34 kW.

The other scenarios were excluded from this type of evaluation.

Table 8 Absorption heat pump features and cost for each energy scenario

Model Heat pump	**Energy scenario**	***P***	**10kW**	**11kW**	**12kW**	**13kW**	**15kW**	**17kW**	**26.4kW**
GAHP Line W LB Series Robur		**% of coverage**	32%	37%	41%	46%	57%	70%	100%
Ground Source Gas Fired Absorption Heat Pump COP = 1.25	**n°users x HP**		1	3	1	1	1	2	1
	Total Peak load		10kW	33kW	12kW	13kW	15kW	34kW	26.4kW
	Heat pump Capacity					35kW			
	$CAD/user		15000	5000	15000	15000	15000	7500	15000

For the electrical solution, hydro-geothermal inverter heat pumps have been chosen by the manufacturer Rossato Group [47], which supplies a range of models with different nominal capacities with COP = 4.3.

In the scenario with thermal load coverage with *P*=10kw peak, a heat pump with a capacity of 9.9 kW and a price of 18000$CAD was chosen.

For the energy scenario with *P*=13kW a 28.5 kW heat pump for two users with a total price of 15000$CAD was coupled, for the 17kW scenario a 38kW capacity pump for two users with 17000$CAD was coupled.

Finally, in the total replacement scenario with *P*=26.4kW a 53.5kW model was used, always dividing it for 2 houses with a cost of 20000$CAD.

Table 9 Electric heat pump features and cost for each energy scenario

Model Heat pump	**Energy scenario**	***P***	**10kW**	**11kW**	**12kW**	**13kW**	**15kW**	**17kW**	**26.4kW**
GAHP Line W LB Series Robur		**% of coverage**	32%	37%	41%	46%	57%	70%	100%
Ground Source Gas Fired Absorption Heat Pump COP = 4.3	**n°users x HP**		1	1	1	2	1	2	2
	Total Peak load		10kW	33kW	12kW	13kW	15kW	34kW	26.4kW
	Heat pump Capacity [kW]		9.9	14.2	14.2	28.5	19.1	38.2	53.5
	$CAD/user		18000	20000	20000	15000	25000	17000	20000

4.5.1 Computation of annual savings with GCAHP

The annual savings due to the replacement of the diesel plant and the new geothermal plant were calculated by the following difference:

$$\boldsymbol{Annual\ saving = cost/y\ fuel}_{\boldsymbol{furnace}} \boldsymbol{- cost/y\ fuel}_{\boldsymbol{geothermal\ plant}}\ [\$CAD/y] \qquad \boldsymbol{(4.13)}$$

The annual cost of both types of plant i has been calculated by multiplying the price of the fuel, fixed at 1.5$CAD/l [12] , by the annual quantity L_{fuel} of the latter consumed:

$$\boldsymbol{COST_{TOT} = \frac{L_{fuel}}{y}\ x\ 1.50\ \$CAD/l}\ \ [\$CAD] \qquad \boldsymbol{(4.14)}$$

the actual amount of diesel required was calculated dividing by the energy supplied by the fuel (E_{fuel}) by the calorific value *PCI*, which for fuel is equal to 10.72 kWh/l:

$$\frac{L_{fuel}}{y} = {E_{fuel}\,[kWh/y]}\Big/{PCI\,[kWh/y]} \quad [l/y] \qquad \textbf{(4.15)}$$

While $E_{eff,\,fuel}$ is the net energy supplied by the fuel during the combustion phase, net of the efficiency during the combustion phase, which according to the values provided in the literature [49] has been assumed to be equal to η=0.83:

$$E_{eff,\ fuel} = T_{fuel}\ \left[\frac{kW}{h}\right] x\,\eta \quad [kWh] \qquad \textbf{(4.16)}$$

Where T_{fuel} is the thermal load to be supplied by the diesel and changes according to the type of plant.

For the diesel plant this obviously corresponds to the *Annual thermal load* (33.58 MWh/y).

For a geothermal plant, this varies according to the base load to be covered with the geothermal probes and the *GUE* or *COP*.

1. In the case of total replacement, this will be given by the thermal load supplied by the diesel of the heat pump.
2. In the case of integration with a hybrid system this will be given by the sum of the amount of thermal load supplied by the diesel of the heat pump and that of the boiler.

In both cases the thermal load to be supplied given by the diesel will be given by the following report:

$$T_{fuel} = T_{fuel}(heat\ pump) + T_{fuel}\,(furnace) \quad [kWh] \qquad \textbf{(4.17)}$$

$$T_{fuel}(heat\ pump) = T_{heat\ pump} - G_{load}\ [kWh] \qquad \textbf{(4.18)}$$

with:

$T_{heat\ pump}$: the total thermal load provided by the heat pump;

G_{load}: the ground thermal load calculated as:

$$G_{load} = \frac{(COP-1)}{COP}\ x\ T_{BHE}\ [kWh] \qquad (4.19)$$

where T_{BHE} is the thermal load supplied by the probes.

4.5.2 Computation of annual saving with GCEHP

For the annual cost calculation of the GCEHP, the actual energy supplied by the diesel was calculated considering the quantity of diesel needed to produce the quantity of electrical energy that must feed the electric heat pump, neglecting losses, with the efficiency of the off-grid production plant in Kuujjuaq powered by diesel, equal to $\eta_E = 0.35$.

$$\boldsymbol{E_{eff,\ fuel}} = \boldsymbol{E_{eff,\ fuel}}\ off\text{-}grid\ plant + \boldsymbol{E_{eff,\ fuel}}\ \boldsymbol{furnace}\ [kWh] \qquad (4.20)$$

With:

$$\boldsymbol{E_{eff,\ fuel}}\ off\text{-}grid\ plant\ = \frac{\boldsymbol{E\ compressor}}{\boldsymbol{\eta E}}\ \ [kWh] \qquad (4.21)$$

$$\boldsymbol{E_{eff,\ fuel}}\ \boldsymbol{furnace}\ = \boldsymbol{T_{furnace}}\ \left[\frac{\boldsymbol{kW}}{\boldsymbol{h}}\right] / \boldsymbol{\eta}\ \ \ [kWh] \qquad (4.22)$$

With the thermal load given by the compressor ($E_{compressor}$) obtained by the difference between the thermal load of the heat pump and the ground thermal load G_{load}:

$$\boldsymbol{E_{compressor}} = \boldsymbol{T_{heat\ pump}} - \boldsymbol{G_{load}}\ \ [kWh] \qquad (4.23)$$

4.6 CO_2 emissions calculation

Finally, the amount of annual savings of CO_2 emitted by the new plants compared to the diesel plant was calculated:

$$CO_{2emission}\ saving = CO_{2\ emission}\ diesel\ plant - CO_{2emission}\ geothermal\ plant\ [t/y] \quad \textbf{(4.24)}$$

$$\boldsymbol{CO_2\ emission} = \frac{L_{fuel}}{y}\ \boldsymbol{x}\ \frac{2.68}{1000}\ [t/y] \quad \textbf{(4.25)}$$

with 2.68 representing the kilograms of CO_2 equivalent emitted for each litre of fuel [50].

4.7 Numerical simulations of the BHE's performance

The second part of the work focused on the study of the real feasibility of the system studied compatibly with the technologies and means available.

As already explained in chapter 2, the heat pump is influenced by the inlet and outlet temperature of the heat transfer fluid coming from BHE.

The selected heat pumps have an inlet limit temperature of approximately $EWT_{(GCAHP)}$ =-12°C and $EWT_{(GCEHP)}$=-5°C. Below this value, the efficiency of the system, that of the ground where the BHEs are installed could be lowered.

For coherence with the value used in the G.POT and for precautionary reasons, the EWT reference value for the absorption heat pump has been taken to be a value equal to -10°C.The presence of permafrost and a low thermal gradient are limits in this sense.

The FEFLOW® code was used to analyse the thermal response of the ground and simulate the temperature trend of the heat carrier fluid for 20 years.

The simulations took place in the case of integration of the existing plant with a GCHAP.

The scenarios chosen were those that meet the following criteria:

1. Scenarios in which it is possible to effectively couple the chosen heat pump with *GUE*=1.25 and a thermal operating capacity of 35kW;
2. Percentage value of coverage of the heat requirement with peak power *P(kW)* extracted from the ground equal to or submultiple and never higher than the heat capacity of the heat pump chosen (35kW);
3. Scenarios with the lowest possible *PBT*;

The only two scenarios that meet these criteria are the scenario with 32% and 70% coverage.

Both scenarios involve sharing the heat pump with 3 users in the first case and 2 in the second. Covering 32% of the thermal load means that the heat pump provides a thermal power up to a peak of 11kW which, when added to two other users, is 33kW very close to the 35kW of the heat pump capacity. In the second case, in which it is assumed to cover 70% of the demand up to powers of 17kW, adding this power to another utility will reach a value of 34kW.

For the sake of completeness of analysis, the first scenario was chosen with a 32% H requirement coverage to appreciate the temperature trend of the heat carrier fluid circulating inside the BHE as the diameter of the drilling ($D_{drilling}$) and the length (L_{BHE}) of the latter varied.

Once the scenarios to be simulated had been chosen, the results obtained were evaluated on the basis of two parameters:

- *Pf* (kW): heat output exchanged between heat carrier fluid and heat pump of the heat pump inlet and outlet temperature during the entire simulation time;
- *EWT* entering water temperature (°C).

The calculation of the temperature of the heat transfer fluid is the fundamental element that determines the performance of the heat pump.

In fact, the heat pump exchanges with the heat transfer fluid coming from the probe a thermal power Pf which, in the case of a good design of the probe, must be compatible with the thermal power required by the user (*P*).

In closed loop systems the thermal power is expressed by the following formula:

$$\boldsymbol{Pf = (\rho_c)_f\, Q_f\, \Delta t_f \quad [kW]} \qquad \textbf{(4.26)}$$

With *Qf* the circulation flow rate of the heat carrier fluid [m3/s], ρ_c its thermal mass [J/m3K] and finally $\Delta t = Tin - Tout$ the temperature difference of the fluid between the return and the delivery temperature to the geo-exchange circuit.

As already explained in chapter 4, since no sizing was done, this formula was used to verify the results obtained, verifying that the power exchanged during the months of operation over a period of 20 years, maintained values similar to the Ground peak load.

The *EWT* (°C) represents the heat pump inlet temperature which, based on the efficiency of the heat pump *GUE*=1.25 and the characteristics of the heat transfer fluid defined in paragraph 4.9.2 and Table 17, has been set at an *EWT* limit value of -10°C. Higher values could lead to a lowering of the *GUE* and therefore compromise the efficiency of the entire system. This value has been chosen according to the minimum Ambient operating temperature (-12°C) given in the technical data sheet of the Robur absorption heat pump.

Therefore, the conditions of verification are:

1. $Pf \sim P$
2. $EWT \leq -10°C$

FEFLOW® is a finite element calculation code through which it is possible to model underground heat and hydraulic processes.

Through this numerical code a basic model of the study area has been created for the numerical simulations of geothermal probes in function of 9 different scenarios $f(D_{drilling}, L_{BHE})$.

In par 4.7.1 the phases for the model elaboration are described: mesh construction, initial conditions, boundary conditions, thermal and hydrogeological properties of the materials and the "problem settings" in FEFLOW®.

4.7.1 Set-up

A rectangular area has been identified in the municipality of Kuujjuaq. The domain has dimensions of *190 x190m*. The well has been positioned inside a private internal area with respect to the main streets shared with the other houses. With respect to the quadrangular area, it was positioned centrally with coordinates (*x=535371,232, y=6440504,087, Coordinate system and projection NAD83 / UTM 19N*) and at *95 m* from the edges, considered adequate to consider the effects of the latter negligible.

Fig. 43 Limits of the model and position of the BHE

From an operational point of view the creation of the mesh is done through the algorithm "triangle" (the domain is divided into triangles) and going to edit appropriate parameters for the generation of the mesh. In this and the following step, attention is paid to the definition of an adequate positioning of the nodes around the BHE.

For a good mesh quality to facilitate convergence, the latter in numerical modelling is reduced to an internal SPC (singular point condition) well occupied by a single node in the case of a horizontal view of a mesh of a 3D finite element model.

The need to precisely edit the first nodes around the well arises from the following considerations:

simulation with heat exchangers is similar to simulations of the flow rate of a pumping well where the node represents the well from which a flow rate Q is pumped. During the pumping phase often the water table of the well does not

represent exactly the physical radius of perforation r_b but it will have a different radius called "virtual" which is often greater than the latter (Fig. 44).

It has been shown that this difference in the simulations depends on the discretization of the mesh on the nodal distance Δ around the node.

In order to make these rays correspond, it is necessary to find an ideal nodal distance.

The formula by which this distance has been calculated is as follows:

$$\Delta = e^{\alpha} r_{virtual}\ [m] \qquad \textbf{(4.27)}$$

$$\alpha = \frac{2\pi}{n \tan\frac{\pi}{n}} \qquad \textbf{(4.28)}$$

where n represents the number of nodes you want to insert, which in the case of triangular meshes is equal to $n=6$. In this way $r_b = r_{virtual}$ [51].

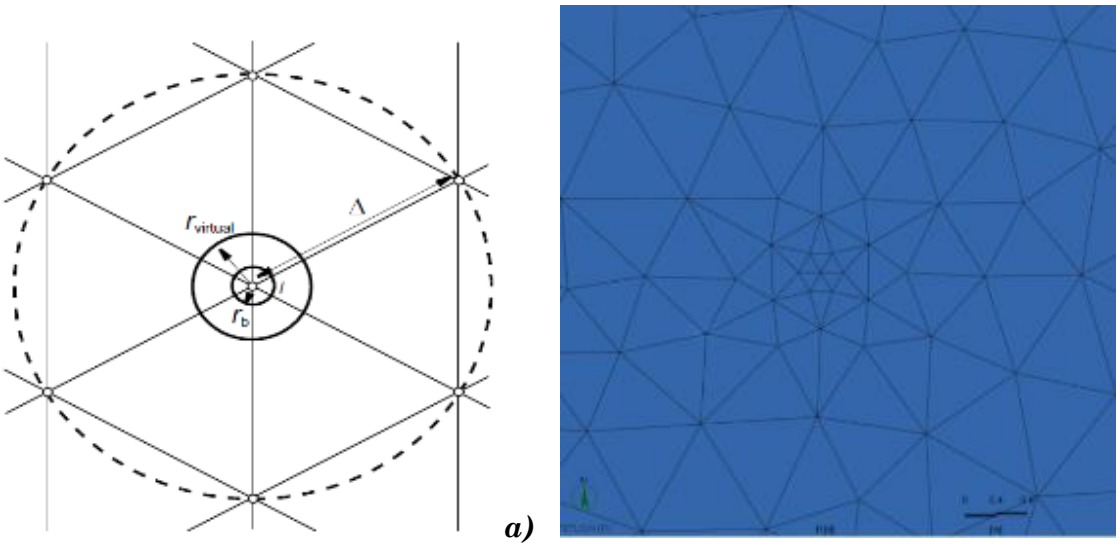

a) ***b)***

Fig. 44 a)Spatial discretization (n=6) around a BHE "well" node. b)Spatial discretization in the model around the BHE.

The next step is represented by the "refinement" of the mesh, which consists in concentrating the presence of nodes in the areas of greatest interest in order to make the processing more precise and less dense. Through the appropriate commands, the presence near the well has been intensified.

Through the "smoothing" operation FEFLOW® allows to adjust the triangles to make them as equilateral as possible and to obtain the right conditions.

An indicator of mesh quality is Delaunay's criterion.

The Delaunay's criterion in the case of 2-D triangulations, this is often called the "empty circumcircle criterion". This criterion is verified when the circumference associated with each triangle has no vertices within it. In this way, the angles will be close to 60°, which is the ideal condition.

The figure Fig. 45 shows the case in which the criterion is satisfied (left) and in which it is violated (right) [52].

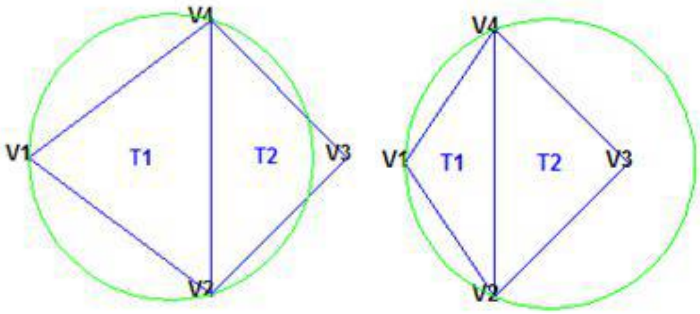

Fig. 45 Triangles that satisfy the Delaunay criterion (left)and triangles that violate it (righ); (source: www.mathworks.com/help/matlab/math/delaunay-triangulation.html).

Of course, this criterion is also valid for the 3D model where the triangles are replaced by a tetrahedron and the associated circumference by a sphere.

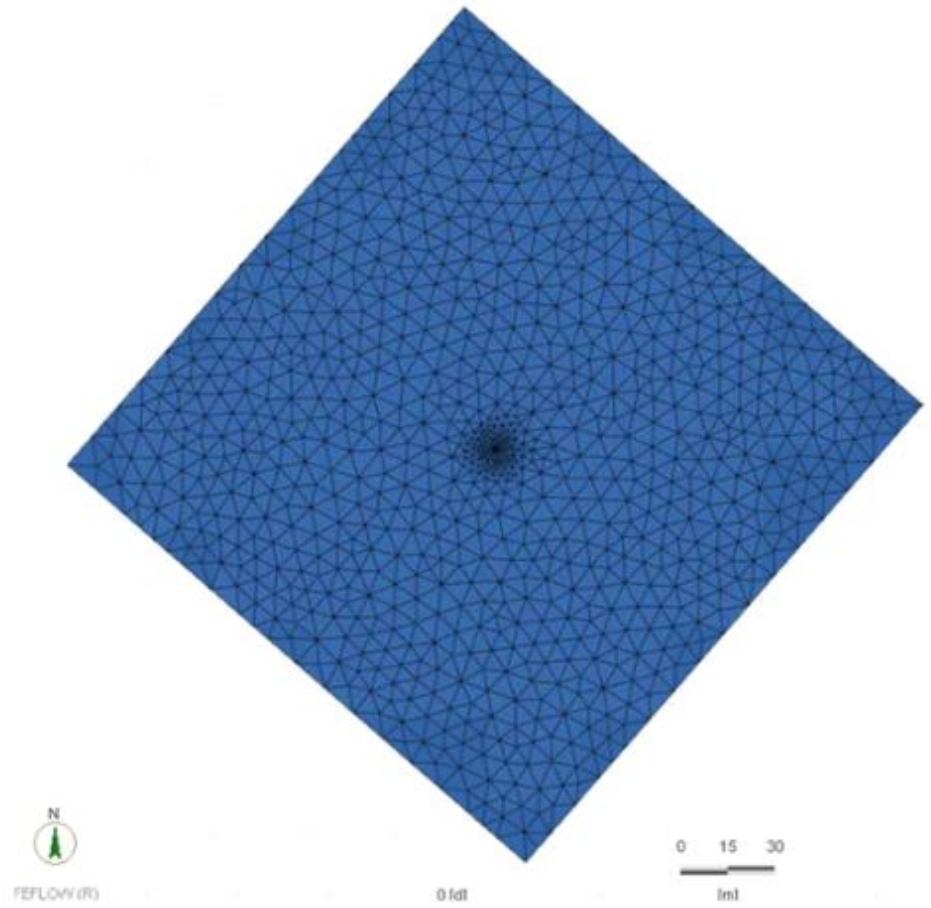

Fig. 46 Final mesh refinement of the elements around the BHE.

The 3D model was then developed. Since this is a simplified model and given the flat topography of the area under examination, a flat surface has been defined. We added the number of slices with which to divide the domain, taking care to report the exact thicknesses of the various layers. Assuming as zero altitude the "elevation" of the downstream edge that represents the country floor, the slices were inserted with increasing intervals as the depth increased until they reached an *depth* of -350m.

The model represents a volume of subsoil with unconfined aquifer and piezometric gradient with a value of *0m* consistent with the situation found site. The depth of the groundwater table is less than *50 cm* at the chosen site, so it was assumed to coincide with the ground level for simplification.

The model is divided into two layer (

Table 10): a layer of satured alluvial deposits and a layer of bedrock consisting of diorites. The first layer in turn is divided by 6 *slices* equidistant from each other

by 5m, except for *slice* n°2, which is distant from the surface of 1m. This choice derives from the need to avoid the interference in the simulation phase between the boundary conditions of the nodes of the first slice with the node of the BHE.

The diorite layer has been divided into 29 *layers* with a gradual decrease thickness as the depth increased. Care was taken to maintain a dense mesh in the thickness affected by the probe in order to obtain a more precise study in those layers.

Table 10 Stratigraphy of the model

Depth	**Geological formation**
m	-
0-25	Alluvial sediment and glacial till
25-350	diorite

The flow of the aquifer, being a simplified system and given the existing piezometric condition, is equal to 0 and has been reproduced through a boundary condition of the 1st type (Dirichlet BC) assigning a hydraulic load to the north-west and south-east faces of the domain equal to the share of the entire volume.

As already explained to avoid weighing down the model and given the very low subjection of the aquifer we preferred to consider the volume totally saturated.

In the same way the thermal flow has been reproduced as a boundary condition of 2th type by assigning to the lower face of the volume a heat flux equal to *-0.045 W/m^2* (Fig. 49), with a negative sign since in FEFLOW®, except for BHE an incoming flow has a negative sign, while the outgoing flow has a positive sign (Fig. 47).

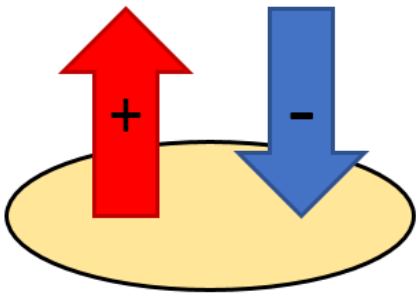

Fig. 47 Algebric sign for boundary conditions in FEFLOW.

The thermal profile of the entire volume, as shown in Table 11, was reproduced by manually assigning the temperature in slice (1th type boundary condition). This profile was defined starting from the measurement of the temperatures carried out in a well near the study area during the studies conducted by the INRS[53].

Going down in depth in the first few meters below the surface reaches a peak of minimum 0 ° C and then grow back to the values present on the surface, from -25m on, the geothermal gradient is about +20 ° C/km.

Table 11 Temperature profile assigned in the model

Depth	**Temperature**	**Depth**	**Temperature**
m	°C	m	°C
0	0,9	80	1.4
10	0,03	90	1.9
20	0	115	2.3
25	0,03	160	3.2
30	0,5	190	3.8
40	0,8	220	4.4
50	0,9	250	5
60	1	300	6
70	1,2	350	7

The heat exchange with the outside air has been reported by assigning to the top slice a boundary condition of the 1st type, with variable temperature value (Fig. 48) for each month of the year through the definition of a timeseries.

As far as the values are concerned, we relied on the measurement of the daily temperature, which was carried out by the INRS at a depth of 1m below ground level for an entire calendar year between 2017-2018 in Kuujjuaq.

Starting from the daily data, the monthly average temperatures were calculated using the Excel spreadsheet and then the timeseries of 12 monthly average temperatures values (Table 12) for an entire year were edited.

Table 12 Timeseries superficial temperature

Timeseries	
day	**temperature**
0	0.75
30	0.75
60	0.26
90	0.16
120	0.26
150	0.27
180	0.71
210	7.58
240	10.26
270	8.65
300	4.47
330	1.92
360	0.96
365	0.75

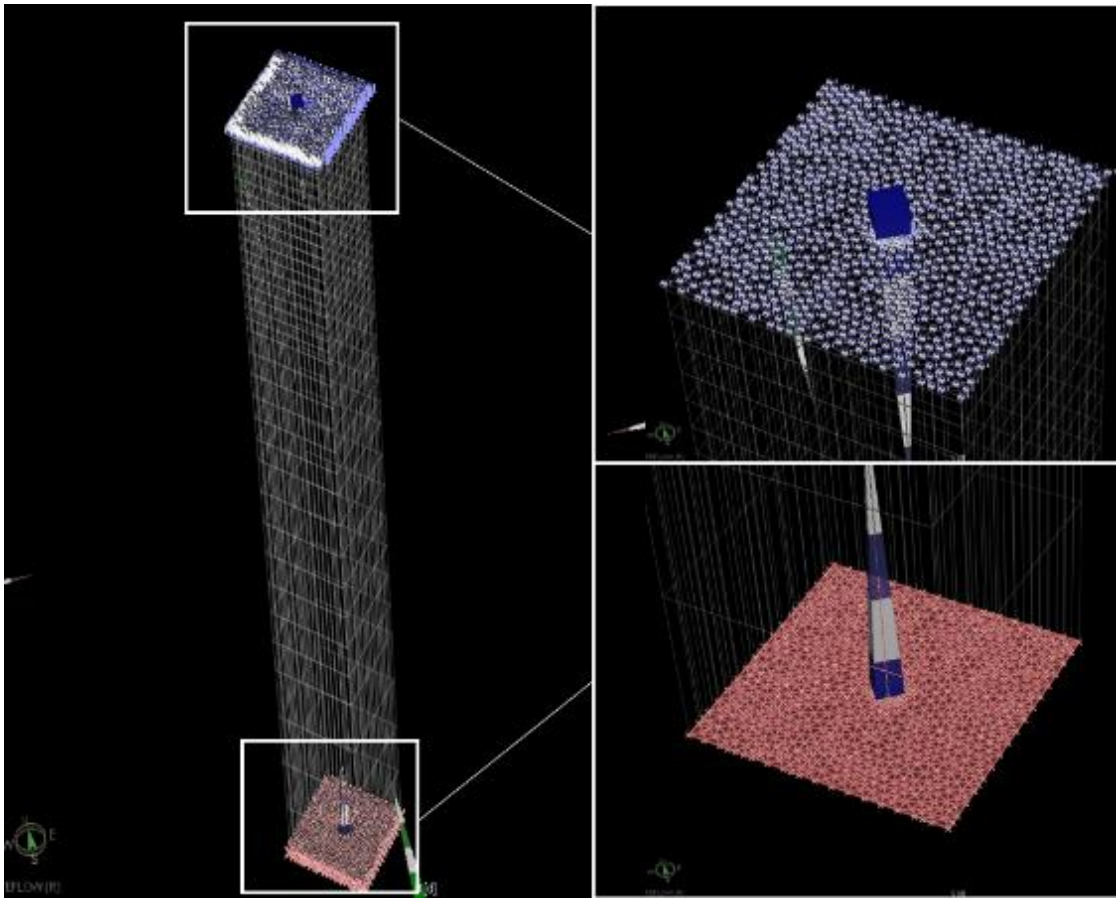

Fig. 48 Boundary condition: temperature at the top (blu) and heat flux at the bottom (red).

The initial condition for the water flow is the distribution of the hydraulic load. This distribution must be consistent with the associated boundary conditions. Therefore, a hydraulic load equal to the height of the entire volume (350m) has been defined (Fig. 49a).

The initial temperature condition, on the other hand, was achieved through a simplified procedure, starting a simulation under stationary flow conditions: through the flow, the distribution of the temperature profile is linearly interpolated over the entire volume (Fig. 49b).

a) 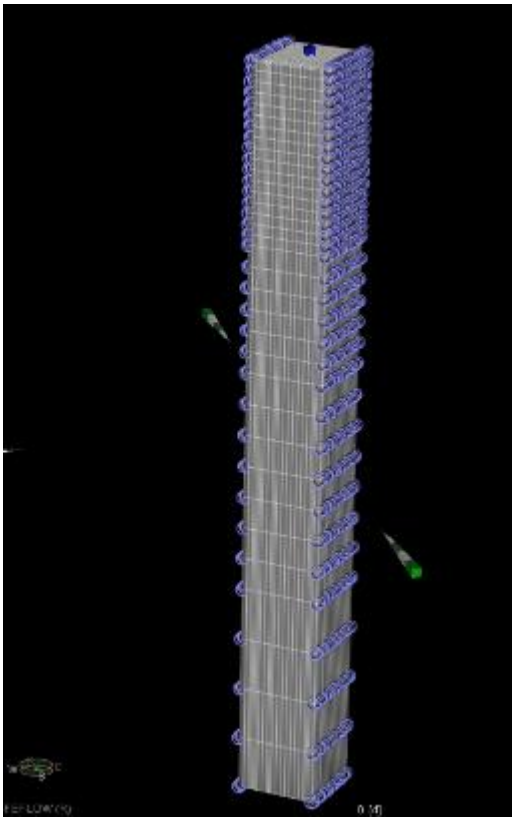 b) 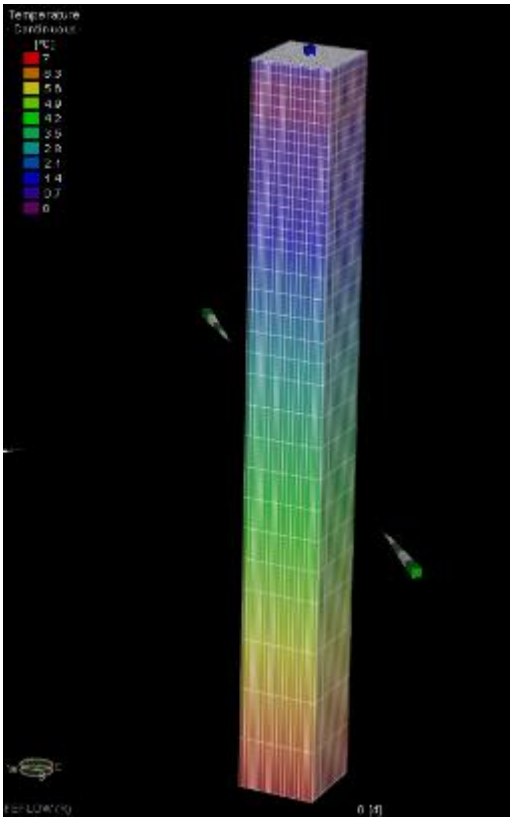

Fig. 49 a) Initial condition flow of water. b) Initial condition temperature.

Following an appropriate analysis for the purposes of this thesis work, only certain properties have been changed to assign the real values of the site, while others have been left fixed equal to the default value of FEFLOW®.

Below are the parameters:

- *Hydraulic conductivity*:
  alluvial sediments Kxx, Kyy =1x10e^{-5} m/s; Kzz=1x10e^{-6} m/s;
  diorite Kxx, Kyy = 1x10e^{-10} m/s; Kzz=01x10e^{-11} m/s.
  Kzz values were assumed based on anisotropy ratio.

- *Porosity*: Indicates the ratio between the volume of water released from an aquifer saturated sample by gravitational drainage alone and the total volume of the sample, values measured by the INRS were used.
  alluvial sediments ε =0.35;
  diorite ε =0.05.

- Thermal conductivity fluid, solid:
  alluvial sediments λfluid=0.58 W/mK; λsolid=2.5 W/mK;
  diorite λfluid=0.58 W/mK; λsolid=3 W/mK.

- Volumetric thermal capacity fluid, solid:
  alluvial sediments ρfluid=4.2 MJ/m3K; ρsolid= 2.4 MJ/m3K;
  diorite ρfluid=4.2 MJ/m3K; ρsolid= 2.3 MJ/m3K.

The implementation of the wells and their properties (position, flow rate, depth to top, depth to bottom and the id relative to the thermal load – shown in Table 13) is carried out by creating an excel sheet in which the characteristics are indicated. After having connected the parameters with the "Multilayer well", the excel sheet loaded is assigned to the domain and the wells model is obtained (Fig. 50).

Table 13 BHE parameters

	X	Y	Z	Flow Rate	Depth to top	Depth to bottom
L100	535371.232	6440504.087	350	1.6	1	100
L200	535371.232	6440504.087	350	1.6	1	200
L300	535371.232	6440504.087	350	1.6	1	300

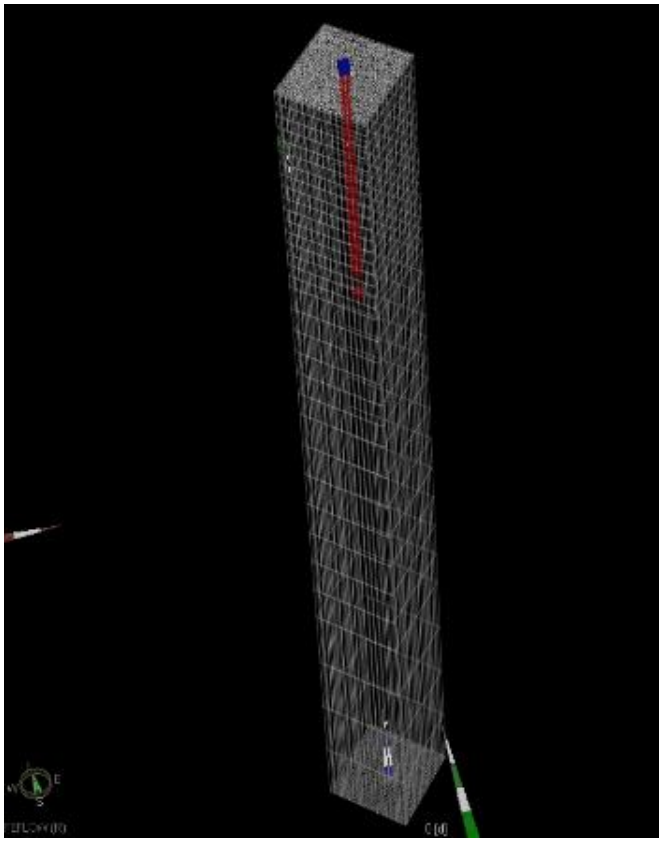

Fig. 50 Multi-layer well

Definition of the *Timeseries*: the thermal load was set according to the peak thermal load obtained during the preliminary calculation phases following the G.POT.

A heat extraction was assumed for 9 months (from September to May) with a constant thermal load value corresponding to the ground peak load (2.2kW in the case of the scenario with 11kW and 3.5kW (Fig. 51) in the case of 17 kW (Fig. 52)).

The G_{peak} values has been divided by the number of BHE required (paragraph 4.3). In both scenarios, if only on BHE is needed, the G_{peak} values remained unchanged.

The choice of distribution over 275 days is since the system operates only in heating mode, therefore in the remaining 90 days the load is zero.

The use of constant values with monthly variation of the thermal load and of a peak value derives on the one hand from the desire to analyse the thermal response of the soil and the temperature of the heat transfer fluid over time in the most severe conditions possible, and on the other hand not to further weigh down the model and speed up its simulation times.

The distribution has been implemented as a "time series" in the simulation with cyclical evolution because it has a total duration of 20 years.

The values of the thermal load, following Algebric sign in FEFLOW® relative to BHE, being an extracted heat flow coming out of the volume, have been inserted with negative values.

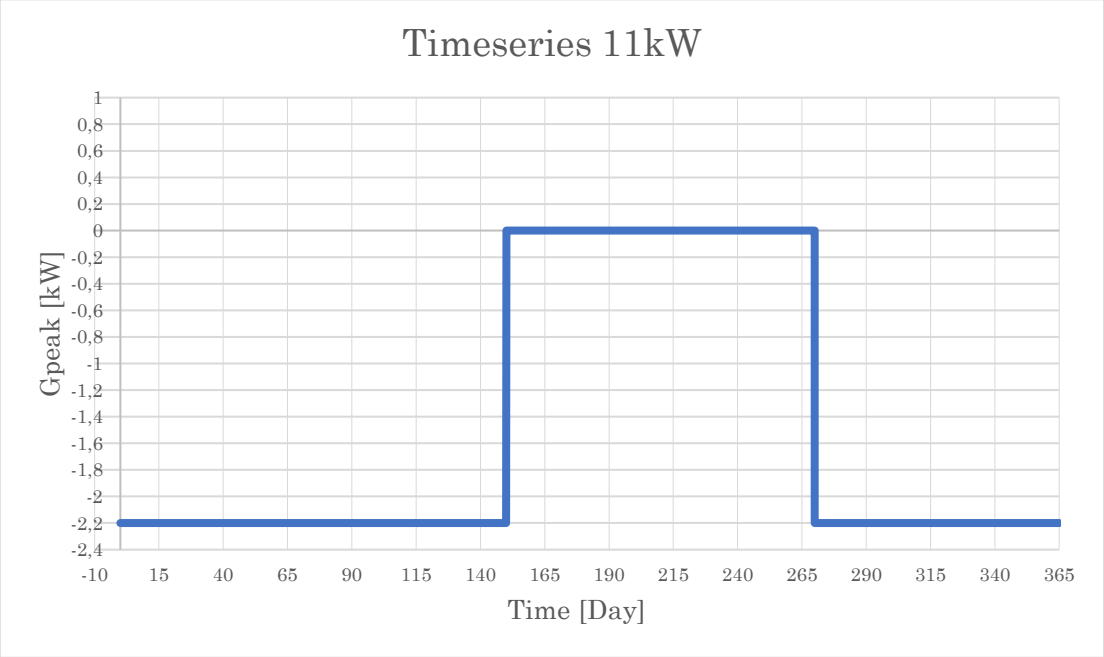

Fig. 51 Time series G_{peak}=2KW

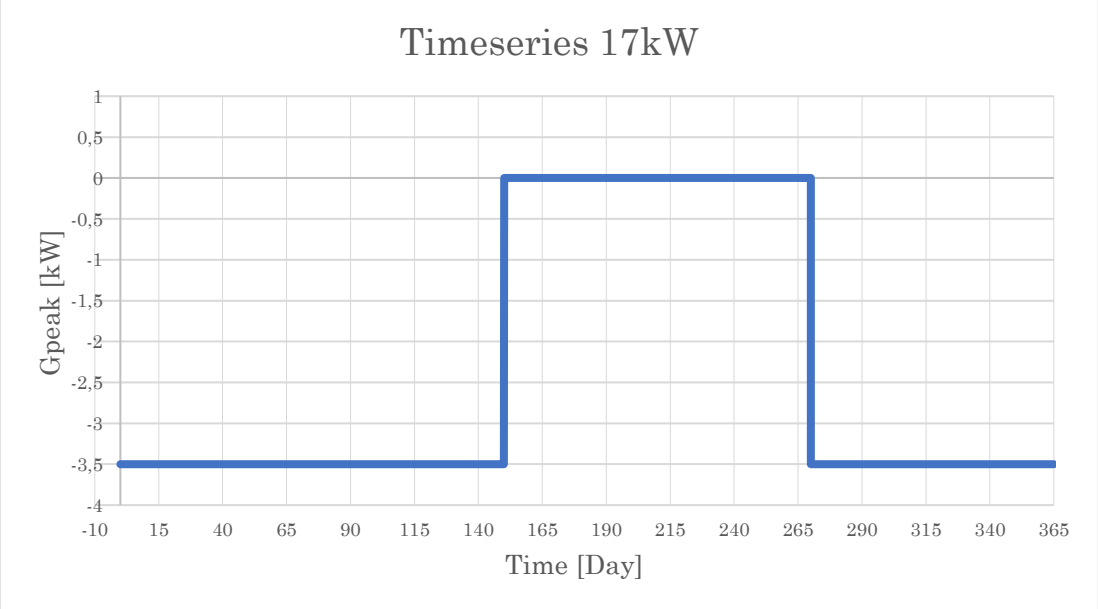

Fig. 52 Time series G_{peak} =3.5kW

To record and display the thermal response of the soil in the post-simulation phase, observation points were manually placed near the BHE at the following distances: 0.3 - 1.1 - 2.1 - 3.4 - 5.5 - 8.9 m (Fig. 53) placed at the following depths: 1 - 40 - 65 - 100 - 150 - 200 - 300m.

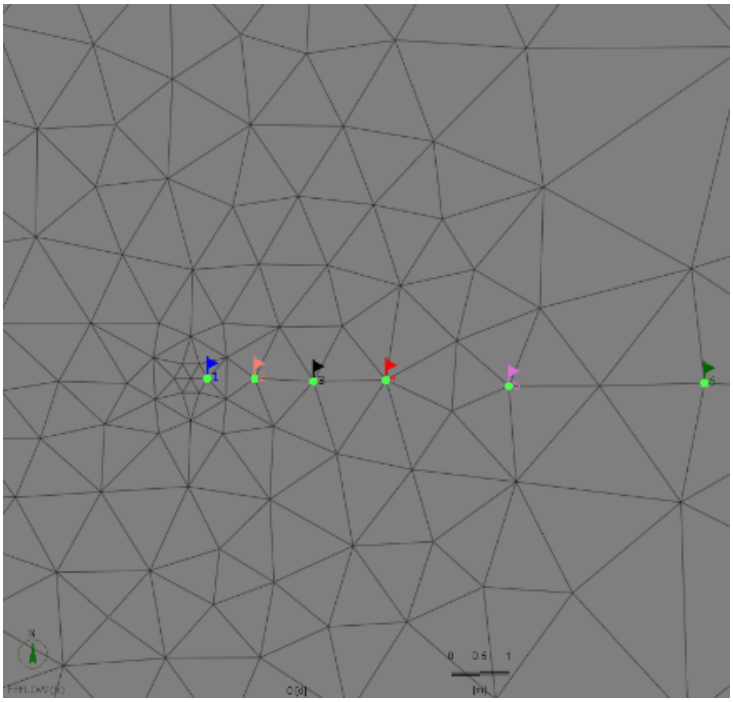

Fig. 53 observation points

The last step before starting the simulations is the setting of the "problem settings":

Table 14 Problem setting parameters

Time step	10 d
Final simulation time	7300 d (20 years)
Initila time-step lenght	0.001 d
Maximum number of iteration per time step	1
Error tolerance	$0.001^{*}\ 10^{-3}$
Symmetric-Matrix system solver Termination criterion	$1e^{-12}$

All the other parameters have been associated with the default values.

4.7.2 BHE parameters and VersaGLD

Using the VersaGLD software, the characteristics of the refrigerant to be edited in "Edit BHE Datasets" in FEFLOW have been set.

This happened for 3 different BHE scenarios based on the drilling diameter that can be made in Kuujjuaq (2.97-3.77-6 inch) with probe length (100-200-300m).

The pipes used are in PE whose characteristics have been found in the catalogue "Versaprofiles"[44].

In the case of del $D_{drilling}$= 2.97 and 3.77 inch a 1U-pipe configuration was chosen while for $D_{drilling}$ = 6inch 2U-pipe.

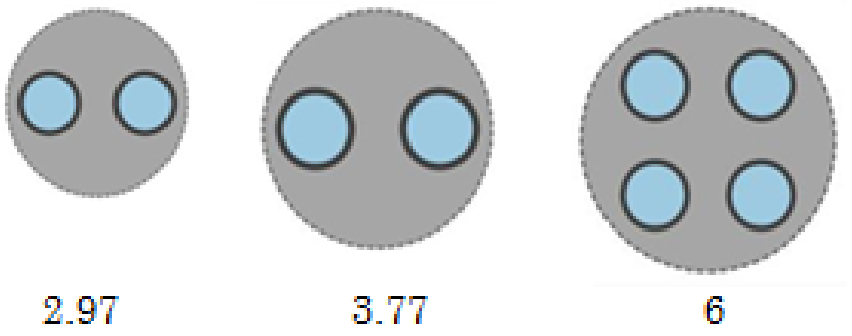

Fig. 54 3 Different scenarios based on diameters that can be drilled in Kuujjuaq

The data and the pipes used are shown below:

Table 15 BHE and pipes parameters

Scenario	$D_{drilling}$		Setup	D_{pipe}	Tickness	Thermal conductivity	Spacing	Grout volume thermal conductiviy
	inch	mm		mm	mm	W/m°K	mm	Js/m/K
1	2.97	75.44	1-Upipe	26.7	2.67	0.70	40	1.5
2	3.77	95.76	1-Upipe	33.4	3.30	0.70	52	1.5
3	6	152,4	2-Upipe	33.4	3.30	0.70	90	1.5

These data were entered into the VersaGLD software together with the geometrical characteristics of the pipe alignment hole. Subsequently, once the *GUE* = 1.25 of the heat pump chosen in the economic analysis and the *EWT* =-10°C had

been fixed, the *quantity of refrigerant (%)* was calculated in an iterative and automatic manner, so as to guarantee a *freezing point* of -15°C, 5°C less than the *operating temperature limit* (tlim= -10°C) fixed in the G.POT method.

The flow rate has also been calculated in an iterative manner, so as to guarantee that the heat transfer fluid is in turbulent motion or by verifying that the *number of Reynolds* resulting is greater than 4000. The software, depending on the amount of antifreeze inserted, calculates the variation of the properties of the entire solution of the heat carrier fluid:

- *Density [kg/m3]*
- *Capacity [kJ/m3°C]*
- *Conductivity [W/m°C]*
- *Viscosity [mPa s]*

the already mentioned number of Reynolds depends on these.

In this case it was decided to use Propylene glycol.

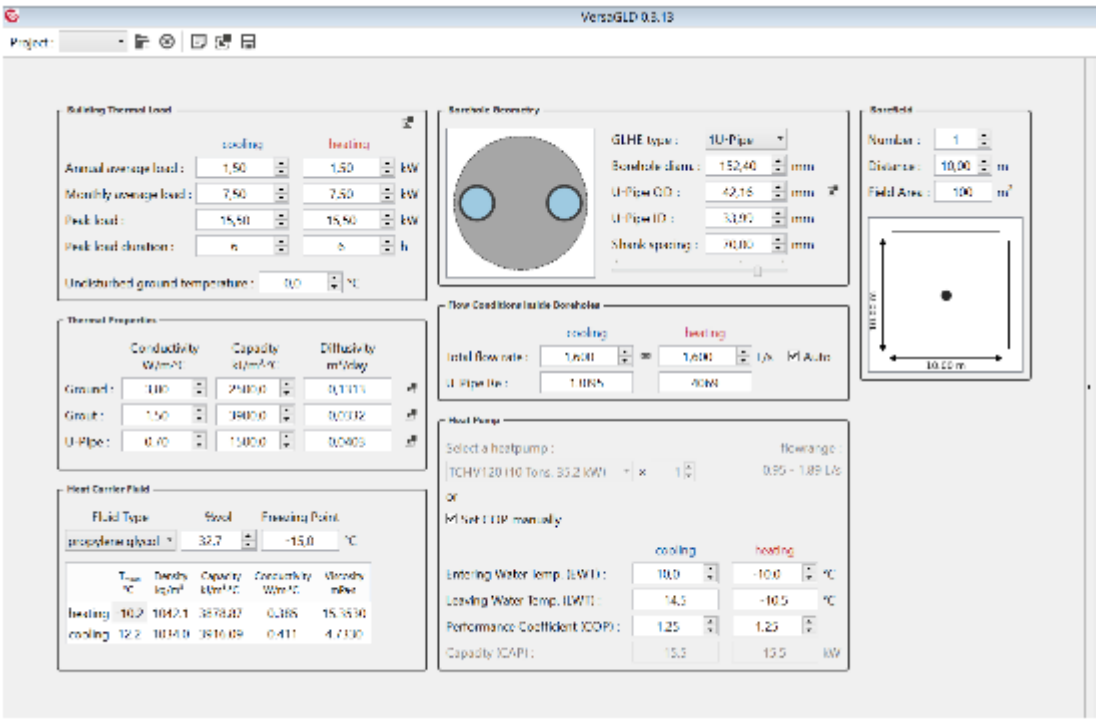

Fig. 55 Graphical interface VersaGLD

The results obtained are shown below:

Table 16 Input parameters

Scenario	D_{pipe}	GUE	EWT	Refrigerant	Freezing point	Flow Rate
	mm		°C	(%)	°C	l/s
1	26.7	1.25	-10	32.7	-15	1.6
2	33.4	1.25	-10	32.7	-15	1.6
3	33.4	1.25	-9	27.0	-15	1.6

The data inserted in the BHE editor Datasets are instead:

Table 17 Heat carrier fluid parameters

Scenario	density	capacity	conductivity	viscosity	Re
	Kg/m3	J/m3/K	J/m/s/K	Kg/m/s	Js/m/K
1	1.042	3.87	0.385	15.35	5745
2	1.042	3.87	0.385	15.81	4594
3	1.036	3.949	0.41	8.45	4147

4.8 Plugin FTM

In the simulation phase, a FEFLOW® Plug in developed by Anbergen et al 2015 [54] was used. The FTM plugin take into account the phase changes that the water undergoes in the vicinity of the BHE.

As already explained in paragraph 3.2, during the freezing and thawing phases, latent heat is released, and the physical properties of the water are modified.

As a preliminary analysis, we wanted to observe the use of the *plugin* and observe the difference in results compared to a non-use of it, leaving the operating conditions of the probe unchanged.

5 RESULTS AND DISCUSSION

5.1 Calculation of shallow geothermal potential with G.POT

Below are the results of the calculation of the geothermal potential using the G.POT method for the 9 different scenarios depending on the diameter and length of the probes:

Table 18 Shallow geothermal potential calculated with G.POT method for 3 different drilling diameters and 3 BHE lengths.

	Drilling Diameter (inches)		
	2.97	**3.77**	**6**
L	$\bar{Q}_{BHE}$	$\bar{Q}_{BHE}$	$\bar{Q}_{BHE}$
m	**MWh/y**	**MWh/y**	**MWh/y**
100	11,0	10.6	12.7
200	23,5	22.6	27.0
300	38,3	36.8	44.0

Dividing the calculated thermal demand of 33.58 MWh/y by the $\bar{Q}_{BHE}$ potential, the number of probes required to satisfy this thermal load was calculated as a first approximation. Here are the results:

Table 19 Number of BHE and total drilling length required to satisfy the annual thermal demand

	n° BHE required			**Total lenght BHE (m)**		
	D	**D**	**D**	**D**	**D**	**D**
L	**2.97**	**3.77**	**6**	**2.97**	**3.77**	**6**
m	**inch**	**inch**	**inch**	**inch**	**inch**	**inch**
100	3	3	3	300	300	300
200	2	2	1	400	400	200
300	1	1	1	300	300	300

Each diameter has been associated with a drilling price including cementation and material laying. In this way, a first cost estimate was given for all 9 scenarios:

Table 20 Drilling cost for each scenario

Total cost $CAD			
L	**D2.97**	**D3.77**	**D6**
m	**inch**	**inch**	**inch**
100	60000	67500	102000
200	80000	90000	68000
300	60000	67500	102000

Below is the map showing the shallow geothermal potential according to BHE length (100-200-300m) and drilling diameter (2.97 inch) made by Simone et al. 2018 [22].

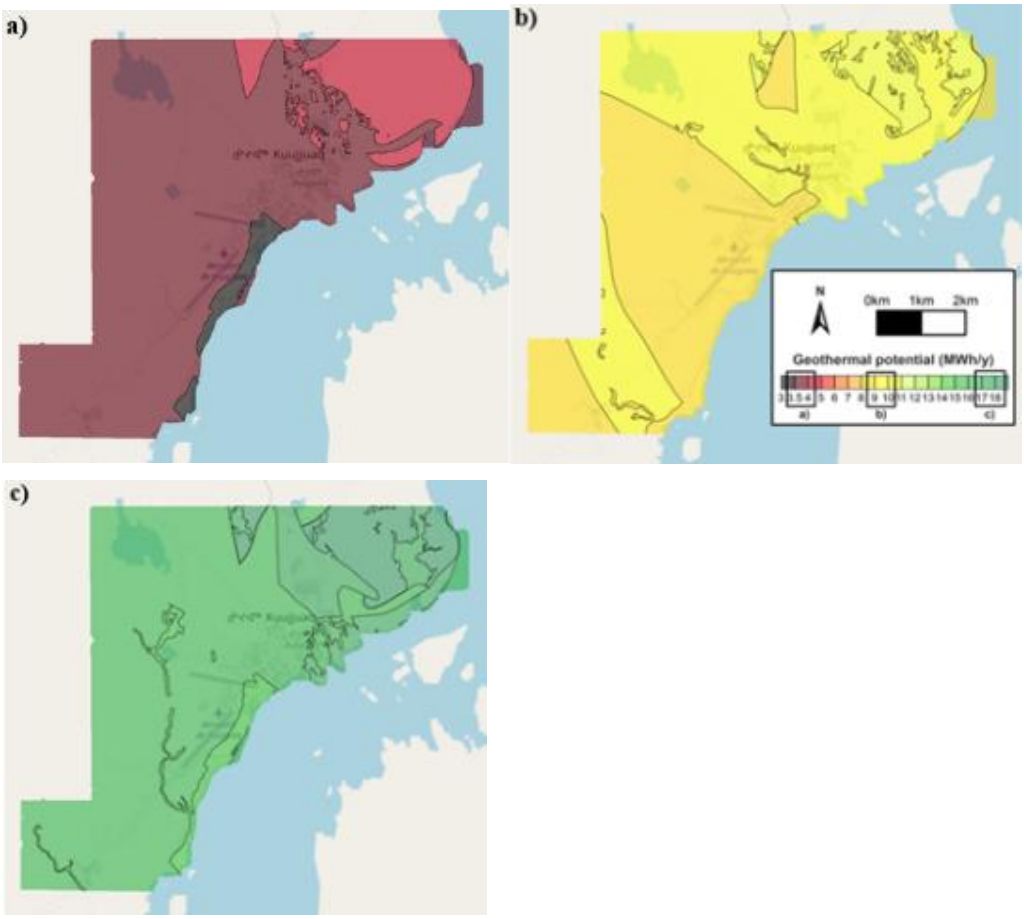

Fig. 56 Shallow geothermal potential in Kuujjuaq according to different BHE lengths: a) 100 m; b) 200 m; c) 300 m; (Source: Della Valentina et al. 2018)

Table 21 Shallow geothermal potential in Kuujjuaq and number of BHE required calculated by Della Valentina et al. 2018.

D 2.97		
L	$\bar{Q}_{BHE}$	**n° BHE required**
m	**MWh/y**	**-**
100	3.7	12
200	9.0	5
300	16.5	3

As you can observe respect there is a greater number of probes than that calculated in this work. In the case of L100 they are 2÷3 times greater, while in L300 they have the same number. The differences in values are essentially due to the difference in thermal load (43 MWh/y) and some different input parameters (t_{lim} =-3°C) used by Della Valentina et al. 2018.

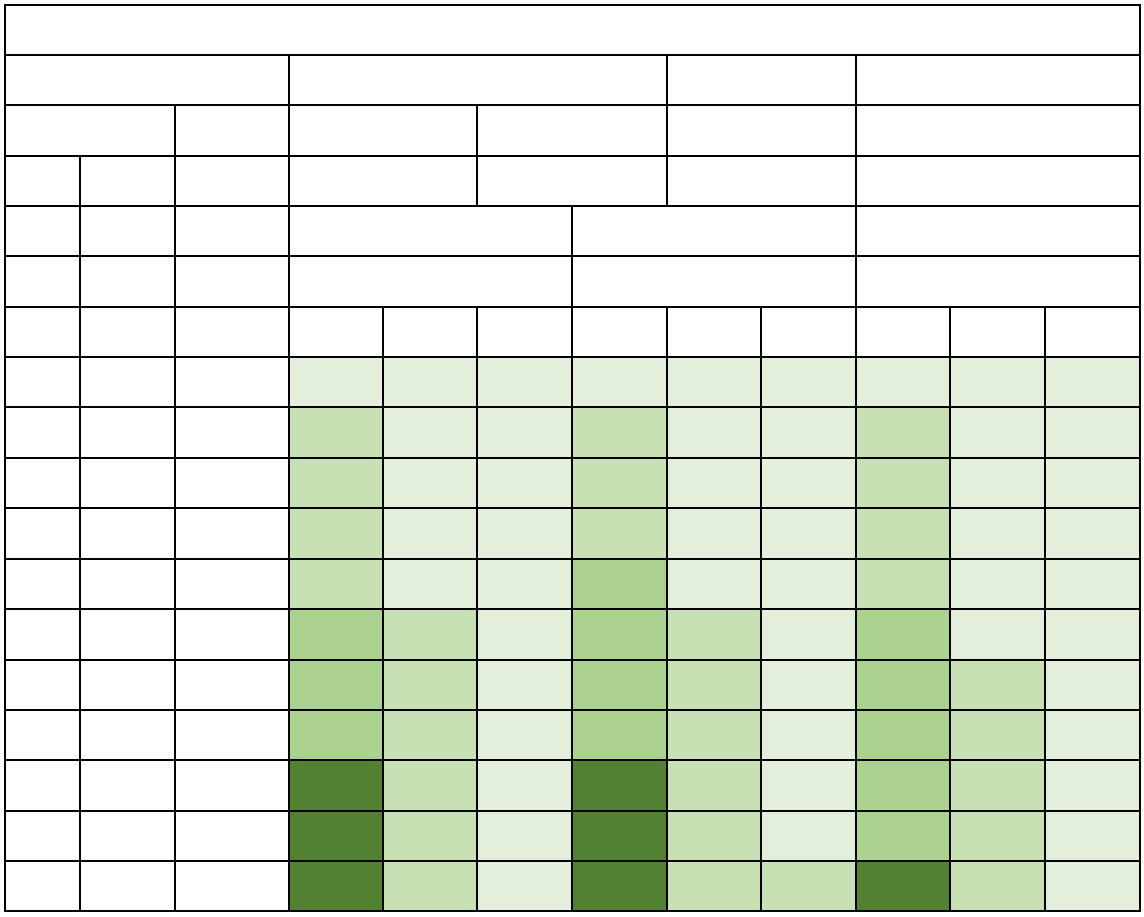

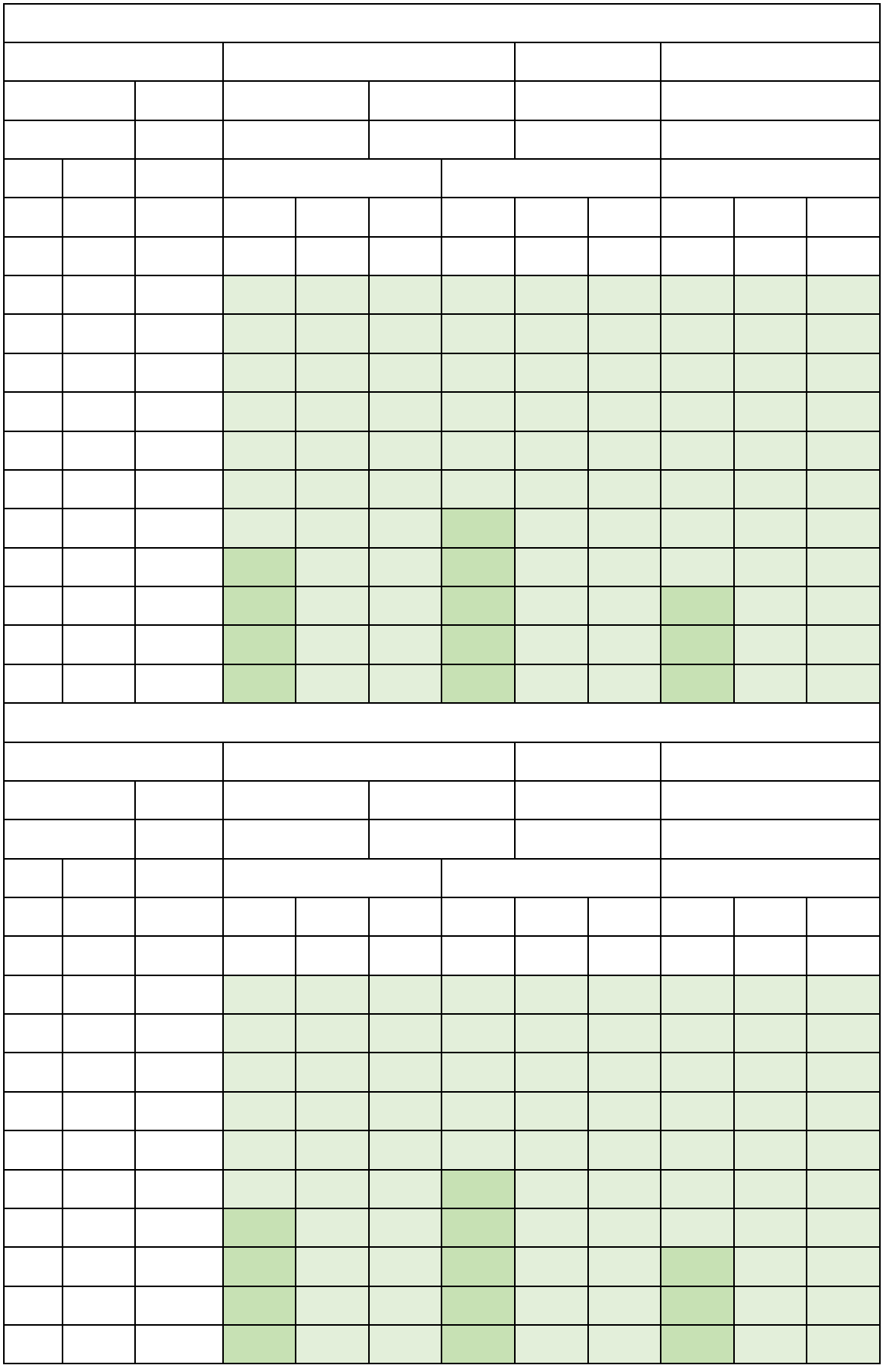

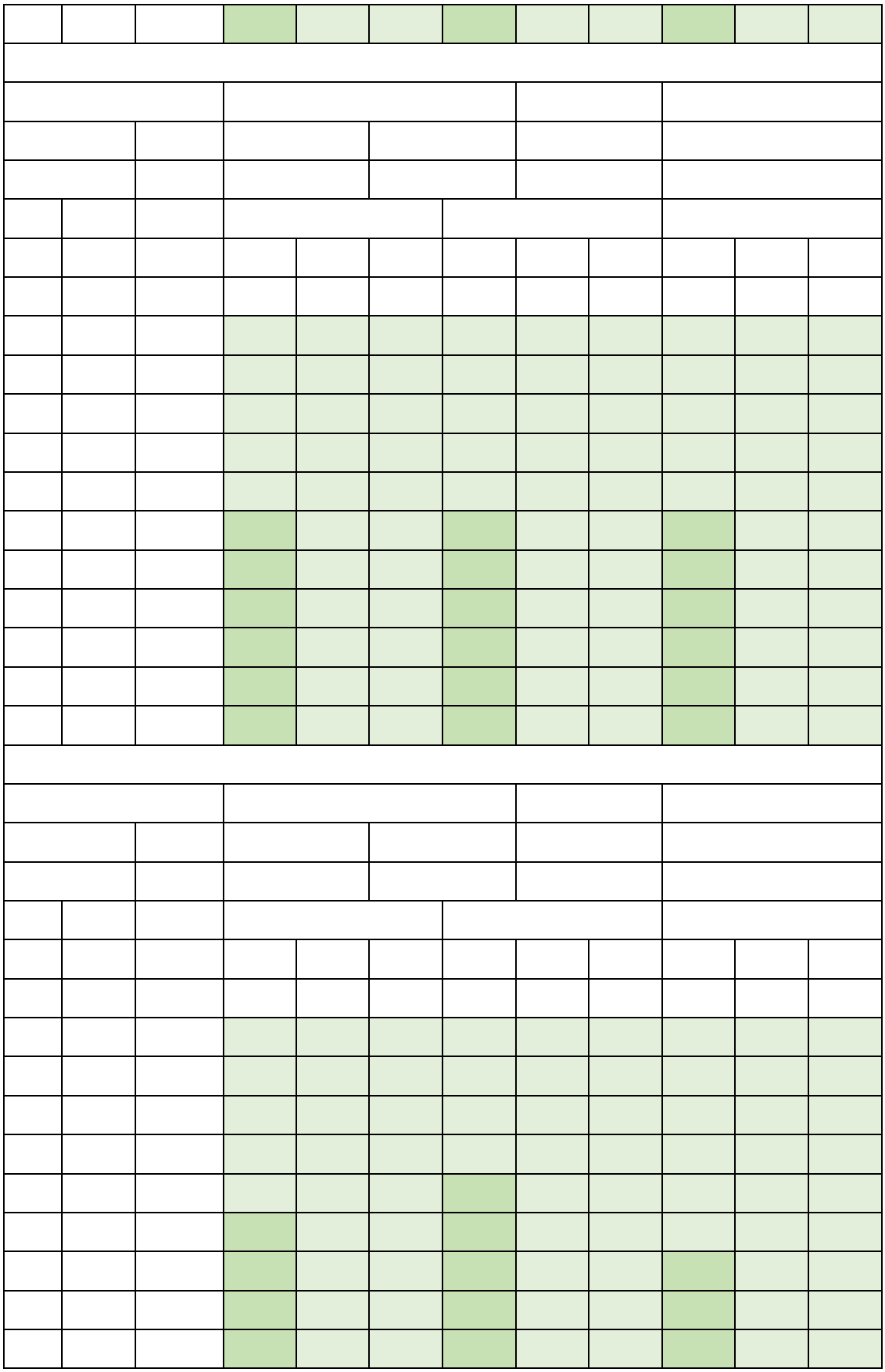

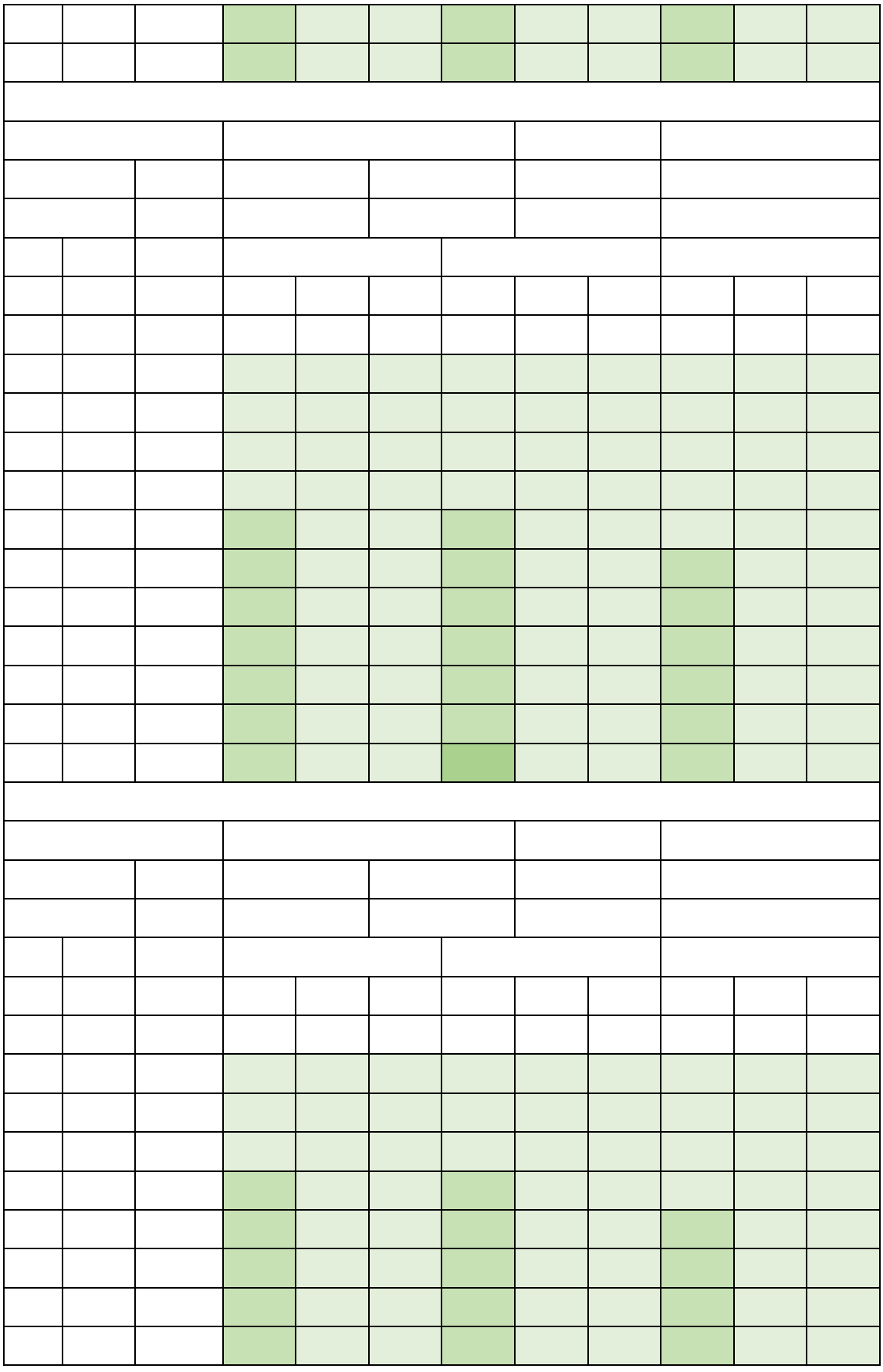

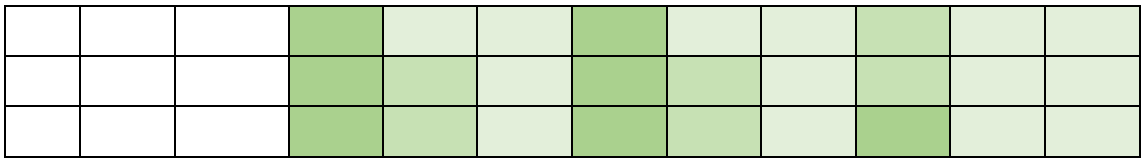

When an absorption heat pump is considered, the number of probes decreases compared to those calculated using the G.POT method, since part of the heat energy will be supplied by the pump. In this case, since it is an absorption heat pump, the thermal energy will be given by that part of the heat deriving from the combustion of the diesel used to compress the refrigerant fluid. Depending on the *GUE* value, the heat input provided by the combustion changes: for increasing *GUE*, this decreases and, on the contrary, the heat extracted from the probes increases and, consequently, their number increases.

It should be noted (***Table 22***)that for a GUE=1.25 with a partial coverage of the heating thermal load, it is sufficient to install only one probe per housing unit. The number of probes remains constant as the diameter and length of the drill vary.

Only in the case of total coverage for a length of 100m the probe requires at least 2.

With the coupling of an electric heat pump, the actual number of BHEs (*Table 23*) reaches a maximum of 6 and a minimum of 1 between all scenarios.

Differently from the previous case, with the GCEHP system the number increases as the diameter and length of the perforation decrease. In the case of total replacement, as the *COP* varies, the number of probes remains constant and assumes a value of 6 for a length of 100m and a diameter of 2.97, and a minimum value of 2 for probes with a length of 200m.

Table 22 Number of BHE coupled with adsorption heat pump(GUE=1.25) depending on the percentage of coverage of the Heat load, Drilling diameters and BHE length.

GUE=1.25	**n° BHE**								
	D 2.97			**D 3.77**			**D 6**		
%of H	**L100**	**L200**	**L300**	**L100**	**L200**	**L300**	**L100**	**L200**	**L300**
32%	1	1	1	1	1	1	1	1	1
37%	1	1	1	1	1	1	1	1	1

41%	1	1	1	1	1	1	1	1	1
46%	1	1	1	1	1	1	1	1	1
57%	1	1	1	1	1	1	1	1	1
70%	1	1	1	1	1	1	1	1	1
100%	2	1	1	2	1	1	2	1	1

Table 23 Number of BHE coupled with eletric heat pump(COP=4.3) depending on the percentage of coverage of the Heat load, Drilling diameters and BHE length.

COP=4.3	**n° BHE**								
	D 2.97			**D 3.77**			**D 6**		
%of H	**L100**	**L200**	**L300**	**L100**	**L200**	**L300**	**L100**	**L200**	**L300**
32%	3	2	1	3	2	1	2	1	1
37%	3	2	1	3	2	1	2	1	1
41%	3	2	1	3	2	1	3	1	1
46%	3	2	1	3	2	1	3	2	1
57%	4	2	1	4	2	1	3	2	1
70%	4	2	2	4	2	2	4	2	1
100%	6	3	2	6	3	2	5	3	2

The results of the calculation of the number effective of probes coupled to an absorption heat pump according to the GUE and COP, are shown in the appendix in Table 34 and Table 35.

For each scenario of energy coverage that takes place through a GCHP system, 99 different scenarios have been obtained with the relative number of BHE needed.

In total, multiplying the 7 energy coverage scenarios by 99, 693 different scenarios were obtained.

With an absorption heat pump, considering all scenarios, a maximum number of 4 probes per user and a minimum of one are reached.

In the scenarios of partial coverage of the heat requirement *H(MWh)* for a range of *GUE* between 1÷1.25 and for the L_{BHE} lengths equal to 200 and 300m for all 3 drilling diameters, only one probe is required, except in the case of coverage of 70% where for *GUE* between 1.9÷2 as many as 2 probes/user are required.

In the case of total replacement with 100% coverage, the number of probes varies between (3÷4) when the *GUE* (1.4÷2) increases and for $D_{drilling}$ = 2.97 inches.

The number of probes increases as the length of the *BHE* (L_{BHE}) decreases and at the same time increases, even if in a less marked way, as the $D_{drilling}$ diameter of *BHE* decreases.

With electric heat pump, in scenarios with partial replacement, the number of probes does not change when the *COP* changes. In particular, for covers of (32-37-41-46%) the number of probes varies between 1÷3, while with higher percentages (57-70%) a number of 4 probes can be reached with L_{BHE} =100.

5.2 Initial investment cost

The number of probes and the total length to be drilled reflects on the drilling cost and consequently on the initial investment. On average, it represents 76% of the total cost, except for the scenario (32% of H) where it reaches 91%.

In the latter case this peak is caused by the low price of the heat pump (5000$CAD) or 3 times less than the other scenarios (Table 24). Despite the little influence of the cost of the heat pump (about 9%) in the scenario (*37%*) and 25% (70%H scenario), its reduction as analyzed in paragraph 4.6 with a reduction of its original cost (15000 $CAD) respectively of 66% and 50%, allows to lower the initial investment costs.

Table 24purchase cost of the heat pum $CAD/users for GCAHP and GCEHP depending on percentage of covering of annual thermal load H(MWh) and the peak load P(kW).

P(kW)		**26.4**	**10**	**11**	**12**	**13**	**15**	**17**
Covering W (%)		100%	32	37	41	46	57	70
Heat pump cost $CAD	**GCAHP**	15000	5000	15000	15000	15000	15000	7500
	GCEHP	18000	20000	20000	15000	25000	17000	20000

The initial investment cost already allows to give a first idea on which are in economic terms the best choices.

With a coverage of *H* of 37% you get to a minimum investment value of 25000$CAD hile for a coverage of 70% you get a minimum value of 27500$CAD. The

maximum investment cost while you reach with a coverage of 100% with 151000 $CAD about 5 times the minimum cost.

Taking into consideration only the values with *GUE*= 1.25 it is possible to observe in Fig. 57 how the initial investment costs present the lowest values for L_{BHE}=100m with absolute minimum values in the scenario (37%) with 25000$CAD.

With 70% of *H* you have a minimum value of 27500$CAD for L_{BHE}=100 $D_{drilling}$=2.97 while 30000$CAD for $D_{drilling}$.=3.77.

A total replacement of the boiler system with a GCAHP with *GUE*=1.25 at best would have an investment cost of 55000$CAD for the drilling diameter $D_{drilling}$=2.97 and lengths L_{BHE}=100 -200m.

Finally, it should be noted that the use of a diameter of 6 inches with a length of L_{BHE}=200-300m and a diameter of L_{BHE}=300m exceeds in any scenario the 70000$CAD cost.

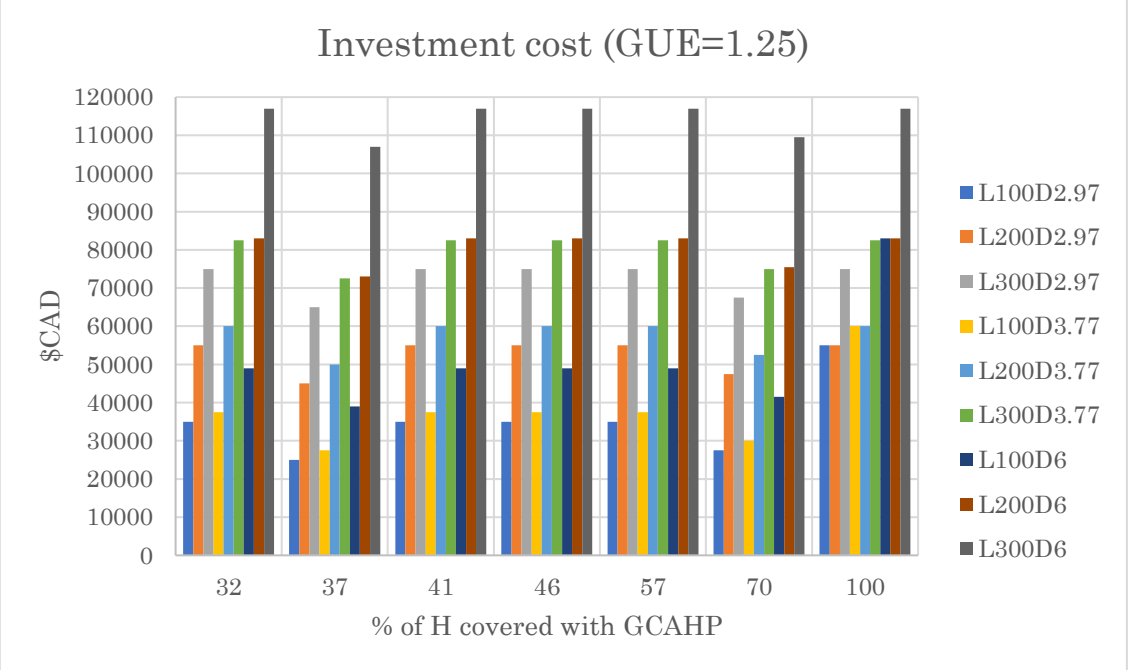

Fig. 57 Investment cost with an Adsorption heat pump with GUE=1.25.

As with GCAHP, the investment cost of a GCEHP system increases with increasing depth and drilling diameters. With an electric heat pump COP=4.3 Investment cost with an electric heat pump with COP=4.35. the absolute minimum cost of $6,000 CAD is 3 times higher than the minimum cost with a GCHAP system.

In the scenario with total replacement of the boiler system (100%) we reach a minimum cost of $ 120000 and a maximum cost that exceeds $ 200.000CAD.

The percentages of coverage with which lower values are obtained are 41% and 48% with the latter representing the best choice.

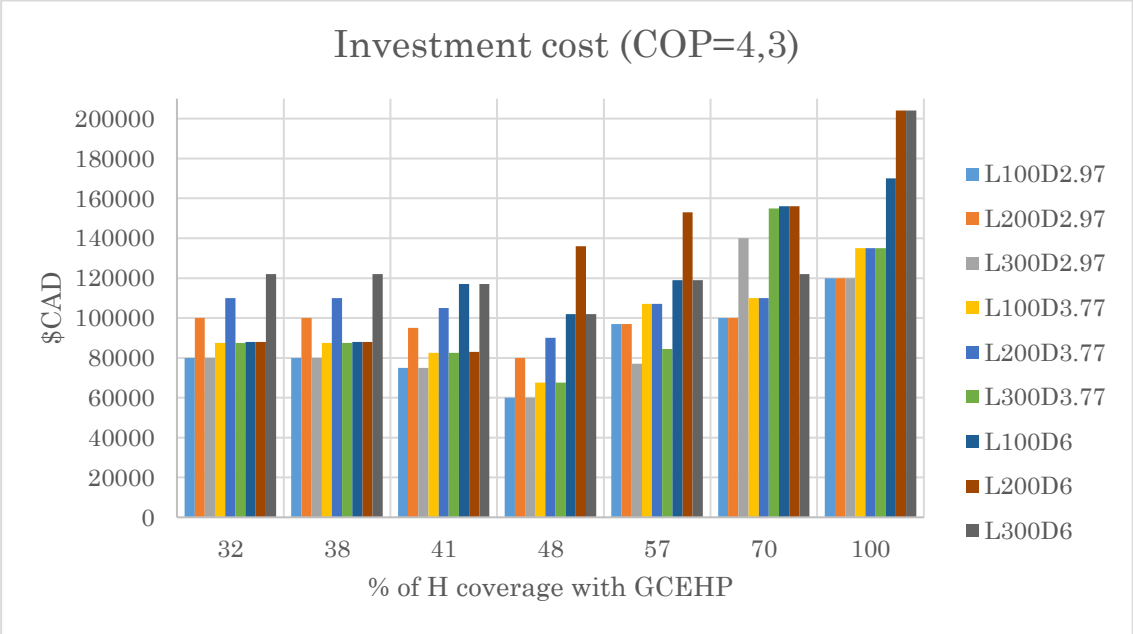

Fig. 58 Investment cost with an electric heat pump with COP=4.35.

With *COP* higher than those of the absorption heat pump, more probes are needed, thus increasing drilling costs in some cases by up to 90%.

The initial investment costs depending on GUE (1.1÷2)/COP(3.5÷4.5),$D_{drilling}$ and L_{BHE} are laid down in the Appendix (*Table 36* - Table 37),

5.3 Annual savings with GCAHP and GCEHP

The *Annual savings* that would be obtained with the installation of the new geothermal system GCAHP (*Table 29*), compared to the annual cost of the diesel boiler (Table 27), derive directly from the difference between the amount of annual diesel (L_{fuel}) required for the operation of the diesel boiler plant and GCAHP respectively. The calculated amount of diesel is such as to generate a thermal energy ($E_{eff,\ fuel}$) which, net of the efficiency (η) of the boiler and the absorption heat pump burner, fully covers the rate of *H* (kWh/y) to be provided by the combustion of the diesel (T_{fuel} *(kW)*).

The value of T_{fuel}, which incorporates the value of thermal energy supplied by the combustion phase of the diesel inside the heat pump burner (T_{fuel}), varies according to the percentage with which it is assumed to cover H(MWh/y). It decreases with increasing *GUE* due to the increasing percentage of thermal energy extracted from the ground.

Table 25 T_{fuel},$E_{eff,\ diesel}$, L_{diesel} and Annual Cost Furnace plant

	Furnace plant			
η	**T_{fuel}**	**$E_{eff,\ fuel}$**	**L_{fuel}**	**Annual Cost**
-	**kWh**	**kWh**	**l/y**	**CAD/y**
0.83	33579	40456,63	3774	5661

With a GCAHP system, as shown in the table Table 29, as the *GUE* and the percentage of coverage of H increase, the annual saving increases to maximum values of 3397 $CAD with *GUE*=2.5 and coverage of 100% of H.

The growth of the savings, starting from the scenario with *GUE*=1.1 and *% of H*=32, is constant and takes into account the increasing contribution of thermal energy extracted from the ground at the expense of the diesel used by the heat pump in the case of *GUE* and the diesel used by the boiler in the case of (% of H).

Relative to a value of *GUE*=1.25, a maximum and minimum saving of 1132 $CAD and 367 $CAD respectively is obtained for percentages of coverage of H of 100% and 32%. For a coverage of 100% the quantity of diesel is equal to 3019 l/y with an annual cost of $ 4526 CAD while in the worst case with 32% of H, there is an annual cost higher than 15% (5294 $CAD) and a relative consumption of diesel equal to 3529 l/y.

Naturally a high value of annual saving means to increase the value of the denominator in the calculation of the payback time and tends to favour its shortening. Simultaneously to a high annual saving corresponds a cost of increasing investment as observed in the paragraph 5.3.

The annual savings values vary according to the GUE (1.1÷2) and the percentage of coverage of the requirement (32÷100% of H) and are shown in yellow-green colour scale in Table 29. The values in yellow represent lower savings while the values in green represent higher annual savings.

The values of ($T_{fuel,\ heat\ pump}$), (T_{fuel}), effective energy, (E_{ff}) supplied by the diesel, the annual quantity of diesel (L_{fuel}) and the annual operating cost of a GCAHP system depending on *GUE* and the percentage (%) of the heat requirement *H* (kWh/y) are laid down in Appendix (Table 38).

Table 26 GCAHP-Annual saving ($CAD and %) depending on GUE and percentage (%) of covering of H(kWh/y).

Annual saving GcAHP														
	$CAD/y							%						
GUE	**32%**	**38%**	**41%**	**48%**	**57%**	**70%**	**100%**	**32%**	**38%**	**41%**	**48%**	**57%**	**70%**	**100%**
1.1	167	188	210	238	294	362	515	3	3	4	4	5	6	9
1.2	306	344	385	436	539	665	943	5	6	7	8	10	12	17
1.25	**367**	**413**	**462**	**523**	**647**	**797**	**1132**	**7**	**7**	**8**	**9**	**11**	**14**	**20**
1.3	424	477	533	604	747	920	1306	8	8	9	11	13	16	23
1.4	525	590	660	748	924	1139	1617	9	10	12	13	16	20	29
1.5	612	689	770	872	1079	1329	1887	11	12	14	15	19	24	33
1.6	689	775	866	982	1213	1495	2123	12	14	15	17	21	26	38
1.7	756	851	951	1078	1332	1642	2331	13	15	17	19	24	29	41
1.8	816	918	1026	1163	1438	1772	2516	14	16	18	21	25	31	44
1.9	870	979	1094	1240	1533	1889	2681	15	17	19	22	27	33	47
2	918	1033	1155	1309	1618	1994	2830	16	18	20	23	29	35	50

The values of the annual saving ($CAD, %) that would be obtained with the installation with a GCEHP (Table 31) system, compared to the cost of the GCAHP configuration is influenced by the cost of producing the electrical energy that must power the compressor of the electric pump and by the efficiency that characterizes it. The price of diesel is linked to the electric energy ($E_{compressor}$) that the compressor needs to operate, which is produced by the diesel plant for off-grid electricity production located near the community of Kuujjuaq. A part of the cost of the diesel is instead tied to the quantity of diesel consumed by the diesel boiler of the user, which with the variation of the *COP* remains constant while it increases with the variation of the percentage of the coverage of the thermal requirement *H* (kWh/y).

Table 27 GCEHP- Annual saving ($CAD and %) depending on COP and percentage (%) of covering of H(kWh/y)

Annual saving GCEHP

	$CAD/y							%						
COP	**32%**	**38%**	**41%**	**48%**	**57%**	**70%**	**100%**	**32%**	**38%**	**41%**	**48%**	**57%**	**70%**	**100%**
3,5	592	666	745	844	1043	1286	1825	11	12	13	15	18	23	32
3,6	627	705	788	893	1104	1361	1932	11	13	14	16	20	24	34
3,7	659	742	829	940	1162	1432	2033	12	13	15	17	21	25	36
3,8	690	777	868	984	1216	1499	2128	12	14	15	17	22	27	38
3,9	720	810	905	1026	1268	1563	2219	13	14	16	18	22	28	39
4	748	841	940	1066	1317	1623	2305	13	15	17	19	23	29	41
4,1	774	871	973	1104	1364	1681	2387	14	15	17	20	24	30	42
4,2	800	900	1005	1140	1409	1736	2465	14	16	18	20	25	31	44
4,3	**824**	**927**	**1036**	**1174**	**1451**	**1788**	**2539**	**15**	**16**	**18**	**21**	**26**	**32**	**45**
4,4	847	953	1065	1207	1492	1838	2610	15	17	19	21	26	33	46
4,5	869	978	1092	1238	1530	1886	2678	15	17	19	22	27	33	47

In one year a GCEHP system with *COP*=4.3 in the case of total coverage of the heat requirement has a saving compared to the boiler system of 45%, and 55% more, in the same condition of energy coverage, of the system powered by heat pump absorption.

This result is due to a higher *COP* value which corresponds to a greater extraction of heat from the ground of about 74% and at the same time a lower use of diesel. This result, if isolated, suggests that an electric compression heat pump allows greater annual savings than the absorption one, but not the certainty of having a lower payback time. In fact, as already analyzed in the paragraph, the use of this system implies the use of a number of probes on average 3 times higher and therefore higher initial investment costs are necessary.

The values of $E_{compressor}$, $E_{eff,\ fuel}$ *off-grid plant*, E_{eff} *furnace*, the annual quantity of diesel (*Ldiesel*) and the annual operating cost of a GCEHP system depending on

COP and the percentage (%) of the *H*(kWh/y) heat requirement, are laid down in Appendix (*Table* 39).

5.4 CO_2 emission

Below is the table in colour scale of the CO2 saved values with each type of configuration studied. The red colour indicates a low percentage of CO2 saved, while the green colour indicates a high percentage that gives the scenario the most "ecological" configuration. The line with the values relating to the case study with GUE = 1.25 is also highlighted, where in the case of total substitution 20%/y of CO2 emissions is reached.

As the GUE and the coverage of requirements with geothermal plant increases, the percentage of annual savings increases, reaching peaks of up to 50% in the case of GUE=2 and total replacement of the diesel plant.

Table 28 CO2 Saving emission GCAHP

GUE	Saving CO2/y GCAHP													
	Ton CO2/y							%						
-	32%	38%	41%	46%	57%	70%	100%	32%	38%	41%	46%	57%	70%	100%
1,1	0,30	0,34	0,38	0,43	0,53	0,80	0,92	3	3	4	4	5	8	9
1,2	0,55	0,62	0,69	0,78	0,96	1,47	1,69	5	6	7	8	10	15	17
1,25	0,66	0,74	0,83	0,94	1,16	1,76	2,02	6	7	8	9	11	17	20
1,3	0,76	0,85	0,95	1,08	1,33	2,03	2,33	7	8	9	11	13	20	23
1,4	0,94	1,05	1,18	1,34	1,65	2,52	2,89	9	10	12	13	16	25	29
1,5	1,09	1,23	1,38	1,56	1,93	2,94	3,37	11	12	14	15	19	29	33
1,6	1,23	1,38	1,55	1,75	2,17	3,31	3,79	12	14	15	17	21	33	38
1,7	1,35	1,52	1,70	1,93	2,38	3,63	4,16	13	15	17	19	24	36	41
1,8	1,46	1,64	1,83	2,08	2,57	3,92	4,50	14	16	18	21	25	39	44
1,9	1,55	1,75	1,95	2,22	2,74	4,18	4,79	15	17	19	22	27	41	47
2	1,64	1,85	2,06	2,34	2,89	4,41	5,06	16	18	20	23	29	44	50
COP	Saving CO2/y GCEHP													
	Ton CO2/y							%						
	32%	38%	41%	46%	57%	70%	100%	32%	38%	41%	46%	57%	70%	100%
-	1,06	1,19	1,33	1,51	1,86	2,84	3,26	10	12	13	15	18	28	32
3,5	1,12	1,26	1,41	1,60	1,97	3,01	3,45	11	12	14	16	20	30	34
3,6	1,18	1,33	1,48	1,68	2,08	3,16	3,63	12	13	15	17	21	31	36
3,7	1,23	1,39	1,55	1,76	2,17	3,31	3,80	12	14	15	17	21	33	38
3,8	1,29	1,45	1,62	1,83	2,27	3,45	3,96	13	14	16	18	22	34	39
3,9	1,34	1,50	1,68	1,90	2,35	3,59	4,12	13	15	17	19	23	35	41
4	1,38	1,56	1,74	1,97	2,44	3,72	4,26	14	15	17	19	24	37	42
4,1	1,43	1,61	1,80	2,04	2,52	3,84	4,40	14	16	18	20	25	38	44
4,2	1,47	1,66	1,85	2,10	2,59	3,95	4,54	15	16	18	21	26	39	45
4,3	1,51	1,70	1,90	2,16	2,67	4,06	4,66	15	17	19	21	26	40	46
4,4	1,55	1,75	1,95	2,21	2,73	4,17	4,78	15	17	19	22	27	41	47

4,5	1,59	1,79	2,00	2,27	2,80	4,27	4,90	16	18	20	22	28	42	48

With an electric heat pump, on the other hand, a maximum of 46% CO2 saving is achieved, i.e. more than twice as much as with the absorption pump chosen.

5.5 Pay Back Time

Having a reasonable *PBT* or one that is less than the useful life of the plant (~50 years) is of great importance for its feasibility.

Below (Table 33) are the above-mentioned payback time values in chromatic scale with red color the highest values and blue for the lowest values.

The most interesting results, of course, are to be found among the values in blue.

Table 29 GCAHP-Payback time values (years) depending on GUE, Ddrilling, LBHE and percentage (%) of H coverage.

Payback Time PBT (y)									
32%									
GUE	**D 2,97**			**D3,77**			**D6**		
-	**L100**	**L200**	**L300**	**L100**	**L200**	**L300**	**L100**	**L200**	**L300**
1,1	210	329	449	225	359	494	293	497	701
1,2	114	180	245	123	196	270	160	271	382
1,25	**95**	**150**	**204**	**102**	**163**	**225**	**133**	**226**	**319**
1,3	83	130	177	88	142	195	116	196	276
1,4	67	105	143	71	114	157	93	158	223
1,5	57	90	123	61	98	135	80	136	191
1,6	80	80	109	87	87	120	71	121	170
1,7	73	73	99	79	79	109	65	110	155
1,8	67	67	92	74	74	35	102	102	143
1,9	63	63	86	69	69	95	95	95	134
2	60	60	82	65	65	90	90	90	127
38%									
GUE	**D 2,97**			**D3,77**			**D6**		
-	**L100**	**L200**	**L300**	**L100**	**L200**	**L300**	**L100**	**L200**	**L300**
1,1	133	240	346	146	266	386	208	389	570
1,2	73	131	189	80	145	210	113	212	311
1,25	**60**	**109**	**157**	**67**	**121**	**175**	**94**	**177**	**259**
1,3	52	94	136	58	105	152	82	153	224
1,4	42	76	110	47	85	123	66	124	181

1,5	65	65	94	73	73	105	57	106	155
1,6	58	58	84	65	65	94	50	94	138
1,7	53	53	76	59	59	85	86	86	126
1,8	49	49	71	54	54	79	79	79	116
1,9	46	46	66	51	51	74	75	75	109
2	44	44	63	48	48	70	71	71	104
41%									
GUE	**D 2 ,97**			**D3,77**			**D6**		
-	**L100**	**L200**	**L300**	**L100**	**L200**	**L300**	**L100**	**L200**	**L300**
1,1	167	262	357	179	286	393	233	395	557
1,2	91	143	195	97	156	214	127	216	304
1,25	**76**	**119**	**162**	**81**	**130**	**179**	**106**	**180**	**253**
1,3	66	103	141	70	113	155	92	156	220
1,4	53	83	114	57	91	125	74	126	177
1,5	71	71	97	78	78	107	64	108	152
1,6	64	64	87	69	69	95	96	96	135
1,7	58	58	79	63	63	87	87	87	123
1,8	54	54	73	58	58	80	81	81	114
1,9	50	50	69	55	55	75	76	76	107
2	48	48	65	52	52	71	72	72	101
46%									
GUE	**D 2 ,97**			**D3,77**			**D6**		
-	**L100**	**L200**	**L300**	**L100**	**L200**	**L300**	**L100**	**L200**	**L300**
1,1	147	231	315	158	252	347	206	349	492
1,2	80	126	172	86	138	189	112	190	268
1,25	**67**	**105**	**143**	**72**	**115**	**158**	**94**	**159**	**223**
1,3	58	91	124	62	99	137	81	137	194
1,4	74	74	100	80	80	110	66	111	156
1,5	63	63	86	69	69	95	95	95	134
1,6	56	56	76	61	61	84	85	85	119
1,7	51	51	70	56	56	77	77	77	109
1,8	47	47	64	52	52	71	71	71	101
1,9	44	44	60	48	48	67	67	67	94
2	42	42	57	46	46	63	63	63	89
57%									
GUE	**D 2,97**			**D3,77**			**D6**		
-	**L100**	**L200**	**L300**	**L100**	**L200**	**L300**	**L100**	**L200**	**L300**
1,1	119	187	255	127	204	280	167	282	398
1,2	65	102	139	70	111	153	91	154	217
1,25	**54**	**85**	**116**	**58**	**93**	**127**	**76**	**128**	**181**
1,3	47	74	100	50	80	110	66	111	157
1,4	59	59	81	65	65	89	90	90	127

1,5	51	51	70	56	56	76	77	77	108
1,6	45	45	62	49	49	68	68	68	96
1,7	41	41	56	45	45	62	62	62	88
1,8	38	38	52	42	42	57	58	58	81
1,9	36	36	49	39	39	54	54	54	76
2	46	34	46	51	37	51	51	51	72
70%									
GUE	**D 2,97**			**D3,77**			**D6**		
-	**L100**	**L200**	**L300**	**L100**	**L200**	**L300**	**L100**	**L200**	**L300**
1,1	76	131	186	83	145	207	114	208	302
1,2	41	71	102	45	79	113	62	114	165
1,25	**34**	**60**	**85**	**38**	**66**	**94**	**52**	**95**	**137**
1,3	52	52	73	57	57	82	45	82	119
1,4	42	42	59	46	46	66	66	66	96
1,5	36	36	51	40	40	56	57	57	82
1,6	32	32	45	35	35	50	50	50	73
1,7	29	29	41	32	32	46	46	46	67
1,8	38	27	38	42	30	42	43	43	62
1,9	36	46	36	40	52	40	40	40	58
2	34	44	34	38	49	38	38	38	55
100%									
GUE	**D 2,97**			**D3,77**			**D6**		
-	**L100**	**L200**	**L300**	**L100**	**L200**	**L300**	**L100**	**L200**	**L300**
1,1	68	107	146	73	117	160	95	161	227
1,2	58	58	79	64	64	87	88	88	124
1,25	**49**	**49**	**66**	**53**	**53**	**73**	**73**	**73**	**103**
1,3	42	42	57	46	46	63	64	64	90
1,4	46	34	46	51	37	51	51	51	72
1,5	40	50	40	44	56	44	62	44	62
1,6	35	45	35	39	49	39	55	71	55
1,7	41	41	32	45	45	35	50	65	50
1,8	38	38	30	42	42	33	47	60	47
1,9	35	35	50	39	39	56	44	56	44
2	34	34	48	37	37	53	53	53	41

From Table 33 it is possible to observe how Payback Time tends to decrease with the increase of *GUE* and with the decrease of diameters and lengths of perforation of BHE.

In some cases, however, it is possible to observe how, for fixed length and diameter, the minimum value of *PBT* is not reached for the greater value of *GUE*.

This happens because of the initial investment costs that increase abruptly with the increase in the probes required for drilling that is still so high that, despite the relative annual savings, results in higher *PBT* compared to the previous scenario.

The only cases in which the *PBT* varies linearly with a minimum value for maximum *GUE* are those in which there is a constant initial investment cost and therefore an equal number of probes. This happens in the scenarios with $D_{drilling}$ =6inch and L_{BHE}=100m and 200m.

In general, the lowest values for each percentage scenario (%) of *H* coverage are found in the lower-left part of the table, i.e. for small $D_{drilling}$ of 2.97 Inch and *GUE*.

Below in Table 34 are the *PBT* values for a GCEHP system:

Table 30 GCEHP-Payback time values (years) depending on COP, Ddrilling, LBHE and percentage (%) of H coverage.

Payback Time PTB (y)									
32%									
COP	**D 2,97**			**D3,77**			**D6**		
-	**L100**	**L200**	**L300**	**L100**	**L200**	**L300**	**L100**	**L200**	**L300**
3,5	135	101	135	110	110	148	149	149	206
3,6	128	96	128	140	104	140	140	140	195
3,7	121	91	121	133	99	133	133	133	185
3,8	116	87	116	127	94	127	127	127	177
3,9	111	83	111	122	90	122	122	122	169
4	107	80	107	117	87	117	118	118	163
4,1	103	77	103	113	84	113	114	114	158
4,2	100	125	100	109	81	109	110	110	153
4,3	**97**	**121**	**97**	**106**	**134**	**106**	**107**	**107**	**148**
4,4	94	118	94	103	130	103	104	104	144
4,5	92	115	92	101	127	101	101	101	140
38%									
COP	**D 2,97**			**D3,77**			**D6**		
-	**L100**	**L200**	**L300**	**L100**	**L200**	**L300**	**L100**	**L200**	**L300**
3,5	120	150	120	131	165	131	132	132	183
3,6	113	142	113	124	156	124	125	125	173
3,7	108	135	108	118	148	118	119	119	164
3,8	103	129	103	113	142	113	113	113	157
3,9	99	123	99	108	136	108	109	109	151

4	95	119	95	104	131	104	105	105	145
4,1	92	115	92	100	126	100	101	101	140
4,2	89	111	89	97	122	97	98	98	136
4,3	**86**	**108**	**86**	**94**	**119**	**94**	**95**	**95**	**132**
4,4	84	105	84	92	115	92	92	92	128
4,5	82	102	82	90	113	90	125	90	125

41%

COP	**D 2,97**			**D3,77**			**D6**		
-	**L100**	**L200**	**L300**	**L100**	**L200**	**L300**	**L100**	**L200**	**L300**
3,5	101	128	101	111	141	111	157	111	157
3,6	95	121	95	105	133	105	148	105	148
3,7	90	115	90	100	127	100	141	100	141
3,8	86	109	86	95	121	95	135	96	135
3,9	83	105	83	91	116	91	129	92	129
4	80	101	80	88	112	88	124	88	124
4,1	77	98	77	85	108	85	120	85	120
4,2	75	94	75	82	104	82	116	83	116
4,3	**72**	**92**	**72**	**80**	**101**	**80**	**113**	**80**	**113**
4,4	70	89	70	77	99	77	110	78	110
4,5	69	87	69	76	96	76	107	138	107

46%

COP	**D 2,97**			**D3,77**			**D6**		
-	**L100**	**L200**	**L300**	**L100**	**L200**	**L300**	**L100**	**L200**	**L300**
3,5	101	124	101	110	136	110	150	110	150
3,6	95	118	95	104	129	104	142	180	142
3,7	90	112	90	98	122	98	135	171	135
3,8	86	107	86	94	117	94	129	164	129
3,9	83	102	83	90	112	90	124	157	124
4	80	99	80	87	108	87	119	151	119
4,1	77	95	77	84	104	84	115	146	115
4,2	75	92	75	81	101	81	111	141	111
4,3	**72**	**89**	**72**	**79**	**98**	**79**	**108**	**137**	**108**
4,4	70	87	70	77	95	77	105	133	105
4,5	69	85	69	75	93	75	103	130	103

57%

COP	**D 2,97**			**D3,77**			**D6**		
-	**L100**	**L200**	**L300**	**L100**	**L200**	**L300**	**L100**	**L200**	**L300**
3,5	93	93	74	81	103	81	114	147	114
3,6	88	88	70	97	97	77	108	139	108
3,7	83	83	66	92	92	73	102	132	102
3,8	80	80	63	88	88	69	98	126	98
3,9	76	76	61	84	84	67	94	121	94

4	74	74	58	81	81	64	90	116	90
4,1	71	71	56	78	78	62	87	112	87
4,2	69	69	55	76	76	60	84	109	84
4,3	**67**	**67**	**53**	**74**	**74**	**58**	**82**	**105**	**82**
4,4	65	65	52	72	72	57	80	103	80
4,5	63	63	50	70	70	55	78	100	78
70%									
COP	**D 2,97**			**D3,77**			**D6**		
-	**L100**	**L200**	**L300**	**L100**	**L200**	**L300**	**L100**	**L200**	**L300**
3,5	78	78	62	86	86	68	95	121	95
3,6	73	73	59	81	81	64	90	115	90
3,7	70	70	98	77	77	61	85	109	85
3,8	67	67	93	73	73	103	81	104	81
3,9	64	64	90	70	70	99	78	100	78
4	62	62	86	68	68	95	75	96	75
4,1	59	59	83	65	65	92	93	93	73
4,2	58	58	81	63	63	89	90	90	70
4,3	**56**	**56**	**78**	**62**	**62**	**87**	**87**	**87**	**68**
4,4	54	54	76	60	60	84	85	85	66
4,5	53	53	74	58	58	82	83	83	65
100%									
COP	**D 2,97**			**D3,77**			**D6**		
-	**L100**	**L200**	**L300**	**L100**	**L200**	**L300**	**L100**	**L200**	**L300**
3,5	76	76	76	84	84	84	103	122	122
3,6	71	71	71	79	79	79	97	115	115
3,7	68	68	68	75	75	75	92	109	109
3,8	65	65	65	72	72	72	88	104	104
3,9	62	62	62	69	69	69	85	100	100
4	60	60	60	66	66	66	82	96	96
4,1	58	58	58	64	64	64	79	93	93
4,2	56	56	56	62	62	62	76	90	90
4,3	**54**	**54**	**54**	**60**	**60**	**60**	**74**	**87**	**87**
4,4	53	53	53	59	59	59	72	85	85
4,5	52	52	52	57	57	57	70	83	83

As in the previous case, shorter *PBT* values are obtained by increasing the *COP* value with values on average higher than the use of absorption heat pumps. The distribution of the lowest values, except for a 100% coverage of the demand is not homogeneous: for 32% coverage the lowest *PBT* are obtained for L_{BHE}=200 m and $D_{drilling}$=2.97-3.77 inch, while in the three following scenarios (37-41-46% of *H*) they are obtained for L_{BHE}=100-300 m. With a coverage of 57% of *H*, we have for

L_{BHE}=300m, and finally for the same diameters we have minimum *PBT* to increase of *COP* for drilling lengths of 100 and 200 m.

Comparing the *PBT* relative to the efficiency values of the heat pumps used in this study (Table 34), chosen during the phase of defining investment costs, it was found that the minimum absolute value obtainable of the *PBT* is 34 years and is obtained by using an absorption heat pump with coverage of the heat requirement *H* of 70% with a diameter and length of peroration respectively equal to $D_{drilling}$ = 2.97 inches and L_{BHE} = 100 m.

The use of an electric heat pump in the best of cases allows instead to reach a minimum *PBT* value equal to 53 years with $D_{drilling}$ = 2.97 inches, L_{BHE} = 300 m and with coverage of the heat requirement of 57%.

Table 31 Payback time values (years) for GCAHP(GUE=1.25) and GCEHP(COP=4.3) depending on, Ddrilling, LBHE and percentage (%) of H coverage.

GUE=1,25	**D2.97**			**D3.77**			**D6**		
%of H	**L100**	**L200**	**L300**	**L100**	**L200**	**L300**	**L100**	**L200**	**L300**
32%	95	150	204	102	163	225	133	226	319
38%	60	109	157	67	121	175	94	177	259
41%	76	119	162	81	130	179	106	180	253
46%	67	105	143	72	115	158	94	159	223
57%	54	85	116	58	93	127	76	128	181
70%	**34**	60	85	38	66	94	52	95	137
100%	49	49	66	53	53	73	73	73	103
COP=4,3	**D2.97**			**D3.77**			**D6**		
%of H	**L100**	**L200**	**L300**	**L100**	**L200**	**L300**	**L100**	**L200**	**L300**
32%	97	121	97	106	134	106	107	107	148
38%	86	108	86	94	119	94	95	95	132
41%	72	92	72	80	101	80	113	80	113
46%	72	89	72	79	98	79	108	137	108
57%	67	67	**53**	74	74	58	82	105	82
70%	56	56	78	62	62	87	87	87	68
100%	54	54	54	60	60	60	74	87	87

These results mean that a geothermal system coupled to an absorption heat pump, with partial coverage of the heat requirement, is the best possible choice from an economic point of view compared to the coupling of the electric heat pump.

These values in the remaining scenarios for 89% of the cases are higher than the nominal life (~50 years) of the system, making them in fact unattainable from an economic point of view.

For this reason, during the simulation phase, this second typology was not taken into consideration.

5.6 FEFLOW simulations

As a preliminary analysis, the difference in the temperature trend of the heat carrier fluid using or not the plugin.

The analysis was done for "scenario 1" for a probe length of 100m.

During the phase change of the water (from fluid to ice) present between the pores of the subsoil, as already explained in chapter 3, latent heat is released.

The heat released allows higher temperatures to be maintained than in a model where this phenomenon is not considered.

The following graphs Fig. 59 show the temperature trend (Simulation time:1year) of the thermo-vector fluid inside the inlet and outlet probes of the system that perform a geo-exchange.

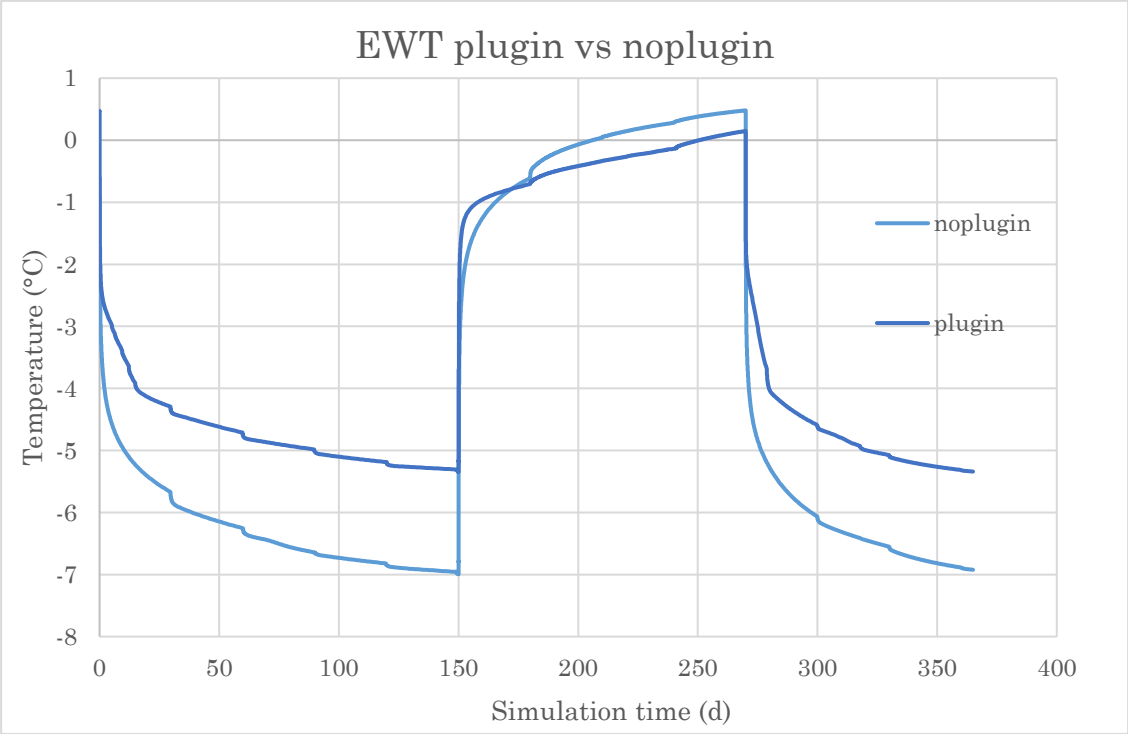

Fig. 59 EWT trend using Plugin and without Plugin, simulation time (365 d), Scenario 1, L_{BHE}=100m, GUE=1.25.

As you can see from the two graphs the temperature in the case of the model with the plugin has average temperatures of 0.8 ° C higher than without the plugin.

This value allows to maintain higher values of minimum temperatures (*EWT*=-10°C) at the exit of the system and with benefits on the *GUE* of the heat pump and the efficiency of the system.

This result shows that with a single probe it is possible to keep within certain operating constraints and how this technology can be used in soils with even colder temperatures.

At the same time, however, the effect of temperature on permafrost and the problems associated with soil swelling and foundations could be underestimated.

The remaining simulations have been carried out using the plugin as it allows to have a model with more realistic simulations.

5.6.1 Results with 32% coverage of heat demand with GCHP

Covering a thermal load of 32%, the G_{peak} is equal to 2.2kW and minimum temperatures are obtained in absolute terms. The results show that as depth increases, the effect of the geothermal gradient (ΔT=+20C°/km) becomes increasingly important. At the same time, as the diameter increases, there is a more efficient heat exchange thanks to a larger contact surface and a lower thermal resistance and therefore a higher *EWT*.

During the 90 days of summer when the heat pump never starts working, the temperature of the heat carrier fluid rises to the next starting value with an average loss of half a degree, which over 20 years remains constant. At the end of the 90th day on which the temperature peak is reached, it begins to fall again and ends the remaining days of the year, starting the cycle of lowering and raising the temperature again.

The minimum peak after 10 years has decreased compared to that of the first year by about 1.5÷2°C and tends to remain constant.

Below are the graphs of the trend of T_{in}(red) and T_{out}(out) of BHE, for the 3 scenarios and lengths (100-200-300) of drilling (Fig. 60Fig. 61Fig. 62).

In Fig. 63 are shown the trend of the power supplied *Pf(kW)* for a simulation time of 7300 d, for the 1ts scenario and lengths(100-200-300), while in Fig. 64 and Fig. 65 are shown the trend of *Pf(kW)* for the 2ts and 3ts scenario and length 100m.

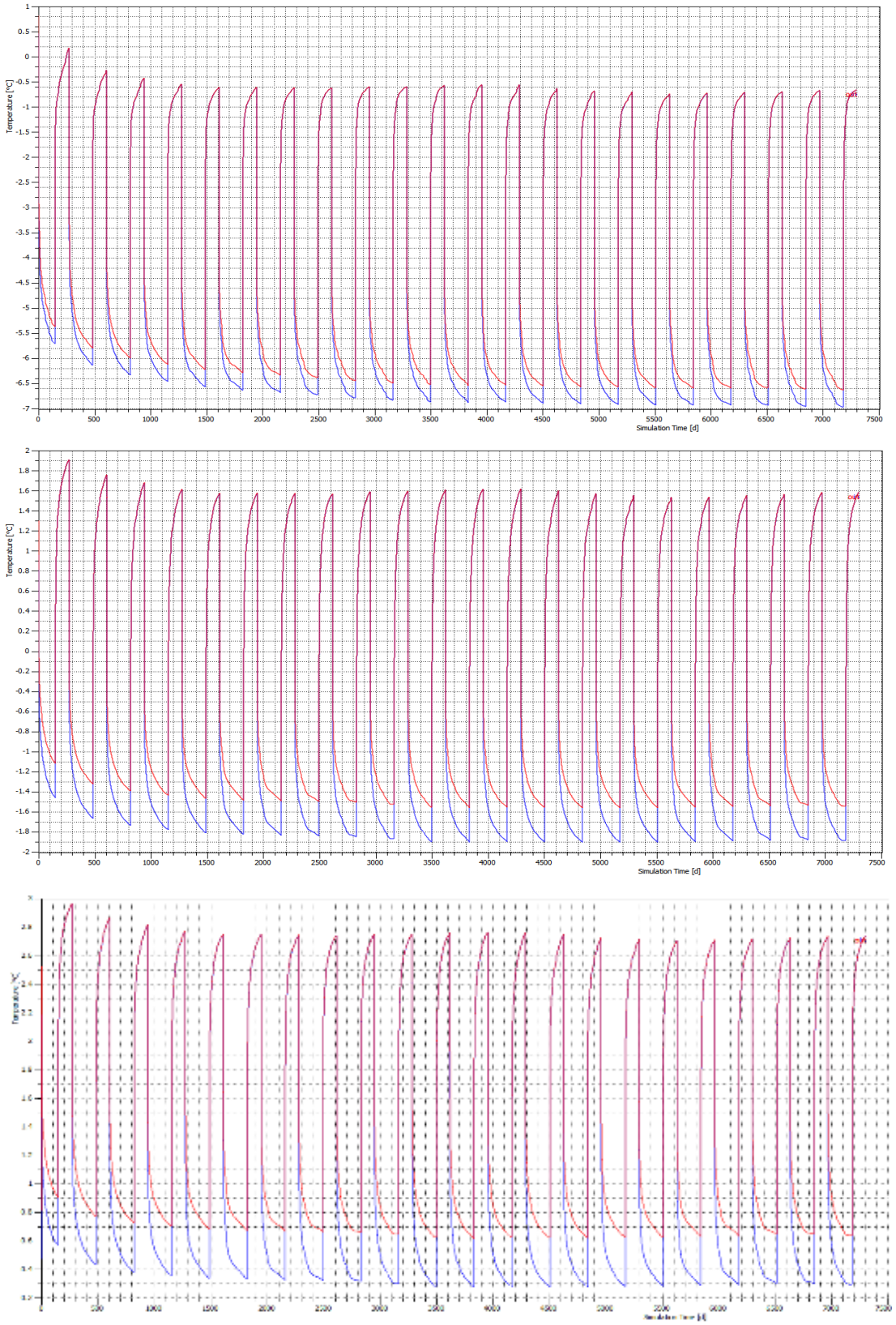

Fig. 60 T_{in}(red) and T_{out}(out) BHE trend Scenario1 ($D_{drilling}$ = 2.97 in.; L_{BHE} = 100 – 200 – 300 m; Simulation time = 7300d).

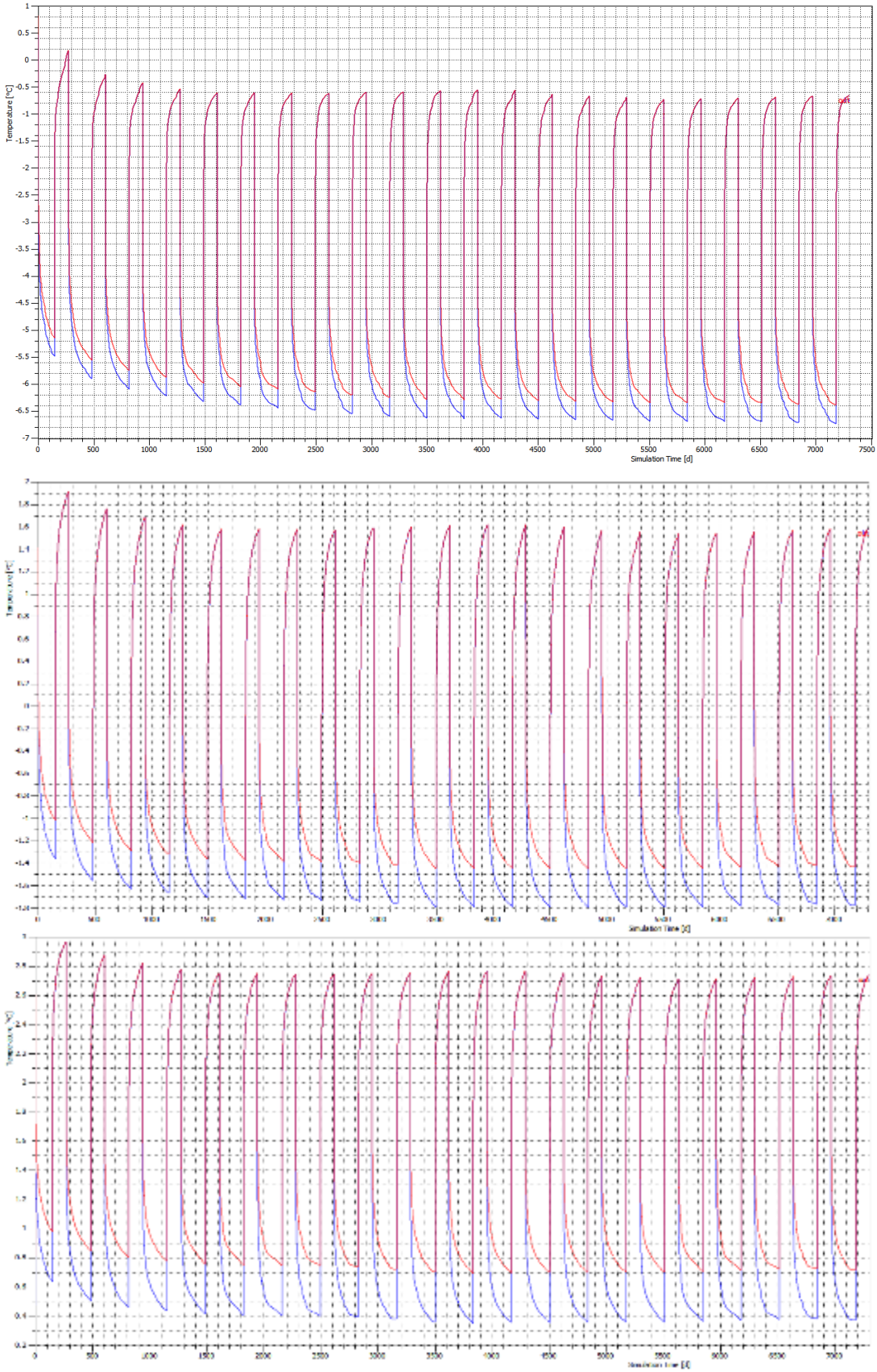

Fig. 61 Tin(red) and Tout(blu) BHE trend Scenario 2 (Ddrilling=3.77inch; LBHE=100-200-300 m; Simulation time=7300d)

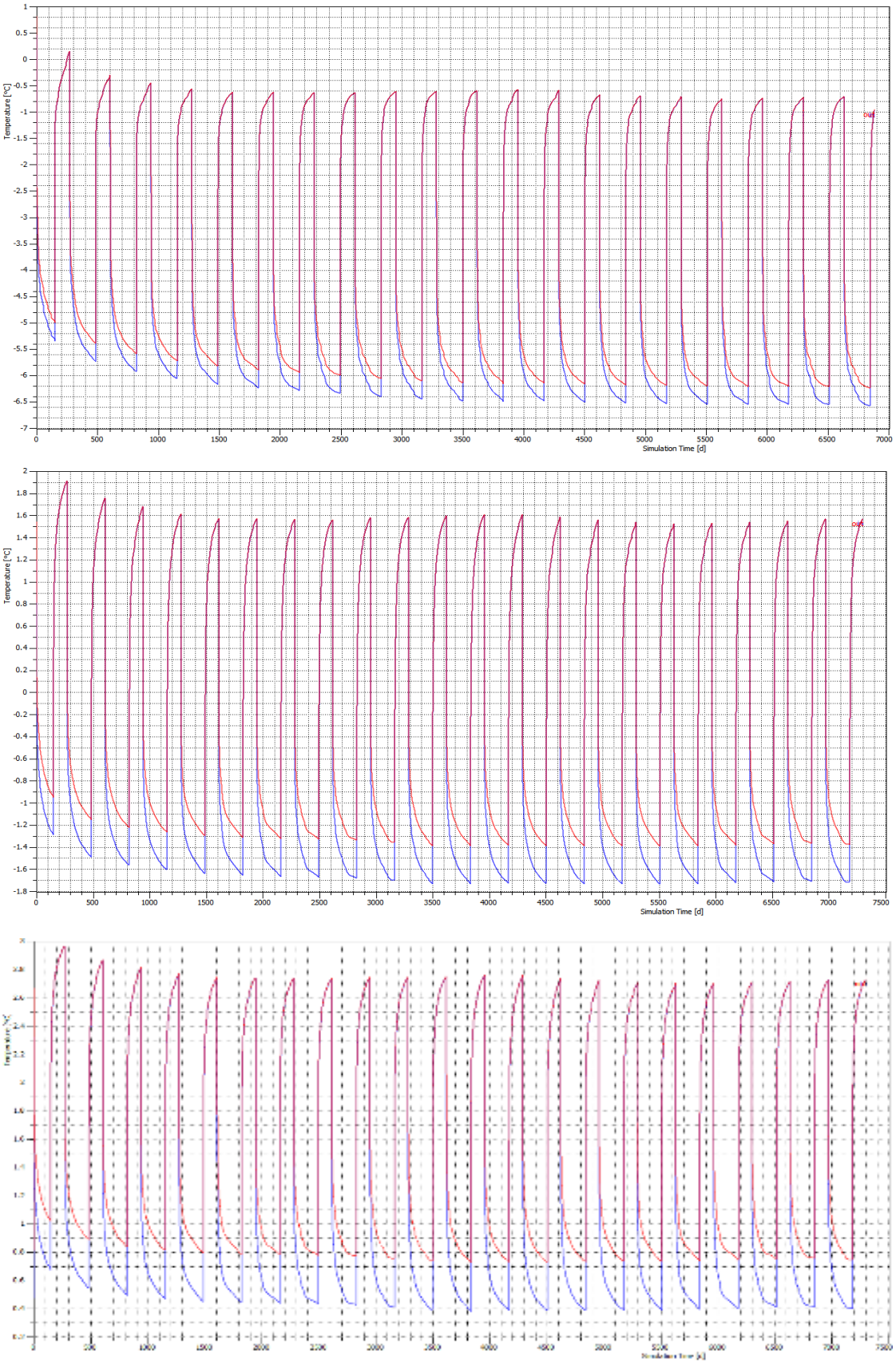

Fig. 62 Tout(blu) and Tin(red) BHE trend Scenario 3 (Ddrilling=6 inch; LBHE=100-200-300 m; Simulation time=7300d)

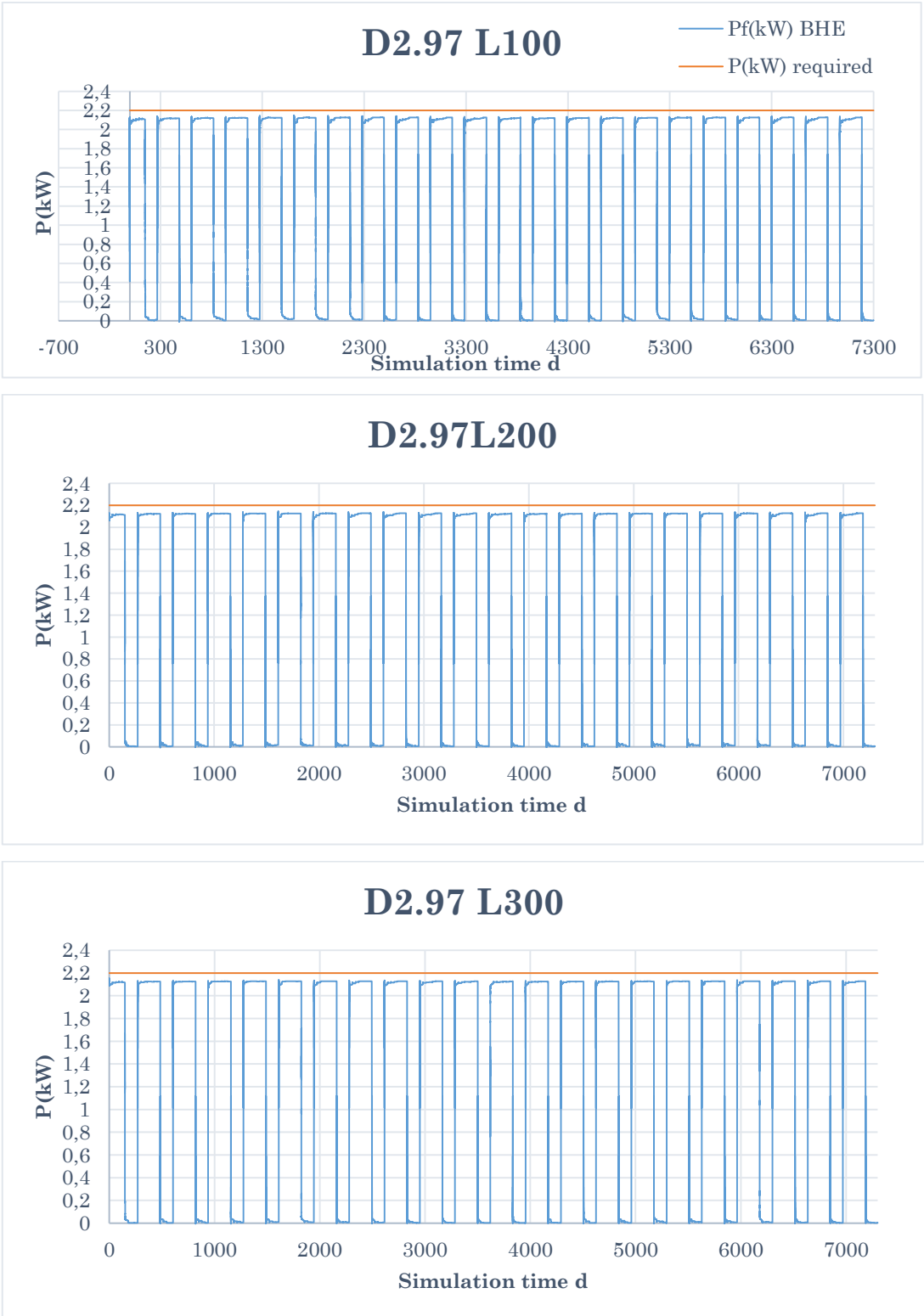

Fig. 63 Pf(kW) (blu) trend Scenario1 (Ddrilling=2.97; LBHE=100-200-300; Simulation time=7300d) and P=2.2kW (red).

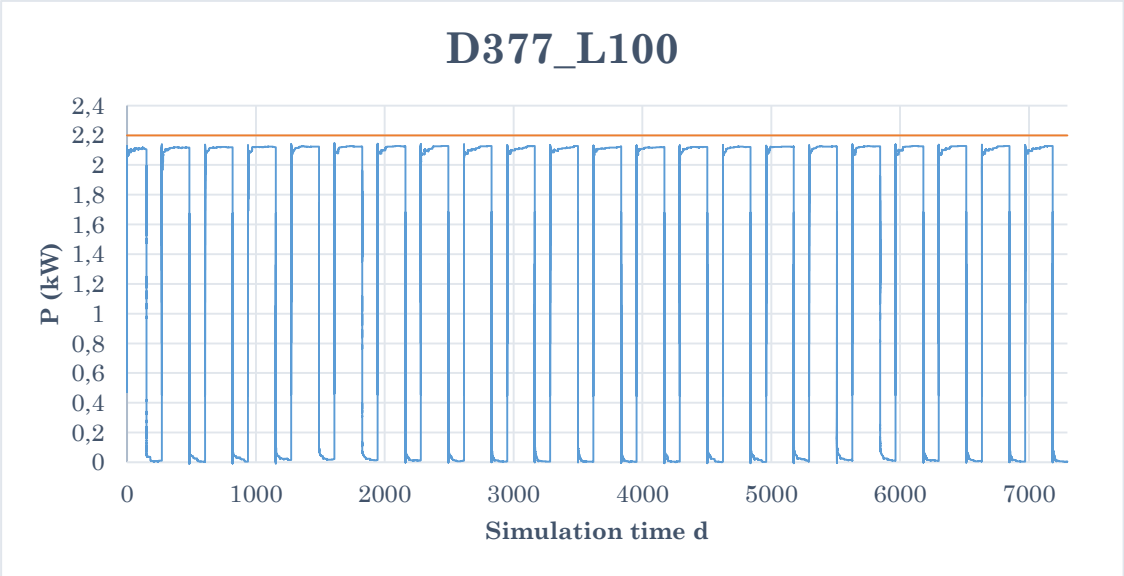

Fig. 64 Pf(kW) (blu) trend Scenario 2(Ddrilling=3.77; LBHE=100; Simulation time=7300d) and P=2.2kW (red).

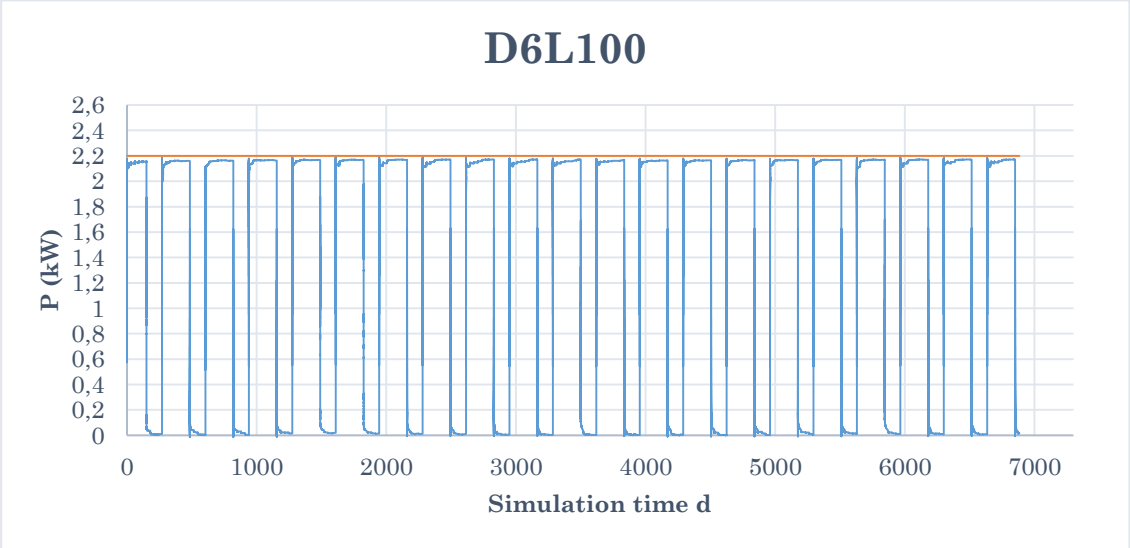

Fig. 65 Pf(kW) (blu) trend Scenario3 (Ddrilling=2.97; LBHE=100; Simulation time=7300d) and P=2.2kW (red).

The results obtained for the 3 Scenarios show that the thermal power extracted is very close to the Peak load ground value with an average of 2.15 kW during the heating period.

This, in line with the trend of the tin and tout temperature of the BHE, has values equal to 0 in the summer periods and peaks in the period of operation, i.e. in the 275 winter days.

The value of *Pf*, although not exactly reaching the required value, is sufficient because in a real plant the thermal load required by the ground will not always be peak but variable.

The minimum temperatures reached by the heat carrier fluid vary according to the 9 scenarios. As the diameter and length of the probe increase, the same results in terms of thermal power are obtained, but with considerably higher operating temperatures that are more favourable to the efficiency of the heat pump.

Below are the values of *EWTmin* during the 7300d simulation of all 3 scenarios:

Table 32 Values of minimum Entering Water Temperature (EWT_{min}).

Scenario 1	
L	**EWTmin**
100	-6.60
200	-1.55
300	0.72
Scenario 2	
L	**EWTmin**
100	-6.40
200	-1.45
300	0.70
Scenario 3	
L	**EWTmin**
100	-6.00
200	-1.40
300	0.74

As you can see in all the values do not exceed the limit value $EWT_{\lim}10°C$ therefore achievable.

The minimum *EWT* values are reached for drilling depths of 100 (-6÷-6.6 °C), while doubling the length reduces the *EWT* value by 76%. For lengths of 300m the *EWT* does not even reach the freezing temperature. This change in efficiency, due to the Tin instead, was measured by recalculating the *GUE* of the heat pump with the

2nd degree empirical polynomial formula for a type of diesel-powered pump proposed by Belzile et al. 2017.

$$\mathrm{GUE} = -1.0812 \cdot 10^{-4} \cdot \mathrm{Tin}^2 + 7.9233 \cdot 10^{-3} T_{in} + 1.4368$$

The following table shows the minimum outlet temperatures and the relative *GUE* calculated with the empirical formula:

Table 33 Tin and GUE calculated with the formula of Belzile et al.2017

Scenario 1		
L	**Tin min (°C)**	**COP (Belzile et al.)**
100	-6.90	1.38
200	-1.90	1.42
300	0.28	1.44
Scenario 2		
L	**Tin min (°C)**	**COP (Belzile et al.)**
100	-6.70	1.38
200	-1.80	1.42
300	0.37	1.44
Scenario 3		
L	**Tout min (°C)**	**COP (Belzile et al.)**
100	-6.4	1.38
200	-1.7	1.42
300	0.4	1.44

It can be observed that as the depth decreases, colder temperatures are reached with lower *GUE* performance compared to longer lengths L_{BHE}.

This result is consistent with the thermal conditions of the soil and the low thermal gradient.

For all three scenarios, probe lengths of 200 and 300 m result in an EWT value of less than -10°C and therefore compatible with heat pumps.

The GUE resulting from the empirical formula confirms, even if in general a decreasing trend in the efficiency of the heat pump as the flow temperature decreases, which makes it preferable to choose probes longer than 100m.

Finally, it can be said that with configurations of this type it does not fully exploit the potential of the ground and the heat pump.

The second scenario in which 70% of H is expected to be covered was then analysed.

5.6.2 Results with 70% coverage of heat demand with GCHP

It was decided to concentrate the studies, in the case of coverage of energy needs up to 17KW, $D_{drilling}$=2.97-3.77 inch, L_{BHE}=100 because they are the configuration, in economic terms with the lowest payback time ever (*PBT*=34 - 38 y). The Fig. 65 shows the trend of the T_{in} and T_{out} of BHE of length 100, for a *Gpeak* of 3.5 kW, with a covering of thermal demand of 70%.

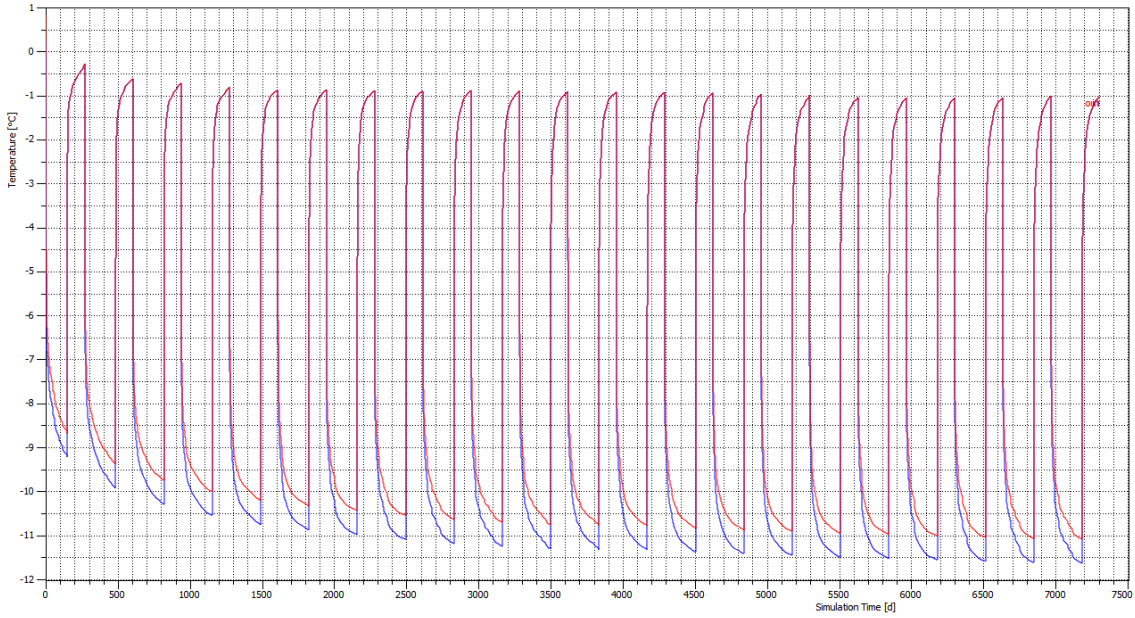

Fig. 66 Tin(blue) and Tout(red) BHE trend Scenario 1 (Ddrilling=6 inch; L_{BHE}=100-m; Simulation time=7300d)

It is evident how the modest depth of the probe and influence the temperature in and out of the heat carrier fluid with *EWT* is close to -11°C and -12°C higher than the *EWT*=-10°C.

The value of power during the year is Pf~3.3 kW, in line with the results obtained with a coverage of 32%.

A value that can be considered acceptable considering that the simplified model of the thermal load has a constant load (17kW) and therefore with the ground that

is subject to "extraction" with a constant value over time of heat and therefore with more severe conditions than are expected in reality.

Considering a minimum temperature T_{in}= -11.5 °C, the efficiency of the heat pump has been calculated with Belzile et al. which was equal to *GUE*(Belzile et al.)=1.33.

Finally, we observe in Fig.67 that increasing the dimeter (Ddrilling=3.77inch) the values of Tin e Tout do not vary.

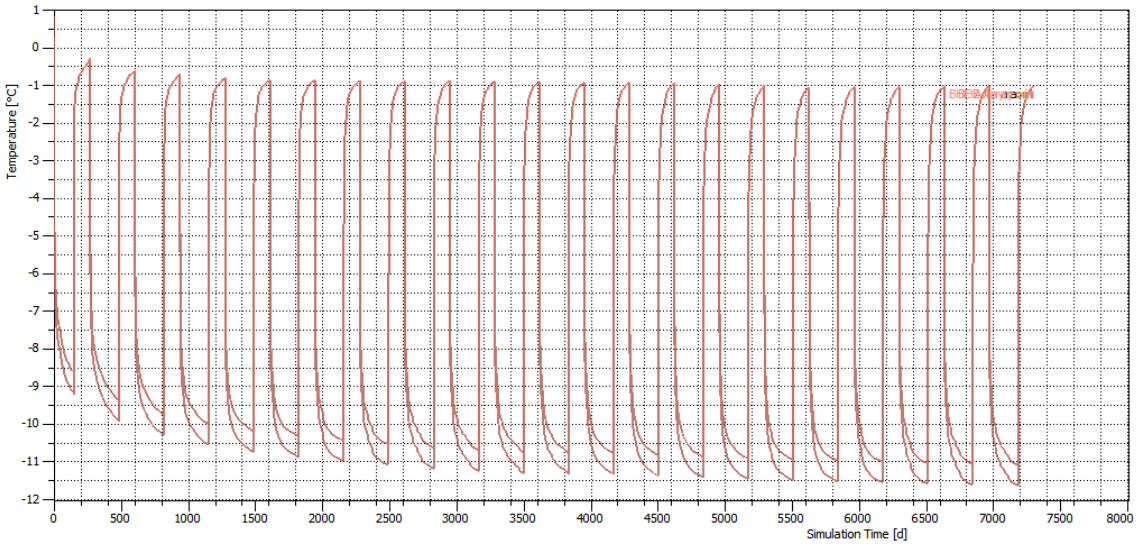

Fig.67 Tin(blue) and Tout(red) BHE trend Scenario 2 (Ddrilling=3.77 inch; LBHE=100-m; Simulation time=7300d)

It can be concluded that a 70% coverage would be preferable because it would not induce cycles of freezing and thawing in the subsoil, risking influencing the stability of the surrounding buildings. Once the system is launched, the temperature of the subsoil would probably remain below the melting T and we should not worry about the stability of the buildings.

From a technical point of view the Tin of the fluid passes -10°C, so technically the heat pump stops working (given the limit defined above). It also does not fit with the GPOT limit (-10°C).

Nevertheless, due to the conservative values of the thermal load model and the EWT, it is possible that the heat pump will work without any problems.

5.6.3 Ground thermal response

A particularly important aspect for the efficiency of geothermal heat pumps is the sustainability of the heat source and care must be taken to avoid the depletion of thermal energy. For this purpose, it is very important to recharge the ground.

As shown in Fig. 68, in fact, after only one working season in heating mode, the soil is able to recharge almost completely naturally, but over a period of 20 seasons it is able to cool the soil constantly with a Δt=-1°C.

The example shows the simplified case of a probe (L_{BHE}=100m, $D_{drilling}$=2.97inch) subject to constant winter load with 70% coverage of the heat requirement and corresponding to a thermal load of 23.65MWh/y.

The probe was placed at a distance of about 5.5 m from the house and thanks to the observation points defined during the modelling phase, the temperature trend was measured for different depths and distance from the BHE. The graph shows the ground temperatures for 7300[d] at a distance of 5m from the probe and at a depth of 1m(black)-40m(blue)-100m(blue)-150m(orange)-200m(red)-300m(brown).

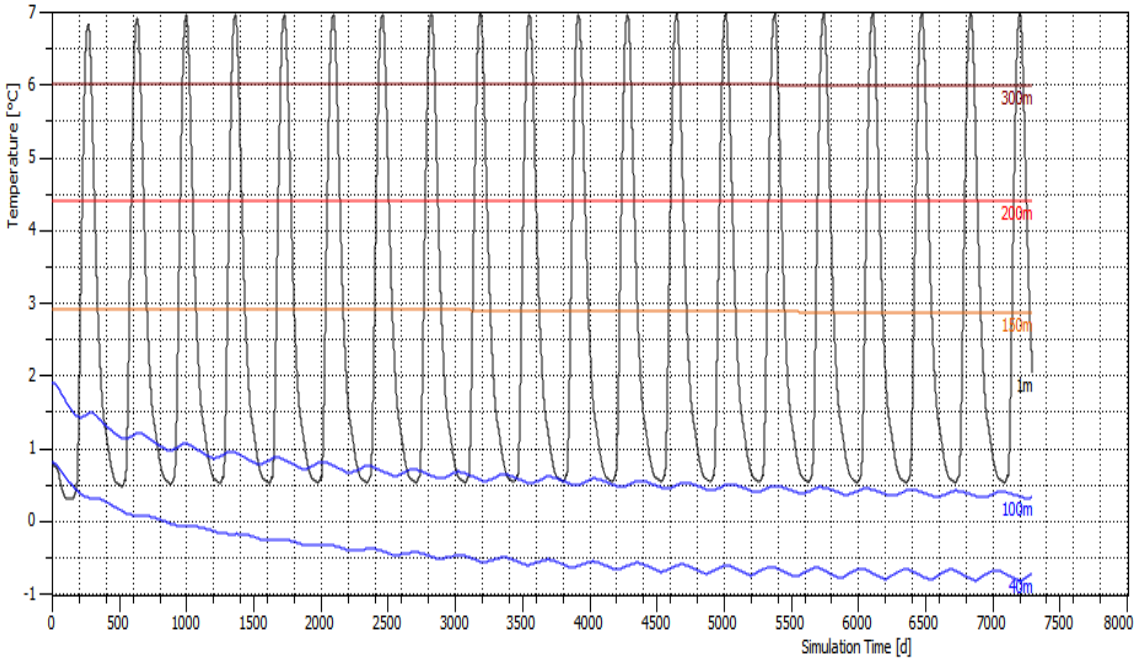

Fig. 68 Ground temperature at 5m from the BHE and at a depth of: 1-40-100-150-200-250-300 m

Three different types of curves can be distinguished from the graph:

In the upper part the 3 curves of 150-200-300m with constant trend of the temperature values; respectively of T_{150}=+3°C, T_{200}=+4.5°C and T_{300}=+6°C. At such depths the ground does not appear to be influenced by the heat extraction activity of the probe, but only by the geothermal gradient coming from below.

The second type is characterised by the temperature curve measured at 1 metre from the ground level. It has a markedly cyclical course where the difference between maximum and minimum is Δt=7.5°C. At this depth the soil is almost exclusively influenced by the atmospheric surface temperature and the solar radiation and therefore with cycles that are exclusively due to the alternation of seasons.

Finally, with the third type of curve, positioned in the lower part of the graph, it can be seen that at a depth of 40 and 100 metres, with the latter corresponding to the depth of the BHE, the average temperature of the ground is reduced by the heat demand from the building to the ground.

As shown in *Fig. 68*, in fact, after only one working season in heating mode, the soil is able to recharge almost completely naturally, but over a period of 20 seasons it is able to cool the soil constantly with a Δt=-1°C, reaching the water freezing temperature.

Interrupting the operation of the plant in the summer period (Fig. 69) allows a recovery of thermal energy that even if minimal, dampens a temperature trend that without this measure would be more pronounced.

This highlights how important it is to allow the thermal regeneration of the soil in the alternation of the summer and winter seasons.

On the other hand, freezing/thawing cycles of the soil can lead to swelling and subsidence of the ground where the foundations of the houses rest.
Moreover, as shown in figure Fig. 71, the lowest temperatures are reached between 20-25m in correspondence of quaternary deposits. This geological formation, having a higher porosity, has a higher water content inside the pores and therefore more pronounced freezing phenomena.

For this reason, it is important to ensure that during the period of heat extraction the thermal plume of the probe does not excessively affect the perimeter of the houses, or that temperatures below 0 ° C are not reached.

Since in this model the probe is positioned at a distance of 5.5m, it has been verified that for a depth of 25m in the 7300d of simulation time, which corresponds

to the last day of operation of the plant before the summer period of the 20th year of the life cycle, the thermal plume exceeds the property boundary of the house by a few meters, so the probe should be positioned at a distance of at least 8m.

Assuming to place a probe for each user, given a procedure between the perimeter of the houses of about 30m, it would result in a distance between the probes of about 6m with the resulting mutual interference.

Therefore, during the installation phase, an optimal positioning configuration should be analysed with appropriate distances to the houses probes of 8 metres (Fig. 72).

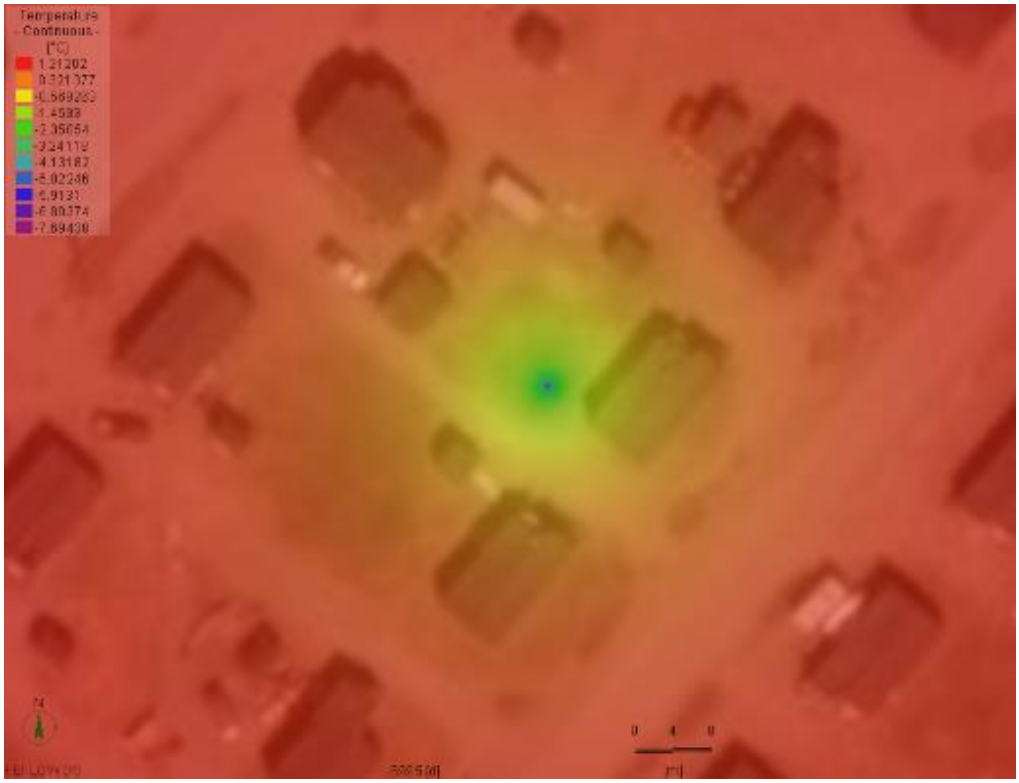

Fig. 69 Ground temperature during summer

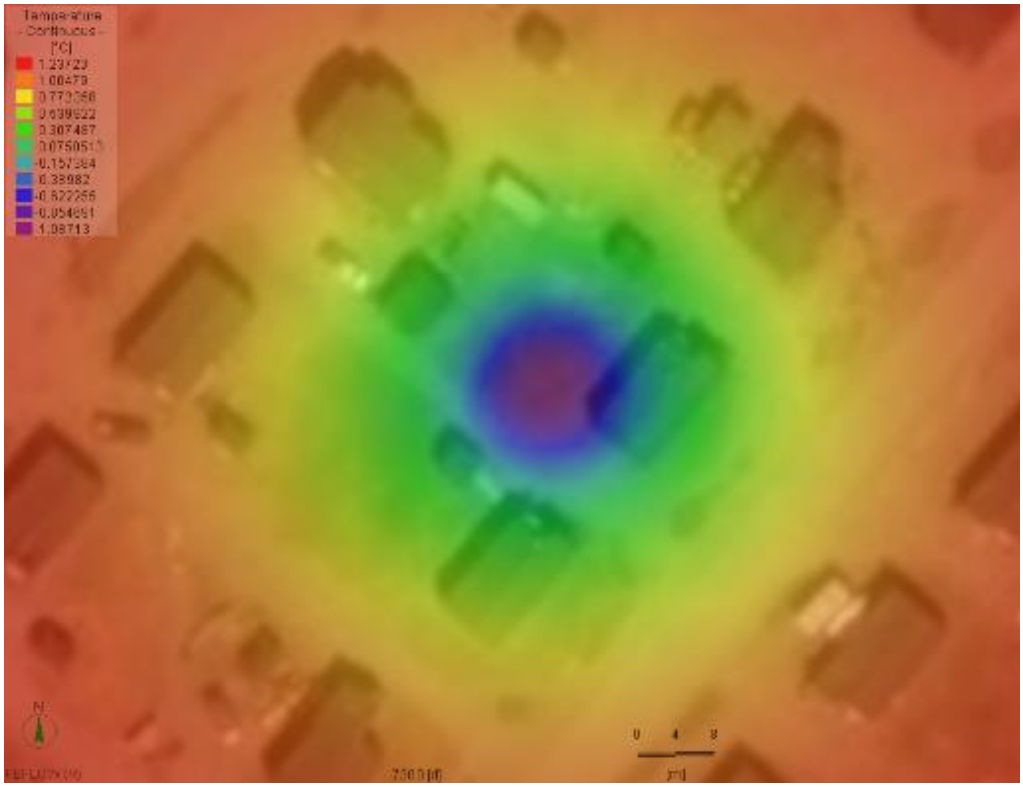

Fig. 70 Ground temperature at the last day of operation in heating mode.

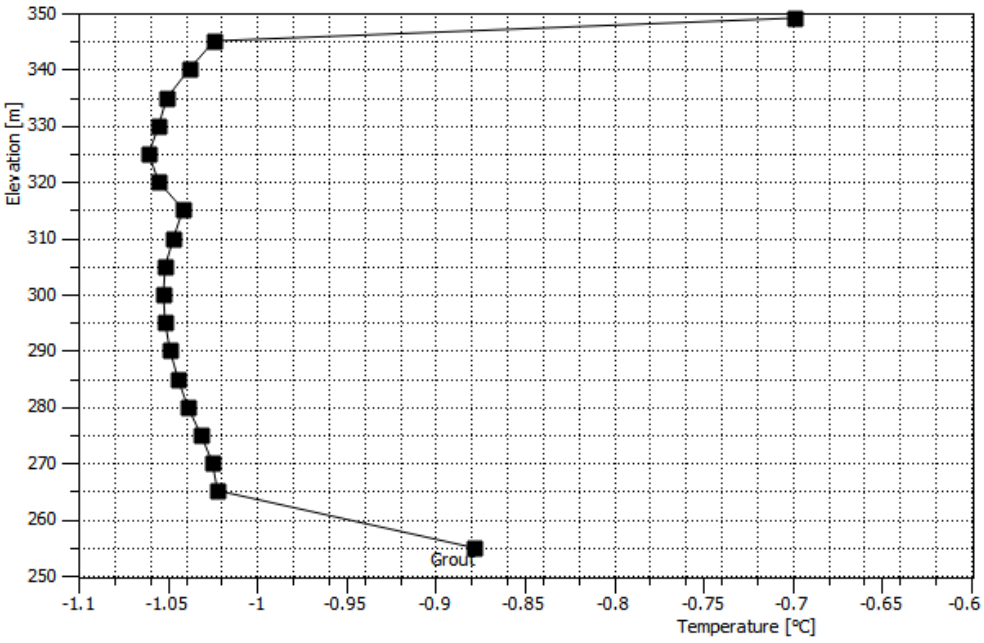

Fig. 71 Temperature of the grout depending on elevation(m).

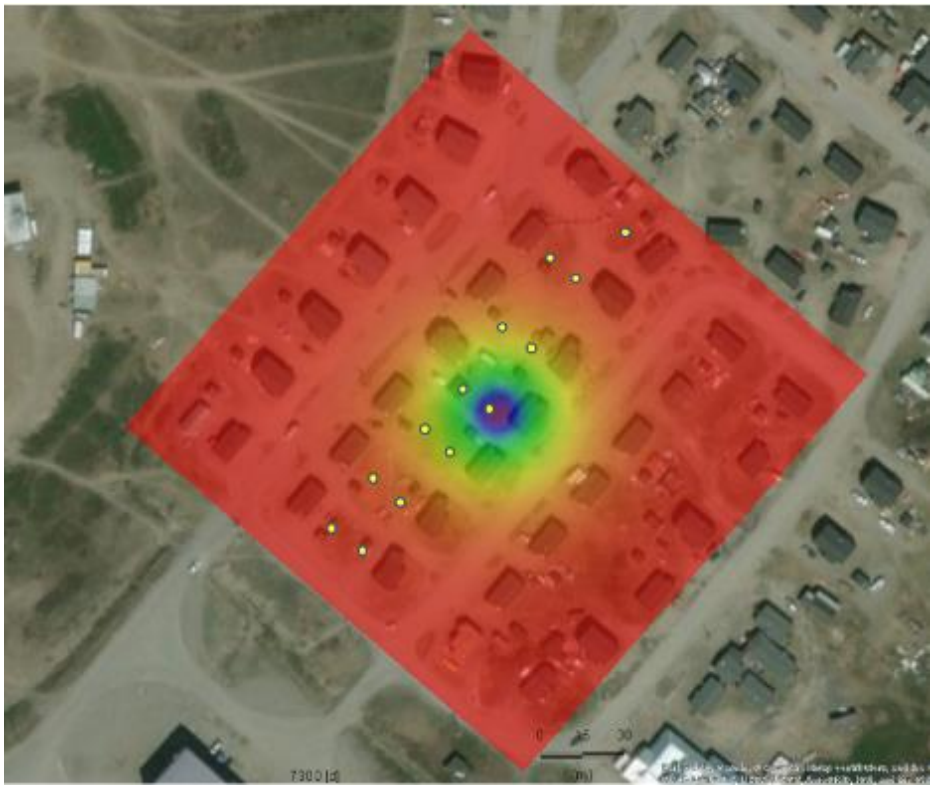

Fig. 72 BHE arrangement.

6 CONCLUSION

Vertical GCHP systems can be installed to extract thermal energy in areas with very low geothermal gradients and provide heat for domestic heating and domestic water and replace heating systems powered by fossil fuels.

Its applicability, however, must be verified through a feasibility analysis that must consider the existing energy context, available technologies and geo-climatic conditions of the area of interest.

Extracting heat at shallow depths in the community of Kuujjaq in northern Quebec involves working with a harsh climate, a very low geothermal gradient (+20°C/km) and the presence of shallow permafrost.

Communities like this, present in the North of Quebec (Nunavik-Canada), in fact, live totally disconnected from the rest of the region producing thermal energy through boilers installed in each housing unit with an estimated heating need of 33.58 MWh/y, and as the only source of power fuel oil.

Given the scarcity of groundwater resources, it was decided to study the feasibility of closed-loop geothermal system.

Three technologies were compared, which are a fuel oil boiler (base case scenario), an absorption geothermal heat pump driven by a diesel engine and a compression geothermal heat pump with electricity geothermal heat pump provided by a diesel generator.

As suggested in the literature due to the low geothermal gradient, the high heat demand and the presence of permafrost, the economic and technological feasibility was studied with total or partial coverage of the heat demand or 32-37-41-46-57-70%.

The commercially available absorption heat pumps generally have a minimum water inlet temperature of -12°C, while those with an electric compressor have a minimum water inlet temperature of -5°C. It has been assumed that the heat pump will be supplied with diesel fuel.

The performance of the GCHP systems made it possible to achieve energy savings compared to a conventional boiler, which was as high as possible, in the case of coverage of 70% and 57% of the heat requirement with a drilling diameter of 2.97 inches and a drilling length of 100 and 200m respectively.

The fuel oil boiler would have required 3774 L of fuel oil per year, at a cost of $5661 CAD. The use of heat pump absorption showed more interesting results with 797 $CAD of savings per year and 532 L of fuel oil while the heat pump with electric compressor showed a saving of 2539$CAD with an annual consumption of diesel equal to 2807 L. The return on investment for a ground absorption heat pump system could be about 34 years, considering an estimated unit heat pump price of $7500CAD and $20000CAD for drilling and installing the BHE, while neglecting the operating costs of the recirculation pump. A heat pump system with electric compressor could have a PBT less interesting than 53 years with heat pump cost of should cost ~17000$CAD.

In both cases such results have been obtained assuming to use to share a heat pump for two users, thus halving the investment costs.

At the same time, it has been recorded that as the GUE/COP increases the PBT values decrease while they tend to increase as the drilling diameter and length of the BHE increases.

While the initial investment costs as the GUE/COP increases also increase, with the influence of drilling costs it is higher than that of the heat pump. The latter has less influence as the GUE/COP increases.

The annual savings show an upward trend, with GUE/COP values and increasing percentages of heat requirement coverage.

Simulations carried out using the FEFLOW numerical code showed that with a GCAHP system a thermal load coverage of 70% is possible to supply a thermal power of about 3.5kW with EWTmin=-11°C, a value considered acceptable given the conservativity of the EWT and thermal load inserted in the model.

In the same way it was observed that the use of a plugin that takes into account the phase change within the pores, increases the values of the EWT thanks to the latent heat released during the phase change and with the increase in thermal conductivity. The higher thermal conductivity of ice water can be considered an advantage over the liquid state of the water in this respect.

The simulations show that the soil freezes and defrosts every year but with a gradual and constant cooling. The probe under the conditions of the last day of operation in heating mode, generates a thermal plume with T<°C that in the absence of underground groundwater flow has a radial-symmetrical expansion, with a maximum radius of about 8 meters. For this reason, during the installation phase,

an installation configuration must be found that keeps the probes sufficiently distant from the houses so as to avoid subisdence of the ground and differential subsidence for the houses and at the same time maintain a sufficient distance between the probes so as to avoid phenomena of thermal interference that could affect the performance of the system.

Future studies can be addressed in the design of diesel heat pumps and in the analysis of thermal interference between the probes.

7 APPENDIX

Table 34 Number of BHE coupled with adsorption heat pump depending on the percentage of coverage of the Heat load, GUE, Ground peak load (Gpeak), ground Energy (E), Drilling diameters and BHE lenght L.

26.4 kW												
FURNACE			**BHE+HEAT PUMP**				**Peak load**			**Heat load**		
MWh		**%**	**MWh**			**%**	**kW**			**MWh/y**		
0		0	33.58			100%	26.4			33.58		
						n° BHE						
GUE	G_{peak}	**E**	**D 2.97**			**D 3.77**				**D 6**		
-	**kW**	**MWh/y**	**L100**	**L200**	**L300**	**L100**	**L200**	**L300**		**L100**	**L200**	**L300**
1.1	2,4	7,10	1	1	1	1	1	1		1	1	1
1.2	4,4	13,02	2	1	1	2	1	1		2	1	1
1.25	5,3	15,63	2	1	1	2	1	1		2	1	1
1.3	6,1	18,03	2	1	1	2	1	1		2	1	1
1.4	7,5	22,33	2	1	1	3	1	1		2	1	1
1.5	8,8	26,05	3	2	1	3	2	1		3	1	1
1.6	9,9	29,30	3	2	1	3	2	1		3	2	1
1.7	10,9	32,18	3	2	1	3	2	1		3	2	1
1.8	11,7	34,73	4	2	1	4	2	1		3	2	1
1.9	12,5	37,02	4	2	1	4	2	1		3	2	1
2	13,2	39,07	4	2	1	4	2	2		4	2	1
10 kW												
FURNACE			**BHE+HEAT PUMP**				**Peak load**			**Heat load**		
MWh		**%**	**MWh**			**%**	**kW**			**MWh/y**		
22.69		68	10.89			32	10			33.58		
						n° BHE						
COP	**P**	**E**		**D 2.97**			**D 3.77**				**D 6**	
-	**kW**	**MWh/y**	**L100**	**L200**	**L300**	**L100**	**L200**	**L300**		**L100**	**L200**	**L300**
1.1	0,9	2,69	1	1	1	1	1	1		1	1	1
1.2	1,7	4,93	1	1	1	1	1	1		1	1	1
1.25	2,0	5,92	1	1	1	1	1	1		1	1	1
1.3	2,3	6,83	1	1	1	1	1	1		1	1	1
1.4	2,9	8,46	1	1	1	1	1	1		1	1	1
1.5	3,3	9,87	1	1	1	1	1	1		1	1	1
1.6	3,8	11,10	1	1	1	2	1	1		1	1	1
1.7	4,1	12,19	2	1	1	2	1	1		1	1	1
1.8	4,4	13,16	2	1	1	2	1	1		2	1	1
1.9	4,7	14,02	2	1	1	2	1	1		2	1	1
2	5,0	14,80	2	1	1	2	1	1		2	1	1
11 kW												
FURNACE			**BHE+HEAT PUMP**				**Peak load**			**Heat load**		

MWh		%	MWh		%		kW		MWh/y		
21.32		63	12.26		37		11		33.58		
						n° BHE					
COP	**P**	**E**		**D 2.97**			**D 3.77**			**D 6**	
-	**kW**	**MWh/y**	**L100**	**L200**	**L300**	**L100**	**L200**	**L300**	**L100**	**L200**	**L300**
1.1	1,0	2,96	1	1	1	1	1	1	1	1	1
1.2	1,8	5,43	1	1	1	1	1	1	1	1	1
1.25	2,2	6,51	1	1	1	1	1	1	1	1	1
1.3	2,5	7,51	1	1	1	1	1	1	1	1	1
1.4	3,1	9,30	1	1	1	1	1	1	1	1	1
1.5	3,7	10,85	1	1	1	2	1	1	1	1	1
1.6	4,1	12,21	2	1	1	2	1	1	1	1	1
1.7	4,5	13,41	2	1	1	2	1	1	2	1	1
1.8	4,9	14,47	2	1	1	2	1	1	2	1	1
1.9	5,2	15,42	2	1	1	2	1	1	2	1	1
2	5,5	16,28	2	1	1	2	1	1	2	1	1
12 kW											
FURNACE			**BHE+HEAT PUMP**				**Peak load**		**Heat load**		
MWh		%	**MWh**		%		**kW**		**MWh/y**		
19.88		59	13.70		41		12		33.58		
						n° BHE					
COP	**P**	**E**		**D 2.97**			**D 3.77**			**D 6**	
-	**kW**	**MWh/y**	**L100**	**L200**	**L300**	**L100**	**L200**	**L300**	**L100**	**L200**	**L300**
1.1	1,1	3,23	1	1	1	1	1	1	1	1	1
1.2	2,0	5,92	1	1	1	1	1	1	1	1	1
1.25	2,4	7,10	1	1	1	1	1	1	1	1	1
1.3	2,8	8,20	1	1	1	1	1	1	1	1	1
1.4	3,4	10,15	1	1	1	1	1	1	1	1	1
1.5	4,0	11,84	2	1	1	2	1	1	1	1	1
1.6	4,5	13,32	2	1	1	2	1	1	2	1	1
1.7	4,9	14,63	2	1	1	2	1	1	2	1	1
1.8	5,3	15,79	2	1	1	2	1	1	2	1	1
1.9	5,7	16,83	2	1	1	2	1	1	2	1	1
2	6,0	17,76	2	1	1	2	1	1	2	1	1
13 kW											
FURNACE			**BHE+HEAT PUMP**				**Peak load**		**Heat load**		
MWh		%	**MWh**		%		**kW**		**MWh/y**		
19.88		54	13.70		46		13		33.58		
						n° BHE					
COP	**P**	**E**		**D 2.97**			**D 3.77**			**D 6**	
-	**kW**	**MWh/y**	**L100**	**L200**	**L300**	**L100**	**L200**	**L300**	**L100**	**L200**	**L300**
1.1	1,2	3,50	1	1	1	1	1	1	1	1	1
1.2	2,2	6,41	1	1	1	1	1	1	1	1	1
1.25	2,6	7,70	1	1	1	1	1	1	1	1	1

1.3	3,0	8,88	1	1	1	1	1	1	1	1	1
1.4	3,7	10,99	1	1	1	2	1	1	1	1	1
1.5	4,3	12,83	2	1	1	2	1	1	1	1	1
1.6	4,9	14,43	2	1	1	2	1	1	2	1	1
1.7	5,4	15,84	2	1	1	2	1	1	2	1	1
1.8	5,8	17,10	2	1	1	2	1	1	2	1	1
1.9	6,2	18,23	2	1	1	2	1	1	2	1	1
2	6,5	19,24	2	1	1	2	1	1	2	1	1
15 kW											
FURNACE			**BHE+HEAT PUMP**				**Peak load**		**Heat load**		
MWh		**%**	**MWh**		**%**		**kW**		**MWh/y**		
14.39		43	19.19		57		15		33.58		
						n° BHE					
COP	**P**	**E**		**D 2.97**			**D 3.77**			**D 6**	
-	**kW**	**MWh/y**	**L100**	**L200**	**L300**	**L100**	**L200**	**L300**	**L100**	**L200**	**L300**
1.1	1,4	4,04	1	1	1	1	1	1	1	1	1
1.2	2,5	7,40	1	1	1	1	1	1	1	1	1
1.25	3,0	8,88	1	1	1	1	1	1	1	1	1
1.3	3,5	10,25	1	1	1	1	1	1	1	1	1
1.4	4,3	12,69	2	1	1	2	1	1	1	1	1
1.5	5,0	14,80	2	1	1	2	1	1	2	1	1
1.6	5,6	16,65	2	1	1	2	1	1	2	1	1
1.7	6,2	18,28	2	1	1	2	1	1	2	1	1
1.8	6,7	19,73	2	1	1	2	1	1	2	1	1
1.9	7,1	21,03	2	1	1	2	1	1	2	1	1
2	7,5	22,20	2	1	1	3	1	1	2	1	1
17 kW											
FURNACE			**BHE+HEAT PUMP**				**Peak load**		**Heat load**		
MWh		**%**	**MWh**		**%**		**kW**		**MWh/y**		
9.93		30	26.65		70		17.5		33.58		
						n° BHE					
COP	**P**	**E**		**D 2.97**			**D 3.77**			**D 6**	
-	**kW**	**MWh/y**	**L100**	**L200**	**L300**	**L100**	**L200**	**L300**	**L100**	**L200**	**L300**
1.1	1,6	4,71	1	1	1	1	1	1	1	1	1
1.2	2,9	8,63	1	1	1	1	1	1	1	1	1
1.25	**3,5**	**10,36**	**1**	**1**	**1**	**1**	**1**	**1**	**1**	**1**	**1**
1.3	4,0	11,95	2	1	1	2	1	1	1	1	1
1.4	5,0	14,80	2	1	1	2	1	1	2	1	1
1.5	5,8	17,27	2	1	1	2	1	1	2	1	1
1.6	6,6	19,43	2	1	1	2	1	1	2	1	1
1.7	7,2	21,33	2	1	1	2	1	1	2	1	1
1.8	7,8	23,02	3	1	1	3	1	1	2	1	1
1.9	8,3	24,54	3	2	1	3	2	1	2	1	1
2	8,8	25,90	3	2	1	3	2	1	3	1	1

Table 35 Number of BHE coupled with electric heat pump depending on the percentage of coverage of the Heat load, COP, Ground peak load (Gpeak), ground Energy (E), Drilling diameters and BHE lenght L.

26.4kW												
FURNACE			**BHE+HEAT PUMP**				**Peak load (P)**			**Heat load (H)**		
MWh		**%**	**MWh**		**%**		**kW**			**MWh/y**		
0		0	33.58		100		26.4			33.58		
						n° BHE						
COP	G_{peak}	**E**	**D 2.97**			**D 3.77**				**D 6**		
-	**kW**	**MWh/y**	**L100**	**L200**	**L300**	**L100**	**L200**	**L300**		**L100**	**L200**	**L300**
3,5	18,9	55,82	6	3	2	6	3	2		5	3	2
3,6	19,1	56,44	6	3	2	6	3	2		5	3	2
3,7	19,3	57,02	6	3	2	6	3	2		5	3	2
3,8	19,5	57,58	6	3	2	6	3	2		5	3	2
3,9	19,6	58,11	6	3	2	6	3	2		5	3	2
4	19,8	58,61	6	3	2	6	3	2		5	3	2
4,1	20,0	59,08	6	3	2	6	3	2		5	3	2
4,2	20,1	59,54	6	3	2	6	3	2		5	3	2
4,3	20,3	59,97	6	3	2	6	3	2		5	3	2
4,4	20,4	60,38	6	3	2	6	3	2		5	3	2
4,5	20,5	60,78	6	3	2	6	3	2		5	3	2
10 kW												
FURNACE			**BHE+HEAT PUMP**				**Peak load**			**Heat load**		
MWh		**%**	**MWh**		**%**		**kW**			**MWh/y**		
22.68		68	10.89		32		10			33.58		
						n° BHE						
COP	G_{peak}	**E**		**D 2.97**			**D 3.77**				**D 6**	
-	**kW**	**MWh/y**	**L100**	**L200**	**L300**	**L100**	**L200**	**L300**		**L100**	**L200**	**L300**
3,5	7,1	4,71	3	1	1	2	1	1		2	1	1
3,6	7,2	8,63	3	1	1	3	1	1		2	1	1
3,7	7,3	10,36	3	1	1	3	1	1		2	1	1
3,8	7,4	11,95	3	1	1	3	1	1		2	1	1
3,9	7,4	14,80	3	1	1	3	1	1		2	1	1
4	7,5	17,27	3	1	1	3	1	1		2	1	1
4,1	7,6	19,43	3	1	1	3	1	1		2	1	1
4,2	7,6	21,33	3	2	1	3	1	1		2	1	1
4,3	7,7	23,02	3	2	1	3	2	1		2	1	1
4,4	7,7	24,54	3	2	1	3	2	1		2	1	1
4,5	7,8	25,90	3	2	1	3	2	1		2	1	1
11 kW												
FURNACE			**BHE+HEAT PUMP**				**Peak load**			**Heat load**		
MWh		**%**	**MWh**		**%**		**kW**			**MWh/y**		
21.32		63	12.26		37		11			33.58		
			n° BHE			**n° BHE**				**n° BHE**		

COP	**P**	**E**		**D 2.97**			**D 3.77**			**D 6**	
-	**kW**	**MWh/y**	**L100**	**L200**	**L300**	**L100**	**L200**	**L300**	**L100**	**L200**	**L300**
3,5	7,9	23,26	3	2	1	3	2	1	2	1	1
3,6	7,9	23,52	3	2	1	3	2	1	2	1	1
3,7	8,0	23,76	3	2	1	3	2	1	2	1	1
3,8	8,1	23,99	3	2	1	3	2	1	2	1	1
3,9	8,2	24,21	3	2	1	3	2	1	2	1	1
4	8,3	24,42	3	2	1	3	2	1	2	1	1
4,1	8,3	24,62	3	2	1	3	2	1	2	1	1
4,2	8,4	24,81	3	2	1	3	2	1	2	1	1
4,3	8,4	24,99	3	2	1	3	2	1	2	1	1
4,4	8,5	25,16	3	2	1	3	2	1	2	1	1
4,5	8,6	25,32	3	2	1	3	2	1	3	1	1

12 kW

FURNACE		**BHE+HEAT PUMP**		**Peak load**	**Heat load**
MWh	**%**	**MWh**	**%**	**kW**	**MWh/y**
19.88	59	13.70	41	12	33.58

			n° BHE			**n° BHE**			**n° BHE**		
COP	**P**	**E**		**D 2.97**			**D 3.77**			**D 6**	
-	**kW**	**MWh/y**	**L100**	**L200**	**L300**	**L100**	**L200**	**L300**	**L100**	**L200**	**L300**
3,5	8,6	25,37	3	2	1	3	2	1	3	1	1
3,6	8,7	25,65	3	2	1	3	2	1	3	1	1
3,7	8,8	25,92	3	2	1	3	2	1	3	1	1
3,8	8,8	26,17	3	2	1	3	2	1	3	1	1
3,9	8,9	26,41	3	2	1	3	2	1	3	1	1
4	9,0	26,64	3	2	1	3	2	1	3	1	1
4,1	9,1	26,86	3	2	1	3	2	1	3	1	1
4,2	9,1	27,06	3	2	1	3	2	1	3	1	1
4,3	9,2	27,26	3	2	1	3	2	1	3	1	1
4,4	9,3	27,45	3	2	1	3	2	1	3	1	1
4,5	9,3	27,63	3	2	1	3	2	1	3	2	1

13 kW

FURNACE		**BHE+HEAT PUMP**		**Peak load**	**Heat load**
MWh	**%**	**MWh**	**%**	**kW**	**MWh/y**
18.05	54	15.23	46	13	33.58

			n° BHE			**n° BHE**			**n° BHE**		
COP	**P**	**E**		**D 2.97**			**D 3.77**			**D 6**	
-	**kW**	**MWh/y**	**L100**	**L200**	**L300**	**L100**	**L200**	**L300**	**L100**	**L200**	**L300**
3,5	9,3	27,49	3	2	1	3	2	1	3	1	1
3,6	9,4	27,79	3	2	1	3	2	1	3	2	1
3,7	9,5	28,08	3	2	1	3	2	1	3	2	1
3,8	9,6	28,35	3	2	1	3	2	1	3	2	1
3,9	9,7	28,61	3	2	1	3	2	1	3	2	1
4	9,8	28,86	3	2	1	3	2	1	3	2	1

4,1	9,8	29,09	3	2	1	3	2	1	3	2	1
4,2	9,9	29,32	3	2	1	3	2	1	3	2	1
4,3	10,0	29,53	3	2	1	3	2	1	3	2	1
4,4	10,0	29,73	3	2	1	3	2	1	3	2	1
4,5	10,1	29,93	3	2	1	3	2	1	3	2	1
15 kW											
FURNACE			**BHE+HEAT PUMP**				**Peak load**		**Heat load**		
MWh		**%**	**MWh**		**%**		**kW**		**MWh/y**		
14.39		43	19.19		57		15		33.58		
			n° BHE			**n° BHE**			**n° BHE**		
COP	**P**	**E**		**D 2.97**			**D 3.77**			**D 6**	
-	**kW**	**MWh/y**	**L100**	**L200**	**L300**	**L100**	**L200**	**L300**	**L100**	**L200**	**L300**
3,5	10,7	31,71	4	2	1	3	2	1	3	2	1
3,6	10,8	32,07	4	2	1	4	2	1	3	2	1
3,7	10,9	32,40	4	2	1	4	2	1	3	2	1
3,8	11,1	32,72	4	2	1	4	2	1	3	2	1
3,9	11,2	33,02	4	2	1	4	2	1	3	2	1
4	11,3	33,30	4	2	1	4	2	1	3	2	1
4,1	11,3	33,57	4	2	1	4	2	1	3	2	1
4,2	11,4	33,83	4	2	1	4	2	1	3	2	1
4,3	11,5	34,07	4	2	1	4	2	1	3	2	1
4,4	11,6	34,31	4	2	1	4	2	1	3	2	1
4,5	11,7	34,53	4	2	1	4	2	1	3	2	1
17 kW											
FURNACE			**BHE+HEAT PUMP**				**Peak load**		**Heat load**		
MWh		**%**	**MWh**		**%**		**kW**		**MWh/y**		
9.93		30	23.65		70		17		33.58		
			n° BHE			**n° BHE**			**n° BHE**		
COP	**P**	**E**		**D 2.97**			**D 3.77**			**D 6**	
-	**kW**	**MWh/y**	**L100**	**L200**	**L300**	**L100**	**L200**	**L300**	**L100**	**L200**	**L300**
3,5	12,1	35,94	4	2	1	4	2	1	3	2	1
3,6	12,3	36,34	4	2	1	4	2	1	3	2	1
3,7	12,4	36,72	4	2	2	4	2	1	3	2	1
3,8	12,5	37,08	4	2	2	4	2	2	3	2	1
3,9	12,6	37,42	4	2	2	4	2	2	3	2	1
4	12,8	37,74	4	2	2	4	2	2	3	2	1
4,1	12,9	38,05	4	2	2	4	2	2	4	2	1
4,2	13,0	38,34	4	2	2	4	2	2	4	2	1
4,3	13,0	38,62	4	2	2	4	2	2	4	2	1
4,4	13,1	38,88	4	2	2	4	2	2	4	2	1
4,5	13,2	39,14	4	2	2	4	2	2	4	2	1

Table 36 Initial investment cost $CAD (drilling cost+ heat pump purchase cost) of a GCAHP system, depending on the percentage of coverage of the Heat load, GUE, Drilling diameters and BHE lenght L.

Initial investment cost $CAD									
100%									
	D 2.97			**D 3.77**			**D 6**		
GUE	**L100**	**L200**	**L300**	**L100**	**L200**	**L300**	**L100**	**L200**	**L300**
1.1	35000	55000	75000	37500	60000	82500	49000	83000	117000
1.2	55000	55000	75000	60000	60000	82500	83000	83000	117000
1.25	**55000**	**55000**	**75000**	**60000**	**60000**	**82500**	**83000**	**83000**	**117000**
1.3	55000	55000	75000	60000	60000	82500	83000	83000	117000
1.4	55000	55000	75000	82500	60000	82500	83000	83000	117000
1.5	75000	95000	75000	82500	105000	82500	117000	83000	117000
1.6	75000	95000	75000	82500	105000	82500	117000	151000	117000
1.7	75000	95000	75000	82500	105000	82500	117000	151000	117000
1.8	95000	95000	75000	105000	105000	82500	117000	151000	117000
1.9	95000	95000	75000	105000	105000	82500	117000	151000	117000
2	95000	95000	75000	105000	105000	150000	151000	151000	117000
32%									
1.1	35000	55000	75000	37500	60000	82500	49000	83000	117000
1.2	35000	55000	75000	37500	60000	82500	49000	83000	117000
1.25	**35000**	**55000**	**75000**	**37500**	**60000**	**82500**	**49000**	**83000**	**117000**
1.3	35000	55000	75000	37500	60000	82500	49000	83000	117000
1.4	35000	55000	75000	37500	60000	82500	49000	83000	117000
1.5	35000	55000	75000	37500	60000	82500	49000	83000	117000
1.6	35000	55000	75000	60000	60000	82500	49000	83000	117000
1.7	55000	55000	75000	60000	60000	82500	49000	83000	117000
1.8	55000	55000	75000	60000	60000	82500	83000	83000	117000
1.9	55000	55000	75000	60000	60000	82500	83000	83000	117000
2	55000	55000	75000	60000	60000	82500	83000	83000	117000
37%									
1.1	25000	45000	65000	27500	50000	72500	39000	73000	107000
1.2	25000	45000	65000	27500	50000	72500	39000	73000	107000
1.25	**25000**	**45000**	**65000**	**27500**	**50000**	**72500**	**39000**	**73000**	**107000**
1.3	25000	45000	65000	27500	50000	72500	39000	73000	107000
1.4	25000	45000	65000	27500	50000	72500	39000	73000	107000
1.5	45000	45000	65000	50000	50000	72500	39000	73000	107000
1.6	45000	45000	65000	50000	50000	72500	39000	73000	107000
1.7	45000	45000	65000	50000	50000	72500	73000	73000	107000
1.8	45000	45000	65000	50000	50000	72500	73000	73000	107000
1.9	45000	45000	65000	50000	50000	72500	73000	73000	107000
2	45000	45000	65000	50000	50000	72500	73000	73000	107000
41%									
1.1	35000	55000	75000	37500	60000	82500	49000	83000	117000
1.2	35000	55000	75000	37500	60000	82500	49000	83000	117000

1.25	**35000**	**55000**	**75000**	**37500**	**60000**	**82500**	**49000**	**83000**	**117000**
1.3	35000	55000	75000	37500	60000	82500	49000	83000	117000
1.4	35000	55000	75000	37500	60000	82500	49000	83000	117000
1.5	55000	55000	75000	60000	60000	82500	49000	83000	117000
1.6	55000	55000	75000	60000	60000	82500	83000	83000	117000
1.7	55000	55000	75000	60000	60000	82500	83000	83000	117000
1.8	55000	55000	75000	60000	60000	82500	83000	83000	117000
1.9	55000	55000	75000	60000	60000	82500	83000	83000	117000
2	55000	55000	75000	60000	60000	82500	83000	83000	117000
				46%					
1.1	35000	55000	75000	37500	60000	82500	49000	83000	117000
1.2	35000	55000	75000	37500	60000	82500	49000	83000	117000
1.25	**35000**	**55000**	**75000**	**37500**	**60000**	**82500**	**49000**	**83000**	**117000**
1.3	35000	55000	75000	37500	60000	82500	49000	83000	117000
1.4	35000	55000	75000	60000	60000	82500	49000	83000	117000
1.5	55000	55000	75000	60000	60000	82500	49000	83000	117000
1.6	55000	55000	75000	60000	60000	82500	83000	83000	117000
1.7	55000	55000	75000	60000	60000	82500	83000	83000	117000
1.8	55000	55000	75000	60000	60000	82500	83000	83000	117000
1.9	55000	55000	75000	60000	60000	82500	83000	83000	117000
2	55000	55000	75000	60000	60000	82500	83000	83000	117000
				57%					
1.1	35000	55000	75000	37500	60000	82500	49000	83000	117000
1.2	35000	55000	75000	37500	60000	82500	49000	83000	117000
1.25	**35000**	**55000**	**75000**	**37500**	**60000**	**82500**	**49000**	**83000**	**117000**
1.3	35000	55000	75000	37500	60000	82500	49000	83000	117000
1.4	55000	55000	75000	60000	60000	82500	49000	83000	117000
1.5	55000	55000	75000	60000	60000	82500	83000	83000	117000
1.6	55000	55000	75000	60000	60000	82500	83000	83000	117000
1.7	55000	55000	75000	60000	60000	82500	83000	83000	117000
1.8	55000	55000	75000	60000	60000	82500	83000	83000	117000
1.9	55000	55000	75000	60000	60000	82500	83000	83000	117000
2	55000	55000	75000	82500	60000	82500	83000	83000	117000
				70%					
1.1	27500	47500	67500	30000	52500	75000	41500	75500	109500
1.2	27500	47500	67500	30000	52500	75000	41500	75500	109500
1.25	**27500**	**47500**	**67500**	**30000**	**52500**	**75000**	**41500**	**75500**	**109500**
1.3	47500	47500	67500	52500	52500	75000	41500	75500	109500
1.4	47500	47500	67500	52500	52500	75000	75500	75500	109500
1.5	47500	47500	67500	52500	52500	75000	75500	75500	109500
1.6	47500	47500	67500	52500	52500	75000	75500	75500	109500
1.7	47500	47500	67500	52500	52500	75000	75500	75500	109500
1.8	67500	47500	67500	75000	52500	75000	75500	75500	109500
1.9	67500	87500	67500	75000	97500	75000	75500	75500	109500
2	67500	87500	67500	75000	97500	75000	109500	75500	109500

Table 37 Initial investment cost $CAD (drilling cost+ heat pump purchase cost) of a GCEHP system, depending on the percentage of coverage of the Heat load, COP, Drilling diameters and BHE lenght L.

Initial investment cost $CAD									
100%									
	D 2.97			D 3.77			D 6		
COP	**L100**	**L200**	**L300**	**L100**	**L200**	**L300**	**L100**	**L200**	**L300**
3,5	120000	120000	120000	135000	135000	135000	170000	204000	204000
3,6	120000	120000	120000	135000	135000	135000	170000	204000	204000
3,7	120000	120000	120000	135000	135000	135000	170000	204000	204000
3,8	120000	120000	120000	135000	135000	135000	170000	204000	204000
3,9	120000	120000	120000	135000	135000	135000	170000	204000	204000
4	120000	120000	120000	135000	135000	135000	170000	204000	204000
4,1	120000	120000	120000	135000	135000	135000	170000	204000	204000
4,2	120000	120000	120000	135000	135000	135000	170000	204000	204000
4,3	**120000**	**120000**	**120000**	**135000**	**135000**	**135000**	**170000**	**204000**	**204000**
4,4	120000	120000	120000	135000	135000	135000	170000	204000	204000
4,5	120000	120000	120000	135000	135000	135000	170000	204000	204000
32%									
3,5	80000	60000	80000	65000	65000	87500	88000	88000	122000
3,6	80000	60000	80000	87500	65000	87500	88000	88000	122000
3,7	80000	60000	80000	87500	65000	87500	88000	88000	122000
3,8	80000	60000	80000	87500	65000	87500	88000	88000	122000
3,9	80000	60000	80000	87500	65000	87500	88000	88000	122000
4	80000	60000	80000	87500	65000	87500	88000	88000	122000
4,1	80000	60000	80000	87500	65000	87500	88000	88000	122000
4,2	80000	100000	80000	87500	65000	87500	88000	88000	122000
4,3	**80000**	**100000**	**80000**	**87500**	**110000**	**87500**	**88000**	**88000**	**122000**
4,4	80000	100000	80000	87500	110000	87500	88000	88000	122000
4,5	80000	100000	80000	87500	110000	87500	88000	88000	122000
38%									
3,5	80000	100000	80000	87500	110000	87500	88000	88000	122000
3,6	80000	100000	80000	87500	110000	87500	88000	88000	122000
3,7	80000	100000	80000	87500	110000	87500	88000	88000	122000
3,8	80000	100000	80000	87500	110000	87500	88000	88000	122000
3,9	80000	100000	80000	87500	110000	87500	88000	88000	122000
4	80000	100000	80000	87500	110000	87500	88000	88000	122000
4,1	80000	100000	80000	87500	110000	87500	88000	88000	122000
4,2	80000	100000	80000	87500	110000	87500	88000	88000	122000
4,3	**80000**	**100000**	**80000**	**87500**	**110000**	**87500**	**88000**	**88000**	**122000**
4,4	80000	100000	80000	87500	110000	87500	88000	88000	122000
4,5	80000	100000	80000	87500	110000	87500	122000	88000	122000
41%									
3,5	75000	95000	75000	82500	105000	82500	117000	83000	117000
3,6	75000	95000	75000	82500	105000	82500	117000	83000	117000
3,7	75000	95000	75000	82500	105000	82500	117000	83000	117000

3,8	75000	95000	75000	82500	105000	82500	117000	83000	117000
3,9	75000	95000	75000	82500	105000	82500	117000	83000	117000
4	75000	95000	75000	82500	105000	82500	117000	83000	117000
4,1	75000	95000	75000	82500	105000	82500	117000	83000	117000
4,2	75000	95000	75000	82500	105000	82500	117000	83000	117000
4,3	**75000**	**95000**	**75000**	**82500**	**105000**	**82500**	**117000**	**83000**	**117000**
4,4	75000	95000	75000	82500	105000	82500	117000	83000	117000
4,5	75000	95000	75000	82500	105000	82500	117000	151000	117000
					46%				
3,5	60000	80000	60000	67500	90000	67500	102000	68000	102000
3,6	60000	80000	60000	67500	90000	67500	102000	136000	102000
3,7	60000	80000	60000	67500	90000	67500	102000	136000	102000
3,8	60000	80000	60000	67500	90000	67500	102000	136000	102000
3,9	60000	80000	60000	67500	90000	67500	102000	136000	102000
4	60000	80000	60000	67500	90000	67500	102000	136000	102000
4,1	60000	80000	60000	67500	90000	67500	102000	136000	102000
4,2	60000	80000	60000	67500	90000	67500	102000	136000	102000
4,3	**60000**	**80000**	**60000**	**67500**	**90000**	**67500**	**102000**	**136000**	**102000**
4,4	60000	80000	60000	67500	90000	67500	102000	136000	102000
4,5	60000	80000	60000	67500	90000	67500	102000	136000	102000
					57%				
3,5	97000	97000	77000	84500	107000	84500	119000	153000	119000
3,6	97000	97000	77000	107000	107000	84500	119000	153000	119000
3,7	97000	97000	77000	107000	107000	84500	119000	153000	119000
3,8	97000	97000	77000	107000	107000	84500	119000	153000	119000
3,9	97000	97000	77000	107000	107000	84500	119000	153000	119000
4	97000	97000	77000	107000	107000	84500	119000	153000	119000
4,1	97000	97000	77000	107000	107000	84500	119000	153000	119000
4,2	97000	97000	77000	107000	107000	84500	119000	153000	119000
4,3	**97000**	**97000**	**77000**	**107000**	**107000**	**84500**	**119000**	**153000**	**119000**
4,4	97000	97000	77000	107000	107000	84500	119000	153000	119000
4,5	97000	97000	77000	107000	107000	84500	119000	153000	119000
					70%				
3,5	100000	100000	80000	110000	110000	87500	122000	156000	122000
3,6	100000	100000	80000	110000	110000	87500	122000	156000	122000
3,7	100000	100000	140000	110000	110000	87500	122000	156000	122000
3,8	100000	100000	140000	110000	110000	155000	122000	156000	122000
3,9	100000	100000	140000	110000	110000	155000	122000	156000	122000
4	100000	100000	140000	110000	110000	155000	122000	156000	122000
4,1	100000	100000	140000	110000	110000	155000	156000	156000	122000
4,2	100000	100000	140000	110000	110000	155000	156000	156000	122000
4,3	**100000**	**100000**	**140000**	**110000**	**110000**	**155000**	**156000**	**156000**	**122000**
4,4	100000	100000	140000	110000	110000	155000	156000	156000	122000
4,5	100000	100000	140000	110000	110000	155000	156000	156000	122000

Table 38 GCAHP-Tfueel(heat pump), Tfuel, Eff,diesel, Ldiesel and Annual cost ($CAD/y) depending on GUE (1.1-2) and percentage (%) of covering of H(kWh/y)

	32%					**37%**				
	Furnace		**BHE+Heat pump**			**Furnace**		**BHE+Heat pump**		
	kWh	**%**	**kWh**	**%**		**kWh**	**%**	**kWh**	**%**	
	22685	68	10894	32		21321	63	12258	37	
GUE	**$T_{fuel\ (heat\ pump)}$**	**T_{fuel}**	**$E_{eff,\ fuel}$**	**L_{fuel}**	**Annual cost**	**Tfuel (heat pump)**	**T_{fuel}**	**$E_{eff,\ diesel}$**	**L_{fuel}**	**Annual cost**
-	**kWh**	**kWh**	**kWh**	**l/y**	**$CAD/Y**	**kWh**	**kWh**	**kWh**	**l/y**	**CAD/Y**
1.1	9903	32589	39263	3663	5494	11144	32465	39114	3649	5473
1.2	9078	31763	38269	3570	5355	10215	31536	37995	3544	5316
1.25	**8715**	**31400**	**37832**	**3529**	**5294**	**9806**	**31127**	**37503**	**3498**	**5248**
1.3	8380	31065	37428	3491	5237	9429	30750	37048	3456	5184
1.4	7781	30467	36707	3424	5136	8756	30077	36237	3380	5070
1.5	7262	29948	36082	3366	5049	8172	29493	35534	3315	4972
1.6	6809	29494	35535	3315	4972	7661	28982	34918	3257	4886
1.7	6408	29093	35052	3270	4905	7211	28532	34375	3207	4810
1.8	6052	28737	34623	3230	4845	6810	28131	33893	3162	4742
1.9	5734	28419	34240	3194	4791	6452	27773	33461	3121	4682
2	5447	28132	33894	3162	4743	6129	27450	33072	3085	4628
	41%					**48%**				
	Furnace		**BHE+Heat pump**			**Furnace**		**BHE+Heat pump**		
	kWh	**%**	**kWh**	**%**		**kWh**	**%**	**kWh**	**%**	
	19882	59	13697	41		18053	54	15526	46	
GUE	**Tfuel (heat pump)**	**Tfuel**	**$E_{eff,\ fuel}$**	**L_{fuel}**	**Annual cost**	**Tfuel(heat pump)**	**Tfuel**	**$E_{eff,\ fuel}$**	**L_{fuel}**	**Annual cost**
-	**kWh**	**kWh**	**kWh**	**l/y**	**$CAD/Y**	**kWh**	**kWh**	**kWh**	**l/y**	**CAD/Y**
1.1	12451	32334	38956	3634	5451	14115	32168	38756	3615	5423
1.2	11414	31296	37706	3517	5276	12938	30991	37339	3483	5225
1.25	**10957**	**30840**	**37156**	**3466**	**5199**	**12421**	**30474**	**36715**	**3425**	**5137**
1.3	10536	30418	36648	3419	5128	11943	29996	36140	3371	5057
1.4	9783	29666	35742	3334	5001	11090	29143	35112	3275	4913
1.5	9131	29013	34956	3261	4891	10351	28404	34221	3192	4788
1.6	8560	28443	34268	3197	4795	9704	27757	33442	3120	4679
1.7	8057	27939	33662	3140	4710	9133	27186	32754	3055	4583
1.8	7609	27492	33122	3090	4635	8626	26679	32143	2998	4498
1.9	7209	27091	32640	3045	4567	8172	26225	31596	2947	4421
2	6848	26731	32206	3004	4506	7763	25816	31104	2901	4352
	57%					**70%**				
	Furnace		**BHE+Heat pump**			**Furnace**		**BHE+Heat pump**		
	kWh	**%**	**kWh**	**%**		**kWh**	**%**	**kWh**	**%**	
	14387	43	19192	57		9928	30	23651	70	
GUE	**Tfuel (heat pump)**	**Tfuel**	**$E_{eff,\ fuel}$**	**L_{diesel}**	**Annual cost**	**Tfuel(heat pump)**	**Tfuel**	**$E_{eff,\ fuel}$**	**L_{fuel}**	**Annual cost**
-	**kWh**	**kWh**	**kWh**	**l/y**	**$CAD/Y**	**kWh**	**kWh**	**kWh**	**l/y**	**CAD/Y**
1.1	17447	31834	38355	3578	5367	21501	31429	37866	3532	5298
1.2	15994	30380	36603	3414	5122	19709	29637	35707	3331	4996
1.25	**15354**	**29741**	**35832**	**3343**	**5014**	**18921**	**28849**	**34758**	**3242**	**4863**
1.3	14763	29150	35121	3276	4914	18193	28121	33881	3161	4741
1.4	13709	28096	33850	3158	4736	16894	26822	32315	3014	4522
1.5	12795	27182	32749	3055	4582	15767	25695	30958	2888	4332
1.6	11995	26382	31785	2965	4448	14782	24710	29771	2777	4166
1.7	11290	25676	30935	2886	4329	13912	23840	28723	2679	4019
1.8	10662	25049	30180	2815	4223	13139	23067	27792	2593	3889

1.9	10101	24488	29504	2752	4128	12448	22376	26959	2515	3772
2	9596	23983	28895	2695	4043	11825	21754	26209	2445	3667

	100%				
	Furnace		**BHE+Heat pump**		
	kWh	**%**	**kWh**	**%**	
	0	0	33580	100	
GUE	**Tfuel (heat pump)**	**Tfuel**	**E eff, fuel**	**L fuel**	**Annual cost**
1.1	30526	30526	36779	3431	5146
1.2	27982	27982	33714	3145	4717
1.25	**26863**	**26863**	**32365**	**3019**	**4529**
1.3	25830	25830	31120	2903	4355
1.4	23985	23985	28898	2696	4044
1.5	22386	22386	26971	2516	3774
1.6	20987	20987	25285	2359	3538
1.7	19752	19752	23798	2220	3330
1.8	18655	18655	22476	2097	3145
1.9	17673	17673	21293	1986	2979
2	16790	16790	20228	1887	2830

Table 39 GCEHP-Ecompressor, Eefffuel off-grid plant, Eeff, furnace, Ldiesel and Annual cost ($CAD/y) depending on COP (3.5-4.5) and percentage (%) of covering of H(kWh/y)

	32%					**37%**				
	Furnace			**BHE+Heat pump**		Furnace			**BHE+Heat pump**	
	kWh	%		**kWh**	%	kWh	%		**kWh**	%
	22685	68		10894	32	**21321**	**63**		12258	37
COP	**E compressor**	**Eeff, fuel plant**	**Eeff,furnace**	**Lfuel**	**Annual cost**	**E compressor**	**Eeff, fuel plant**	**Eeff,furnace**	**Lfuel**	**Annual cost**
-	**kWh**	**kWh**	**kWh**	**l/y**	**$CAD/y**	**kWh**	**kWh**	**kWh**	**l/y**	**CAD/y**
3,5	3112	8893	27332	3379	5069	3502	10007	25688	3330	4995
3,6	3026	8646	27333	3356	5034	3405	9729	25688	3304	4956
3,7	2944	8412	27334	3334	5001	3313	9466	25688	3279	4919
3,8	2867	8191	27335	3314	4970	3226	9217	25688	3256	4884
3,9	2793	7981	27336	3294	4941	3143	8980	25688	3234	4851
4	2723	7781	27337	3275	4913	3065	8756	25688	3213	4820
4,1	2657	7591	27338	3258	4887	2990	8542	25688	3193	4790
4,2	2594	7411	27339	3241	4861	2919	8339	25688	3174	4761
4,3	2533	7238	27340	3225	4837	2851	8145	25688	3156	4734
4,4	2476	7074	27341	3209	4814	2786	7960	25688	3139	4708
4,5	2421	6917	27342	3195	4792	2724	7783	25688	3122	4683
			41%					48%		
	Furnace			**BHE+Heat pump**		Furnace			**BHE+Heat pump**	
	kWh	%		**kWh**	%	kWh	%		**kWh**	%
	19882	59		13697	41	**18053**	**54**		15526	48
COP	**E compressor**	**Eeff, fuel plant**	**Eeff,furnace**	**Lfuel**	**Annual cost**	**E compressor**	**Eeff, fuel plant**	**Eeff,furnace**	**Lfuel**	**Annual cost**
-	**kWh**	**kWh**	**kWh**	**l/y**	**$CAD/y**	**kWh**	**kWh**	**kWh**	**l/y**	**CAD/y**

3,5	3913	11181	23955	3278	4916	4436	12674	21750	3211	4817
3,6	3805	10870	23955	3249	4873	4313	12322	21750	3178	4768
3,7	3702	10577	23955	3221	4832	4196	11989	21750	3147	4721
3,8	3604	10298	23955	3195	4793	4086	11674	21750	3118	4677
3,9	3512	10034	23955	3171	4756	3981	11374	21750	3090	4635
4	3424	9783	23955	3147	4721	3882	11090	21750	3063	4595
4,1	3341	9545	23955	3125	4687	3787	10820	21750	3038	4557
4,2	3261	9317	23955	3104	4656	3697	10562	21750	3014	4521
4,3	3185	9101	23955	3084	4625	3611	10316	21750	2991	4487
4,4	3113	8894	23955	3064	4596	3529	10082	21750	2969	4454
4,5	3044	8696	23955	3046	4569	3450	9858	21750	2949	4423

57%

70%

Furnace		**BHE+Heat pump**		Furnace		**BHE+Heat pump**	
kWh	%	**kWh**	**%**	kWh	%	**kWh**	**%**
14387	**43**	19192	57%	**9928**	**30**	23651	70

COP	**E compressor**	**Eeff, fuel plant**	**Eeff, furnace**	**Lfuel**	**Annual cost**	**E compressor**	**Eeff, fuel plant**	**Eeff, furnace**	**Lfuel**	**Annual cost**
-	**kWh**	**kWh**	**kWh**	**l/y**	**$CAD/y**	**kWh**	**kWh**	**kWh**	**l/y**	**CAD/y**
3,5	5483	15667	17333	3078	4618	6757	19307	1116	2917	4375
3,6	5331	15232	17333	3038	4557	6570	18771	1116	2867	4300
3,7	5187	14820	17333	2999	4499	6392	18263	1116	2819	4229
3,8	5051	14430	17333	2963	4445	6224	17783	1116	2775	4162
3,9	4921	14060	17333	2929	4393	6064	17327	1116	2732	4098
4	4798	13709	17333	2896	4344	5913	16894	1116	2692	4038
4,1	4681	13374	17333	2865	4297	5769	16481	1116	2653	3980
4,2	4570	13056	17333	2835	4252	5631	16089	1116	2617	3925
4,3	4463	12752	17333	2807	4210	5500	15715	1116	2582	3873
4,4	4362	12462	17333	2779	4169	5375	15358	1116	2548	3823
4,5	4265	12186	17333	2754	4130	5256	15016	1116	2517	3775

100%

Furnace		**BHE+Heat pump**	
kWh	**%**	**kWh**	**%**
0	0	33580	100

COP	**E compressor**	**Eeff, fuel plant**	**Eeff, furnace**	**Lfuel**	**Annual cost**
-	**kWh**	**kWh**	**kWh**	**l/y**	**$CAD/y**
3,5	9594	27411	0	2557	3836
3,6	9327	26650	0	2486	3729
3,7	9075	25930	0	2419	3628
3,8	8837	25247	0	2355	3533
3,9	8610	24600	0	2295	3442
4	8395	23985	0	2237	3356
4,1	8190	23400	0	2183	3274
4,2	7995	22843	0	2131	3196
4,3	7809	22312	0	2081	3122
4,4	7632	21805	0	2034	3051
4,5	7462	21320	0	1989	2983

REFERENCES

[1] E. Avard, «The Kuujjuaq Greenhouse Project: Developing a New Type of Northern Food System», n. 5, pag. 14, 2013.

[2] «Nunivaat - Statistics on Estimation Of The Villages Population, 1st Of July 1996-2017». [In linea]. Available at: http://www.nunivaat.org/Table.aspx/Region/Nunavik/Indicator/Population/2014-02-24-04/13343. [Consultato: 19-set-2018].

[3] Société d'habitation du Québec, Direction des affaires intergouvernementales et autochtones, e Société d'habitation du Québec, *Le logement au Nunavik: document d'information*. 2014.

[4] «Kuujjuaq», *Wikipedia*. 02-set-2018.

[5] «Shallow geothermal resource assessments for the northern community of Kuujjuaq, Québec, Canada | Request PDF», *ResearchGate*. [In linea]. Available at: https://www.researchgate.net/publication/325451055_Shallow_geothermal_resource_assessments_for_the_northern_community_of_Kuujjuaq_Quebec_Canada. [Consultato: 14-set-2018].

[6] «PGMR resume_eng.pdf». [In linea]. Available at: http://www.krg.ca/images/stories/docs/Residual%20Material%20Management%20Plan/PGMR%20resume_eng.pdf. [Consultato: 14-set-2018].

[7] G. Duhaime, «SOCIO-ECONOMIC PROFILE OF NUNAVIK», pag. 151.

[8] «Hydro-Québec: Réseaux autonomes, Portrait d'ensemble et perspectives d'avenir. Demande R-3776, HQD-13, (2011), 35 p.» [In linea]. Available at: http://publicsde.regie-energie.qc.ca/projets/40/DocPrj/R-3776-2011-B-0058-DEMANDE-PIECE-2011_08_01.pdf. [Consultato: 14-set-2018].

[9] THE QUÉBEC GOVERNMENT, THE KATIVIK REGIONAL GOVERNMENT, e AND THE MAKIVIK CORPORATION, «Master SAA - 10_09_16 eng 08_15.pdf». [In linea]. Available at: http://www.krg.ca/images/stories/docs/Cost%20of%20Living/Master%20SAA%20-%2010_09_16%20eng%2008_15.pdf. [Consultato: 14-set-2018].

[10] S. Schott, «Alexandra Mallett, Assistant Professor, and», pag. 208.

[11] «Feasibility study of wind-diesel hybrid power system for remote communities in north of Quebec | Request PDF», *ResearchGate*. [In linea]. Available at: https://www.researchgate.net/publication/252326166_Feasibility_study_of_wind-diesel_hybrid_power_system_for_remote_communities_in_north_of_Quebec. [Consultato: 14-set-2018].

[12] «Revue technologique : efficacité énergétique et énergies renouvelables au nord du Québec - PDF». [In linea]. Available at: https://docplayer.fr/65654265-Revue-technologique-efficacite-energetique-et-energies-renouvelables-au-nord-du-quebec.html. [Consultato: 14-set-2018].

[13] «WG1AR5_SPM_FINAL.pdf». .

[14] «CO2EmissionsFromFuelCombustion2017Overview.pdf». [In linea]. Available at: http://www.iea.org/publications/freepublications/publication/CO2EmissionsFromFuelCombustion2017Overview.pdf. [Consultato: 14-set-2018].

[15] «AR4 SYR Synthesis Report - 1 Observed changes in climate and their effects». [In linea]. Available at: http://www.ipcc.ch/publications_and_data/ar4/syr/en/mains1.html. [Consultato: 14-set-2018].

[16] «(1) Allard, M. and M. Lemay (2012). Nunavik and Nunatsiavut: From science to policy. An Integrated Regional Impact Study (IRIS) of climate change and modernization. ArcticNet Inc., Quebec City, Canada, 303p. | Request PDF». [In linea]. Available at: https://www.researchgate.net/publication/264447186_Allard_M_and_M_Lemay_2012_Nunavik_and_Nunatsiavut_From_science_to_policy_An_Integrated_Regional_Impact_Study_IRIS_of_climate_change_and_modernization_ArcticNet_Inc_Quebec_City_Canada_303p. [Consultato: 19-set-2018].

[17] «Plan d'Approvisionnement 2017-2018 Réseaux autonomes R-3986-2016 Hydro Québec, 2016». [In linea]. Available at: http://publicsde.regie-energie.qc.ca/projets/389/DocPrj/R-3986-2016-B-0010-Demande-Piece-2016_11_01.pdf. [Consultato: 14-set-2018].

[18] «Nunavik», *Wikipédia*. 04-set-2018.

[19] «Clima Kuujjuaq: temperatura, medie climatiche, pioggia Kuujjuaq. Grafico pioggia e grafico temperatura Kuujjuaq - Climate-Data.org». [In linea].

Available at: https://it.climate-data.org/america-del-nord/canada/quebec/kuujjuaq-718971/#climate-graph. [Consultato: 18-nov-2018].

[20] R. Fortier, M. Allard, J.-M. Lemieux, e R. Therrien, «Cartographie des dépôts quaternaires des villages nordiques de Whapmagoostui-Kuujjuarapik, Umiujaq, Salluit et Kuujjuaq», pag. 122.

[21] «Progetto CARG - Cartografia geologica e geotematica — Italiano». [In linea]. Available at: http://www.isprambiente.gov.it/it/servizi-per-lambiente/il-servizio-geologico-ditalia/progetto-carg-cartografia-geologica-e-geotematica. [Consultato: 18-nov-2018].

[22] «Della Valentina et al. 2018.pptx». .

[23] T. You, W. Wu, W. Shi, B. Wang, e X. Li, «An overview of the problems and solutions of soil thermal imbalance of ground-coupled heat pumps in cold regions», *Applied Energy*, vol. 177, pagg. 515–536, set. 2016.

[24] M. H. Dickson e M. Fanelli, «What is geothermal energy?», pag. 33.

[25] «Heat Pump Systems | Department of Energy». [In linea]. Available at: https://www.energy.gov/energysaver/heat-and-cool/heat-pump-systems. [Consultato: 21-set-2018].

[26] A. Casasso e R. Sethi, «Tecnologia e potenzialità dei sistemi geotermici a bassa entalpia», pag. 10, 2013.

[27] «2013_03_Linee Guida per la progettazione dei campi geotermici per pompe ....pdf». .

[28] «Pompe di calore a confronto - Che cos'è la pompa di calore | Robur». [In linea]. Available at: https://www.robur.it/area_tecnica/dossier_tecnici/tecnologia_dell_assorbimento_pompe_calore/pompe_di_calore_a_confronto_principi_base. [Consultato: 26-set-2018].

[29] «Delmastro and Noce 2009_GSHP Geotermia a sonde verticali.pdf». .

[30] «Absorption Heat Pumps | Department of Energy». [In linea]. Available at: https://www.energy.gov/energysaver/heat-pump-systems/absorption-heat-pumps. [Consultato: 05-ott-2018].

[31] «idraulica_38.pdf». .

[32] A.-M. Gustafsson e L. Westerlund, «Heat extraction thermal response test in groundwater-filled borehole heat exchanger – Investigation of the borehole thermal resistance», *Renewable Energy*, vol. 36, n. 9, pagg. 2388–2394, 2011.

[33] «2012_Casasso_PhDThesis.pdf». .

[34] D. Banks, *An introduction to thermogeology: ground source heating and cooling*, 2nd ed. Hoboken, NJ: John Wiley & Sons, Ltd, 2012.

[35] «Termodinamica e trasmissione del calore», *www.libreriauniversitaria.it*. [In linea]. Available at: https://www.libreriauniversitaria.it/termodinamica-trasmissione-calore-cengel-yunus/libro/9788838665110. [Consultato: 06-ott-2018].

[36] Russo, «Advective Heat Transport in an Unconfined Aquifer Induced by the Field Injection of an Open-Loop Groundwater Heat Pump», *American Journal of Environmental Sciences*, vol. 6, n. 3, pagg. 253–259, mar. 2010.

[37] A. Casasso e R. Sethi, «Sensitivity Analysis on the Performance of a Ground Source Heat Pump Equipped with a Double U-pipe Borehole Heat Exchanger», *Energy Procedia*, vol. 59, pagg. 301–308, 2014.

[38] M. P. Anderson, «Heat as a Ground Water Tracer», *Ground Water*, vol. 43, n. 6, pagg. 951–968, ago. 2005.

[39] V. Alexiades, A. D. Solomon, e V. J. Lunardini, «Mathematical Modeling of Melting and Freezing Processes», *Journal of Solar Energy Engineering*, vol. 115, n. 2, pag. 121, 1993.

[40] «Freezing of Soil with an Unfrozen Water Content and Variable Thermal Properties», pag. 34.

[41] D. Mottaghy e V. Rath, «Latent heat effects in subsurface heat transport modelling and their impact on palaeotemperature reconstructions», *Geophysical Journal International*, vol. 164, n. 1, pagg. 236–245, gen. 2006.

[42] A. Casasso e R. Sethi, «G.POT: A quantitative method for the assessment and mapping of the shallow geothermal potential», *Energy*, vol. 106, pagg. 765–773, lug. 2016.

[43] «Giordano et al_IGCP636_2017.pdf». .

[44] «Pompa di calore geotermica ad inverter». [In linea]. Available at: http://www.rossatogroup.com/prodotti/pompe-di-calore/pompe-di-calore-geotermia/pompa-di-calore-geotermica-ad-inverter.html#descrizione. [Consultato: 19-ott-2018].

[45] «Simulation de Bâtiment.docx». .

[46] I. Staff, «Payback Period», *Investopedia*, 26-nov-2003. [In linea]. Available at: https://www.investopedia.com/terms/p/paybackperiod.asp. [Consultato: 10-nov-2018].

[47] «Listino prezzi_Pompe di calore.pdf». .

[48] «ROBUR GAHP-W-LB submittal 200710.pdf». .

[49] «Lez05apr11_21.pdf». .

[50] «Annex 5 - Calculations from the case studies.pdf». .

[51] «BHE meshing.pdf». .

[52] «Delaunay Triangulation.pdf». .

[53] N. Giordano, I. Kanzari, M. M. Miranda, C. Dezayes, e J. Raymond, «Stockage souterrain de chaleur pour le chauffage de serres et de l'eau potable à Kuujjuaq et production de chaleur issue des reservoirs géothermique profonds au Nunavik», pag. 34.

[54] H. Anbergen, W. Rühaak, J. Frank, e I. Sass, «Numerical simulation of a freeze–thaw testing procedure for borehole heat exchanger grouts», *Canadian Geotechnical Journal*, vol. 52, n. 8, pagg. 1087–1100, ago. 2015.